Technical Report Documentation Page

1. Report No.	2. Government Accession No.	3. Recipient's Catalog No.
FHWA/TX-08/0-5262-3		

4. Title and Subtitle	5. Report Date
EVALUATION AND RECOMMENDED IMPROVEMENTS FOR MIX DESIGN OF PERMEABLE FRICTION COURSES	December 2007 Published: March 2008
	6. Performing Organization Code
7. Author(s)	8. Performing Organization Report No.
Allex E. Alvarez, Amy Epps Martin, Cindy K. Estakhri, Joe W. Button, Zachary Kraus, Nikornpon Prapaitrakul, and Charles J. Glover	Report 0-5262-3
9. Performing Organization Name and Address	10. Work Unit No. (TRAIS)
Texas Transportation Institute The Texas A&M University System College Station, Texas 77843-3135	11. Contract or Grant No. Project 0-5262
12. Sponsoring Agency Name and Address	13. Type of Report and Period Covered
Texas Department of Transportation Research and Technology Implementation Office P. O. Box 5080 Austin, Texas 78763-5080	Technical Report: September 2005-August 2007
	14. Sponsoring Agency Code

15. Supplementary Notes

Project performed in cooperation with the Texas Department of Transportation and the Federal Highway Administration

Project Title: Optimizing the Design of Permeable Friction Courses (PFC)

URL: http://tti.tamu.edu/documents/0-5262-3.pdf

16. Abstract

This project focuses on the improvement of the mix design and the development of guidelines for construction and maintenance of permeable friction courses (PFC). The study started with an information search documented in Technical Report 0-5262-1 that summarizes information from a worldwide literature review and Texas Department of Transportation (TxDOT) district interviews focused on performance, maintenance, and construction of PFC. The information gathered was used to define an experimental design directed to evaluate four main aspects of PFC mix design: volumetrics, functionality (or drainability), durability, and aging. These aspects were evaluated for mixtures fabricated with both TxDOT asphalt types: PG-76-22 and asphalt rubber.

Dimensional analysis and calculation of the theoretical maximum specific gravity of the mixture were recommended for evaluating total air voids (AV) content and water accessible AV content. The computation of water accessible AV was suggested for future application in design and performance evaluations. In addition, the density specification was modified (from 78-82 percent to 76-80 percent) to ensure adequate drainability. Field evaluation of drainability during construction was recommended to ensure adequate initial functionality properties in terms of permeability. For durability, the draindown test and the Cantabro loss test (conducted in both dry and wet conditions) were recommended. In addition, density requirements for field compaction were suggested to improve the control of functionality and durability.

Technical Report 0-5262-2 constitutes the second interim report and documents construction and maintenance guidelines for PFC.

17. Key Words	18. Distribution Statement
Permeable Friction Courses, Porous Friction Courses, Open-Graded Friction Courses, Mix Design, Asphalt Mixture, Asphalt, Volumetrics, Functionality, Durability, Aging, Permeability, Drainability, Surface Free Energy, X-ray Computed Tomography, Cantabro loss test	No Restrictions. This document is available to the public through NTIS: National Technical Information Service Springfield, Virginia 22161 http://www.ntis.gov

19. Security Classif.(of this report)	20. Security Classif.(of this page)	21. No. of Pages	22. Price
Unclassified	Unclassified	180	

Form DOT F 1700.7 (8-72) **Reproduction of completed page authorized**

EVALUATION AND RECOMMENDED IMPROVEMENTS FOR MIX DESIGN OF PERMEABLE FRICTION COURSES

by

Allex E. Alvarez
Graduate Student, Texas A&M University

Amy Epps Martin
Associate Research Engineer, Texas Transportation Institute

Cindy K. Estakhri
Research Engineer, Texas Transportation Institute

Joe W. Button
Senior Research Engineer, Texas Transportation Institute

Zachary Kraus
Graduate Research Assistant, Texas Transportation Institute

Nikornpon Prapaitrakul
Graduate Research Assistant, Texas Transportation Institute

and

Charles J. Glover
Research Engineer, Texas Transportation Institute

Report 0-5262-3
Project 0-5262
Project Title: Optimizing the Design of Permeable Friction Courses (PFC)

Performed in Cooperation with the
Texas Department of Transportation
and the
Federal Highway Administration

December 2007
Published: March 2008

TEXAS TRANSPORTATION INSTITUTE
The Texas A&M University System
College Station, Texas 77843-3135

DISCLAIMER

The contents of this report reflect the views of the authors, who are responsible for the facts and the accuracy of the data presented herein. The contents do not necessarily reflect the official view or policies of the Texas Department of Transportation (TxDOT) or the Federal Highway Administration (FHWA). This report does not constitute a standard, specification, or regulation. This report is not intended for construction, bidding, or permit purposes. The engineer in charge of the project was Amy Epps Martin, P.E. # 91053.

The United States Government and the State of Texas do not endorse products or manufacturers. Trade or manufacturers' names appear herein solely because they are considered essential to the object of this report.

ACKNOWLEDGMENTS

The authors wish to express their appreciation to the Texas Department of Transportation personnel for their support throughout this project. Special thanks are given to the TxDOT project committee: Richard Izzo (project director), Billy Pigg, Mykol Woodruff, Jeremy Dearing, and Jesse Sisco for providing technical guidance and assistance.

Acknowledgment is also due the staff and personnel at the Texas Transportation Institute. This project was completed in cooperation with TxDOT and FHWA. Special thanks are expressed to the National Science Foundation for providing funds for the acquisition of the X-ray Computed Tomography equipment at Texas A&M University.

The first author, as Associate Professor of the University of Magdalena (Colombia), expresses special thanks to the University of Magdalena and COLCIENCIAS for sponsorship of his graduate studies at Texas A&M University. The remaining authors would like to thank the University of Magdalena and COLCIENCIAS for the sponsorship of Allex Alvarez whose work was invaluable to the successful outcome of this research.

TABLE OF CONTENTS

LIST OF FIGURES ..... **x**

LIST OF TABLES ..... **xiv**

INTRODUCTION **1**

1. SUMMARY OF INFORMATION SEARCH **5**

1.1. ADVANTAGES AND DISADVANTAGES OF OGFC 5

1.2. MIX DESIGN METHODS 5

1.3. CONSTRUCTION PRACTICES 6

1.3.1. Mixture Production Considerations 7

1.3.2. Mixture Storage and Transportation 7

1.3.3. Underlying Surface Profile 7

1.3.4. Mixture Placement 7

1.3.5. Material Compaction and Joint Construction 8

1.3.6. Mixture Acceptance 8

1.4. MAINTENANCE PRACTICES 8

1.4.1. Surface Maintenance 9

1.4.2. Corrective Surface Maintenance 9

1.4.3. Rehabilitation 9

1.5. PERFORMANCE 10

1.5.1. Durability 10

1.5.2. Functionality 10

1.6. TxDOT DISTRICT INTERVIEWS 11

2. EXPERIMENT DESIGN **13**

2.1. MATERIAL SELECTION 13

2.2. SPECIMEN FABRICATION 16

3. VOLUMETRICS **17**

3.1. EXPERIMENT DESIGN 18

3.1.1. Determination of Bulk Specific Gravity of the Compacted Mixture (G_{mb}) and Water Accessible Air Voids 19

3.1.2. Determination of Theoretical Maximum Specific Gravity of the Mixture (G_{mm}) 21

3.1.3. Analysis of X-Ray CT Images 22

3.2. COMPARISON AND VARIABILITY OF THEORETICAL MAXIMUM SPECIFIC GRAVITY OF THE MIXTURE 25

3.3. TOTAL AIR VOIDS CONTENT 27

3.4. ADDITIONAL VARIABILITY IN TOTAL AIR VOIDS CONTENT FOR COMPACTED SPECIMENS 29

3.5. EFFECTS ON OPTIMUM ASPHALT CONTENT (OAC) SELECTION 31

3.6. WATER ACCESSIBLE AIR VOIDS CONTENT 32
3.7. TOTAL AND INTERCONNECTED AIR VOIDS BASED ON ANALYSIS OF X-RAY CT IMAGES 36
3.8. COMPACTION EFFECTS 40
3.9. GRADATION EFFECTS 42
3.10. SUMMARY AND RECOMMENDATIONS 43

4. FUNCTIONALITY 47
4.1. EXPERIMENTAL DESIGN 47
4.2. EVALUATION OF LABORATORY CHARACTERIZATION OF DRAINABILITY 50
4.3. EVALUATION OF FIELD CHARACTERIZATION OF DRAINABILITY 55
4.4. COMPACTION EFFECTS ON DRAINABILITY 58
4.5. SUMMARY AND RECOMMENDATIONS 59

5. DURABILITY 63
5.1. EXPERIMENTAL DESIGN 64
5.1.1. Current Tests for PFC Mix Design 64
5.1.2. Additional Tests for Mixture Performance Evaluation 65
5.1.3. Compaction Effects on Durability 70
5.1.4. Surface Free Energy Measurements 70
5.2. DRAINDOWN AND BOILING TEST RESULTS 76
5.3. EVALUATION OF CANTABRO LOSS TEST RESULTS 77
5.3.1. Effect of Different Conditioning Processes on Cantabro Loss and Selection of Optimum Asphalt Content 80
5.3.2. Effect of Material Quality on Cantabro Loss 81
5.3.3. Effect of Air Voids Content on Cantabro Loss 85
5.4. EVALUATION OF HAMBURG WHEEL-TRACKING TEST AND OVERLAY TEST RESULTS 86
5.5. EVALUATION OF TENSILE STRENGTH RATIO RESULTS 89
5.6. COMPACTION EFFECTS ON DURABILITY 89
5.7. EVALUATION OF RESULTS OF SURFACE FREE ENERGY AND WORK OF ADHESION CALCULATIONS 92
5.7.1. Work of Adhesion 95
5.7.2. Relationship of Cantabro Loss and Bond Strength 97
5.8. COMPARISON OF ASPHALT RUBBER AND PERFORMANCE GRADE MIXTURE SYSTEMS 99
5.9. SUMMARY AND RECOMMENDATIONS 100

6. PFC BINDER RHEOLOGY AND AGING DURABILITY 103
6.1. INTRODUCTION 103

6.2. METHODOLOGY 104
6.2.1. Aging Methods 105
6.2.2. Analytical Measurements 105
6.3. A COMPARISON OF ASPHALT RUBBER AND SBS POLYMER-MODIFIED BINDERS 106
6.4. SPECIAL CONSIDERATIONS FOR ASPHALT RUBBER MATERIALS 116
6.4.1. Introduction 116
6.4.2. Results and Discussion 116
6.5. COMPARISON OF SBS, TIRE RUBBER, AND AR BINDERS 125
6.5.1. Introduction 125
6.5.2. Results and Discussion 125
6.6. COMPARISON BETWEEN PFC ASPHALTS AND DENSE-GRADED ASPHALTS 133
6.7. BINDER AGING IN CANTABRO SPECIMENS 134
6.8. SUMMARY, CONCLUSIONS, AND RECOMMENDATIONS 137
7. RECOMMENDATIONS, FUTURE WORK, AND MIX DESIGN EVALUATION 139
7.1. RECOMMENDATIONS AND FUTURE WORK 139
7.2. MIX DESIGN EVALUATION 142
APPENDIX 145
REFERENCES 159

LIST OF FIGURES

Page

Figure 1. (a) and (b) Aggregate Gradation for PG Mixtures. 15
Figure 2. Aggregate Gradation for AR Mixtures. 15
Figure 3. X-ray CT Setup at Texas A&M University. 23
Figure 4. Theoretical Maximum Specific Gravity (G_{mm}) Comparison for (a) I-35-PG and (b) US-281-AR Mixtures. 25
Figure 5. Theoretical Maximum Specific Gravity (G_{mm}) Variability for (a) PG and (b) AR Mixtures. 27
Figure 6. Comparison of Dimensional and Vacuum Method Total Air Voids Content for (a) I-35-PG and (b) US-281-AR Laboratory Mixtures. 28
Figure 7. Total Air Voids Content Comparison Based on G_{mb} and G_{mm} Calculations for I-35-PG and US-281-AR Laboratory Mixtures. 28
Figure 8. Impact of Volumetric Parameters on Optimum Asphalt Content Selected at 20 Percent Total Air Voids Content for (a) I-35-PG and (b) US-281-AR Laboratory Mixtures. 32
Figure 9. Comparison of Water Accessible and Total Air Voids Content for (a) I-35-PG and (b) US-281-AR Laboratory Mixtures. 33
Figure 10. Comparison of Water Accessible Air Voids Content and Total Air Voids Content for Plant Mixtures. 34
Figure 11. Ratio of Water Accessible Air Voids Content to Total Air Voids Content for (a) Plant Mixtures and (b) Road Cores. 34
Figure 12. Comparison of Air Voids Content Measured Using the Vacuum Method and Dimensional Analysis for Plant Mixtures. 35
Figure 13. X-ray CT Image Analysis (a) Original Grayscale Image, (b) Black and White Image after Threshold and (c) Black and White Image after Interconnected AV Analysis. 36
Figure 14. Total and Interconnected Air Voids Distribution for PMLC Specimens and Road Cores of the US-59Y-PG Mixture. 38
Figure 15. Total and Interconnected Air Voids Distribution for PMLC Specimens of the US-290-AR Mixture. 38

Figure 16. Total and Interconnected Air Voids Distribution for Road Cores of the (a) US-59Y-PG and (b) US-290-AR Mixture. 39
Figure 17. Comparison of Air Voids Distributions for PMLC Specimens and Road Cores of the (a) US-59Y-PG and (b) US -290-AR Mixtures. 39
Figure 18. Comparison of Air Voids Content of Plant Mix Specimens and Road Cores..... 40
Figure 19. Compaction Energy Effect on Air Voids Content Evaluated Using (a) Dimensional Analysis and (b) Vacuum Method. 41
Figure 20. Gradations of Fine PFC Mixtures..... 42
Figure 21. Comparison of Air Voids Content and Water Permeability for (a) PG Plant Mixtures and (b) PG and AR Plant Mixtures. 50
Figure 22. (a) Comparison of Air Voids Content and Water Permeability and (b) Comparison of Water Permeability for Road Cores and Plant Mixture Specimens. 53
Figure 23. Comparison of Water Flow Value and Water Permeability Based on (a) Individual Test Results (Variability) and (b) Average Values. 56
Figure 24. Comparison of Water Flow Values and Water Permeability for PMLC Specimens. . 57
Figure 25. Effect of Field Compaction Pattern on Water Flow Number. 58
Figure 26. Effect of Laboratory Compaction Energy on Water Permeability. 59
Figure 27. Asphalt Rubber Slides Prepared with Original Asphalt Rubber (Left) and Asphalt Rubber Filtered on Sieve 80 (Right). 76
Figure 28. Average Cantabro Loss for Different Conditioning Processes in I-35-PG Mixture. .. 78
Figure 29. Average Cantabro Loss for Different Conditioning Processes in US-281-AR Mixture. 78
Figure 30. Cantabro Loss at Optimum Asphalt Content (OAC) for Different Conditioning Processes. 79
Figure 31. Cantabro Loss Comparison at Optimum Asphalt Content (OAC) for (a) Dry and (b) Temperature Conditioned Specimens. 82
Figure 32. Aggregate Breakage Due to Compaction (I-35-PG Mixture). 83
Figure 33. Cantabro Loss of Plant Mixture Specimens for (a) PG and (b) AR mixtures. 84
Figure 34. Cantabro Loss (Dry Condition) Compared to Total Air Voids (a) and Water Accessible Air Voids (b) for I-35-PG and US-281-AR Mixtures. 86

Figure 35. Hamburg Wheel-Tracking Test Results for (a) I-35-PG and US-59Y-PG and (b) US-281-AR and US-290-AR Mixtures. 87
Figure 36. Overlay Test Results for (a) I-35-PG and US-59Y-PG and (b) US-281-AR and US-290-AR Mixtures. 88
Figure 37. Comparison of Overlay Test Results for (a) PG and (b) AR Plant Mixtures. 88
Figure 38. Tensile Strength Ratio for I-35-PG Laboratory Mixture. 89
Figure 39. (a) Effect of Compaction Energy on Cantabro Loss and (b) US-290-AR Mixture Failure at High Temperature (140°F [60°C]). 90
Figure 40. Effect of Compaction Energy on Cracking Life for (a) US-59Y-PG and (b) US-290-AR Mixtures. 92
Figure 41. Cantabro Loss and Work of Adhesion Comparison in (a) Dry Condition and (b) Wet Condition for the Main Laboratory and Plan Mixtures. 98
Figure 42. Cantabro Loss and Work of Adhesion Comparison in (a) Dry Condition and (b) Wet Condition for Plant Mixtures. 98
Figure 43. Cantabro Ratio at Optimum Asphalt Content (OAC) for Different Conditioning Processes. 99
Figure 44. DSR Map for IH-35-PG-76-22 and US-281-AR Asphalts. 107
Figure 45. Viscosity Curves for IH-35-PG-76-22 (SBS). 108
Figure 46. Viscosity Curve for US-281-AR. 109
Figure 47. Phase Angle Curves for IH-35-PG-76-22 (SBS). 110
Figure 48. Phase Angle Curves for US-281-AR. 110
Figure 49. Ductility versus DSR for IH-35-PG-76-22 (SBS) and US-281-AR. 111
Figure 50. Force Ductility for IH-35-PG-76-22 (SBS). 114
Figure 51. Force Ductility for US-281-AR Asphalt Rubber. 115
Figure 52. DSR Map for US-281-AR and US-288-AR Asphalt Rubber. 118
Figure 53. Asphalt Rubber Phase Angle for Original and Recovered US-281-AR. 120
Figure 54. Asphalt Rubber Viscosity for Original and Recovered US-281-AR. 121
Figure 55. US-281-AR Phase Angle. 122
Figure 56. US-288-AR Phase Angle. 123
Figure 57. US-281-AR Viscosity Master Curves. 124
Figure 58. US-288-AR Viscosity Master Curves. 124

Figure 59. Ductility versus DSR for AR Asphalts. 125
Figure 60. DSR Map of SBS and TR 76-22 Asphalts. 126
Figure 61. Ductility versus DSR Function for SBS and TR PFC Asphalts. 127
Figure 62. Ductility Improvement and Initial Stiffness for the PFC Asphalts. 128
Figure 63. Force Ductility Data for SBS PFC Asphalts. 130
Figure 64. Force Ductility Data for TR Asphalt. 130
Figure 65. Force Ductility Data for AR Asphalts. 131
Figure 66. DSR Map of TR and SBS Asphalts Plus Their Extracted Field Road Cores. 132
Figure 67. Examination of PFC versus Dense-Graded PG-76-22 Asphalt. 133
Figure 68. DSR Map of IH-35-PG-76-22 Binders Aged by Several Methods. 135
Figure 69. Ductility versus DSR Function for IH-35-PG-76-22 Binder, Aged by Several Methods. 136
Figure 70. Cantabro Loss Compared to the DSR Function for the IH-35-PG-76-22 Binder. 137
Figure 71. Summary of the Improved Mix Design Method for Volumetric and Durability Evaluation. 143

LIST OF TABLES

Page

Table 1. Laboratory (LMLC) Mixtures. 13
Table 2. Plant (PMLC) Mixtures. 13
Table 3. Cores (FMFC). 14
Table 4. Variability of Total AV Content for US-281-AR Laboratory Mixture. 30
Table 5. Comparison of Total, Water Accessible, and Interconnected Air Voids for PMLC Specimens. 37
Table 6. Fine PFC Mixtures. 42
Table 7. Average Air Voids Contents for Fine Mixture Specimens. 43
Table 8. Locations and Mixtures Selected for Evaluations of Water Flow Value. 49
Table 9. Coefficients of Correlation for Air Voids Content and Permeability. 51
Table 10. Permeability Values for Laboratory Mixtures. 52
Table 11. Water Permeability Comparison for Specimens Compacted in the Laboratory and in the Field. 54
Table 12. Results of Repeated Determinations of Water Flow Value. 55
Table 13. Mixture Descriptions. 65
Table 14. Parameters and Evaluation Methods for Fabrication of Durability Specimens 68
Table 15. Asphalts Tested for Surface Free Energy Using Unaged Samples. 71
Table 16. Aggregates Tested for Surface Free Energy. 71
Table 17. Surface Free Energy Characteristics of Probe Liquids at 20°C (ergs/cm^2). 73
Table 18. Surface Free Energy Characteristics of Probe Vapors (ergs/cm^2). 74
Table 19. Draindown and Boiling Test Results for Laboratory Mixtures. 77
Table 20. Average Total Air Voids Content (Vacuum Method) of Specimens Tested for Cantabro Loss. 79
Table 21. Effect of Compaction Energy on Hamburg Wheel-Tracking Test Results. 91
Table 22. Components and Total Surface Free Energy of Aggregates (ergs/cm^2). 93
Table 23. Components and Total Surface Free Energy of Unaged Asphalts Based on Receding Contact Angles (Dewetting-Fracture). 93

Table 24. Components and Total Surface Free Energy of Unaged Asphalts Based on Advancing Contact Angles (Wetting-Healing). 94
Table 25. Adhesive Dewetting Work of Adhesion for Both Dry and Wet Conditions. 96
Table 26. Adhesive Wetting Work of Adhesion for Both Dry and Wet Conditions. 96
Table 27. Ductility Values for US-281-AR and IH-35-PG-76-22 (SBS). 113
Table 28. Ductility Ratio Values and PAV*16 DSR Values Divided by 0.0001 for US-281-AR Asphalt Rubber and IH-35-PG-76-22 (SBS). 113
Table 29. Ductility Values for SBS, AR, and TR Asphalts. 128
Table 30. Binders Used for the Examination of PFC vs. Dense-Graded PG-76-22 Asphalt. 134
Table 31. Cantabro Loss Compared to Binder Stiffening..... 136

INTRODUCTION

Porous or permeable friction courses (PFC) are hot-mix asphalt (HMA) mixtures placed at the surface of an asphalt pavement structure in a thin layer to produce several benefits for the traveling public in terms of safety, economy, and the environment (*1*). TxDOT Specifications Item 342 defines a permeable friction course as a surface course of a compacted permeable mixture of aggregate, asphalt binder, and additives mixed hot in a mixing plant (*1*).

The use of PFC reduces the risk of hydroplaning and wet skidding; decreases splash and spray, fuel consumption, tire wear, and pavement noise; improves ride quality and visibility of pavement markings at night and in wet weather; and results in cleaner runoff when compared to dense-graded HMA (*2, 3, 4, 5, 6*). PFC mixtures are new generation open-graded friction courses (OGFC) designed with a minimum 18 percent air void (AV) content to create a permeable structure with an expected service life of 6 to 13 years. The functional life in terms of permeability and noise reduction can be less, ranging from 3 to 9 years (*1*). First-generation OGFC mixtures typically lasted half as long due to: (1) a lower optimum asphalt content (OAC), (2) use of an unmodified asphalt, (3) placement in thinner lifts, and (4) smaller total AV contents (10 to 15 percent) that allowed moisture to become trapped in a less permeable structure, causing disintegration through stripping or expansion due to freezing.

To obtain the benefits described previously, a mix design system that produces both a functional and durable PFC mixture is required. Although a common mix design procedure for these mixtures does not currently exist, many states in the United States use the National Center for Asphalt Technology (NCAT) method recommended in 2000 and modified in 2004 (*7, 8, 9*). This method integrates draindown resistance, minimum total AV content (>18 percent using dimensional analysis), durability in terms of Cantabro abrasion loss, and retained tensile strength ratio (TSR) after moisture conditioning to establish OAC. Evaluation of permeability in the NCAT method is optional, although minimum desirable values are available.

Texas Department of Transportation (TxDOT) Test Method Tex-204-F Part V (*10*) defines the Texas PFC mix design method that is required in Item 342 of the 2004 TxDOT standard specifications book (*11*). The following two types of asphalts are allowed in this specification:

- Type I or II asphalt rubber (AR) meeting requirements of Item 300.2.I with a minimum of 15 percent by weight of Grade C or Grade B crumb rubber meeting requirements in Item 300.2.G, and
- Performance grade (PG) asphalt with a minimum high temperature grade of PG76-XX defined in Item 300.2.J with a minimum of 1.0 percent of lime by weight of the total dry aggregate and a minimum of 0.2 percent of cellulose or mineral fibers by weight of mixture.

Based on the type of asphalt selected, Item 342 provides master aggregate gradation bands. Aggregates must also meet requirements in Item 342 that include coarse aggregate angularity, deleterious materials, soundness, abrasion resistance, and flat and elongated particles. Following selection of materials, two replicate specimens [6 in. (150 mm) in diameter by 4.5 in. (115 mm) in height] at three selected asphalt contents are mixed, oven-cured for 2 hours at the compaction temperature, and compacted in a Superpave Gyratory Compactor (SGC) at an N_{design} of 50. The three asphalt contents differ by 0.5 percent, and the minimum OAC for PG and AR asphalts, respectively, must be 6.0 and 8.0 percent. According to Item 342 the OAC must be between 6 and 7 percent for PG mixtures and between 8 and 10 percent for AR mixtures. An OAC is then selected based on the target laboratory density specified (between a suggested limit of 78 and a maximum of 82 percent according to Item 342 or equivalently between total AV contents of 18 and 22 percent evaluated using dimensional analysis) and the minimum requirements provided. Next, specimens at the selected OAC are produced for an evaluation of draindown (Tex-235-F), durability (Tex-245-F) (*10*), and moisture susceptibility (Tex-530-C) (*12*). However, at present the durability evaluation is performed for informational purposes only.

Although OGFC and PFC mixture performance and service life have improved since the 1990s, mix design, construction, and maintenance still require additional research. This need for additional research motivated TxDOT Project 0-5262 Optimizing the Design of Permeable Friction Courses (PFC). The main objectives of this research project were: (1) the improvement of the PFC mix design method based on an evaluation of the current process used by TxDOT using advanced research tools and (2) the development of guidelines for construction and maintenance of PFC.

This document represents the final research report (Technical Report 0-5262-3) and summarizes the entire project. The following chapter summarizes the interim report (Technical Report 0-5262-1) that documents the information search. Next, the document describes the

overall experiment design, including specimen fabrication procedures and materials used to fabricate laboratory mixed-laboratory compacted (LMLC), field mixed-laboratory compacted (PMLC or plant mixes), and field mixed-field compacted (FMFC or road cores) specimens. The next four chapters present the results of the research project in terms of volumetrics, functionality, durability, and aging. Based on these results, an evaluation of the current TxDOT PFC mix design process, recommendations for improvement, and suggestions for future work are provided. This report concludes with a mix design evaluation proposed for implementation. Technical Report 0-5262-2 constitutes the second interim report and documents construction and maintenance guidelines for PFC.

1. SUMMARY OF INFORMATION SEARCH

This chapter presents a summary of the information search conducted to document the advantages and disadvantages and the state of the practice related to the design, construction, maintenance, and performance of surface courses using porous mixtures. These mixtures include PFC, OGFC, and porous asphalt (PA), which are similar porous mixtures used in Europe.

1.1. ADVANTAGES AND DISADVANTAGES OF OGFC

The main advantages related to the use of OGFC as surface courses are improvements in safety, economy, and the environment. Regarding safety, the following particular advantages can be identified:

- hydroplaning reduction/elimination,
- spray and splash reduction,
- glare reduction, particularly at night, which enhances the visibility of road, and
- frictional resistance improvement (i.e., in wet conditions.)

Reductions in fuel consumption and rate of tire wear represent economic benefits, whereas the environmental advantages are:

- tire-pavement noise reduction,
- higher driver comfort levels, and
- possible integration of recycled products (i.e., crumb rubber from old tires) in the mix.

The disadvantages of OGFC are:

- reduced performance affecting functionality (i.e., drainability and noise reduction capacity),
- high construction materials costs,
- winter maintenance issues, and
- minimal structural contribution.

1.2. MIX DESIGN METHODS

In the United States, there are diverse approaches for OGFC mix design. Until 2000 at least, some departments of transportation (DOTs) were using Federal Highway Administration (FHWA) Technical Advisory T5040.31 (1990), while others were applying diverse criteria to

establish the OAC. These criteria included specific draindown tests, visual evaluation of draindown, retained coating after boiling, and evaluation of the minimum voids in mineral aggregate, among others. At that time, only Oregon specified a minimum AV content.

At present, a significant number of states using OGFC have implemented the design method suggested by NCAT in 2000 that integrates basic parameters: draindown resistance, minimum AV content (>18 percent), abrasion loss (Cantabro test performed using SGC compacted specimens), and retained tensile strength ratio. Evaluation of permeability is still considered optional, although NCAT indicated minimum desirable values for this parameter, which should be evaluated in the laboratory.

Most European design methods for PA establish OAC based on the determination of the maximum asphalt content that permits obtaining a minimum specified AV content. In general, this AV content is greater than 20 percent and can be as high as 26 percent (i.e., in Denmark). The draindown test is also performed to avoid draindown issues during mixing, handling, and placement. The determination of the minimum asphalt content that ensures adequate mixture resistance against disintegration, as determined by applying the Cantabro test, is also used to some extent in Europe. Some European countries currently require not only evaluating the loss of weight in the Cantabro test using dry specimens, but also using moisture conditioned samples. The retained tensile strength ratio is used only for PA design in Switzerland.

PA design parameters do not currently include permeability. In Europe, only the United Kingdom requires a minimum permeability in the field, which is measured immediately after placing the mix.

The use of modified asphalt for fabricating both PA and OGFC has increased notably for maximizing mixture service life. In Europe, The Netherlands and Switzerland are still employing conventional binder, although in Switzerland the use of modified binder is an alternative. The incorporation of fibers has become a common practice in Europe and North America to prevent draindown problems in both PA and OGFC, respectively.

1.3. CONSTRUCTION PRACTICES

Construction of OGFC and PA, in general, utilizes the current techniques applied to construct dense-graded HMA. However, construction of porous layers requires some special considerations throughout the process as summarized below.

1.3.1. Mixture Production Considerations

- OGFC mixture production requires special attention to aggregate moisture control.
- Incorporation of fibers and the use of modified asphalts as required for most OGFC mixtures is successfully performed by adapting conventional asphalt plants (batch and drum plants).
- Both the dry and the wet mixing time should be lengthened to augment fiber (mineral or cellulose) distribution when using a batch plant to produce OGFC mixtures.
- Since draindown susceptibility characterizes OGFC, control of mixing temperature requires particular attention.

1.3.2. Mixture Storage and Transportation

- Limits on mixture storage and transportation times should be required because OGFC are prone to draindown.
- Tarps are necessary to avoid crusting of the OGFC mixture during transportation.
- Requiring insulated truck beds for OGFC transportation is not a generalized practice, but some state DOTs are already applying it.
- Preparation of truck beds by using a full application of an asphalt release agent is recommended for transportation of rich OGFC mixtures.

1.3.3. Underlying Surface Profile

- Since OGFC is not a layer to correct profile distresses or any kind of structural distress, the underlying surface should exhibit adequate conditions before OGFC placement.
- Lateral and longitudinal drainage of the underlying layer must be provided to ensure adequate water discharge from the OGFC.
- Placement of OGFC over an impermeable layer is recommended to prevent problems in underlying layers.

1.3.4. Mixture Placement

- OGFC smoothness is highly dependent on constructive practices; surface depressions are more difficult to correct with OGFC than with dense-graded HMA.

- The use of modified binders and the construction of OGFC in thin layers demand special attention to placement and compaction temperatures.
- Technology for simultaneously placing both layers of the two-layer PA (currently tested in Europe and Japan) is now available in Japan.

1.3.5. Material Compaction and Joint Construction

- Compaction of OGFC mixtures is typically performed using static steel-wheel rollers; 8- to 9-ton tandem rollers are appropriate to complete the compaction process on thin layers.
- Pneumatic-tired rollers are not used for OGFC compaction because their kneading action reduces the mixture drainage capacity by closing surface pores.
- Keeping a maximum distance of 15 m (50 feet) between the roller and the paver is strongly recommended.
- Longitudinal and transverse joints in OGFC require special treatment since they are more difficult to construct than those in dense-graded HMA. Avoidance of longitudinal cold joints is always preferred.

1.3.6. Mixture Acceptance

- The practice in most agencies for mixture approval is based on the evaluation of:
  - binder content,
  - gradation, and
  - visual inspection after compaction to evaluate (qualitatively but not quantitatively) the density, material variability, and segregation.
- Adequate compaction is necessary to prevent raveling. However, specified density in the field is not currently required.
- Almost all agencies specify a minimum smoothness for mixture acceptance.

1.4. MAINTENANCE PRACTICES

OGFC or PA maintenance activities cannot be performed in the same way as for conventional dense-graded HMA. Earlier and more frequent frost and ice formation is a result of the particular open-graded mixtures' thermal properties. In fact, the main problems associated

with OGFC maintenance in the United States are the formation of black ice and extended frozen periods. Consequently, OGFC requires specific winter maintenance practices such as:

- more salt (or deicing agents) and more frequent applications than on dense-graded HMA,
- greater control in the homogeneous supply of deicing chemical, and
- the use of new technology to monitor in real time the road system and support the decision process involving when and how to treat an OGFC surface, which can improve the maintenance process.

Spreading sand to enhance friction and hasten deicing is not recommended because it contributes to the clogging of voids.

1.4.1. Surface Maintenance

There are no reports in the United States on the application of major maintenance for OGFC. Some states using OGFC apply fog seals to perform preventive maintenance. Cleaning of OGFC in the United States is not common practice. However, in some European countries and Japan, different techniques are applied to maintain porosity during the pavement's lifetime. In addition, these countries are testing two-layer PA in order to maximize mixture functionality.

1.4.2. Corrective Surface Maintenance

Most agencies using OGFC and PA apply dense-graded HMA to repair delaminated areas and potholes. Crack filling may generate drainage problems since water flow inside the mixture is diminished.

1.4.3. Rehabilitation

General recommendations and actual practices for rehabilitation of OGFC in the United States include milling and replacing existing OGFC with new OGFC or any other asphalt mixture. However, the ideal set of technical actions for major rehabilitation of OGFC should be milling, recycling, and inlaying.

Once the OGFC has lost its functionality (i.e., permeability and noise reduction capacity) by clogging, its service might still be permitted since it essentially behaves like a dense-graded HMA with low permeability. Direct placement of new dense-graded HMA over a porous mixture

is not recommended because the life of the new layer can be diminished by water accumulation inside the OGFC.

1.5. PERFORMANCE

OGFC performance includes durability and functionality. Whereas durability comprises moisture sensitivity and aging potential, functionality takes into account permeability and noise reduction.

1.5.1. Durability

The service life of OGFC is highly variable and can range from 7 to 10 years. One of the factors that most influences mixture durability is the type of binder used. The majority of agencies reporting successful application of OGFC at present are using modified binders. Tire rubber, styrene butadiene styrene (SBS), and styrene butadiene rubber (SBR) modified asphalt are now more frequently used in OGFC.

Raveling is the distress most frequently reported as the cause of failure in OGFC mixtures. However, delamination is also an important cause of failure in these mixtures. Raveling can be associated with aging binder, which can be the main cause; binder softening generated by oil and fuel drippings; and inadequate compaction or insufficient asphalt content. Important work remains to be done in assessing the aging potential of PFC mixtures and the resulting impact on durability.

1.5.2. Functionality

A functional life between 5 and 8 years is expected for OGFC and PA. Reductions of AV content during service, as a consequence of clogging, affect functionality. Therefore, in the absence of cleaning activities, the initial permeability and noise reduction capacity are expected to decrease such that, at the end of the functional life, OGFC behaves like dense-graded HMA.

When the infrastructure contributes a small amount of debris and high traffic speeds can be ensured, clogging is delayed due to the existence of suction forces generated by high-speed rolling tires that effectively clean the OGFC and PA.

Europe and Japan are pursuing the extended noise reduction capability of PA by means of a combined strategy that involves designing and constructing two-layer PA, limiting construction of PA to high-speed roads only, and applying frequent cleaning with special equipment. However, engineers in different agencies around the world do not agree on the convenience of cleaning techniques, and its practice is still not generalized. New technological developments (i.e., new Japanese cleaning technology) are modifying the current cleaning practices and maximizing the cost-benefit ratio of this practice.

Although high permeability is one of the main properties of OGFC, this parameter is not widely measured since it is integrated into most mix design procedures as AV content, which is considered to be representative of drainability. However, the minimum AV content is not specified by many agencies in the United States. The common approach to measure the drainage capacity of porous mixtures in the field is the determination of the time of discharge of a specific water volume. In the laboratory, permeability has been measured using permeameters with either falling head or constant head.

Comparisons of the structural capacity of OGFC, PA, and dense-graded HMA presented in the literature do not lead to a definitive conclusion on the material properties of porous mixtures. Whereas some authors state that dense-graded HMA, PA, and OGFC are comparable in terms of mechanical response, others suggest that lower modulus are obtained for PA and OGFC in comparison to the modulus on dense mixtures.

Permanent deformation is not generally considered an issue in PA and OGFC. Field measurements and extensive experience in Europe (mainly in Spain, where PA has been used for more than 20 years) suggest that PA mixtures are highly resistant to permanent deformation.

1.6. TxDOT DISTRICT INTERVIEWS

Researchers conducted interviews with 10 TxDOT districts to obtain district personnel's assessment of performance, maintenance, and construction of PFC. Most of the PFC projects placed by these districts are relatively new (less than 3 years old), so maintenance has not yet been an issue. However, overall perceptions of construction and performance are very positive. Some of the primary production and placement issues include the following:

- Mixture temperature—It is important for the mix to be sufficiently hot at the time of placement because the mix does not maintain good workability. Insulated trucks are recommended. It is also important for the screed to be in vibratory mode and to be hot.
- Handwork—Raking or handwork is difficult or impossible. Districts have overcome this problem by staying away from bridge ends, intersections, and crossovers and using a dense-graded mixture in these areas. Another district reports milling down existing surfaces about 2 inches at bridge ends. One district reports that it is better to come back later and grind areas that need tapering rather than allowing any raking.
- Placement—There is a preference for the use of shuttle buggies because they seem to provide more uniformity than other methods.
- Stopping/Starting—Any stopping/starting of the laydown machine can cause a bump. Stopping the rollers can leave marks.
- Pick-Up—One district reported that while the mixture is still hot, it tends to pick up under traffic. Water has been used to cool the mixture prior to allowing traffic onto the roadway.
- Storage—The Austin District reports that a maximum of 12 hours should be allowed in silo.

Performance of the PFC mixtures has been very good, and as a result, their use is increasing. It has been used on top of stone matrix asphalt (SMA), stone-filled mixtures, dense-graded mixtures, jointed concrete, and continuously reinforced concrete, and is almost always used on very high-traffic facilities. Usually an underseal is placed first. One district reports that they would consider PFC on new concrete pavements. Most report safety as the primary reason for the selection of PFC as a wearing course. While the cost is higher than conventional dense-graded mixtures, it seems that the benefits outweigh the additional cost. Areas where PFC has not performed as well are where there is a significant amount of turning traffic, in driveway area turnouts, and where fuel spills have occurred from traffic accidents. Locations where hand raking was attempted have not performed well. The Austin District reports that milled rumble strips are showing signs of raveling, though this has not yet been reported in other districts.

2. EXPERIMENT DESIGN

This chapter presents the overall experiment design, including specimen fabrication, procedures and materials used to fabricate laboratory mixed-laboratory compacted (LMLC or laboratory mixtures), field mixed-laboratory compacted (PMLC or plant mixtures), and field mixed-field compacted (FMFC or road cores) specimens. Different subsets of these specimens were utilized to evaluate volumetrics, functionality, and durability of PFC mixtures (Chapters 3, 4, and 5, respectively) in the laboratory.

2.1. MATERIAL SELECTION

Both asphalt types (PG and AR) and corresponding aggregate gradations as defined in TxDOT Test Method Tex-204-F Part V (*10*) and Item 342 of the 2004 TxDOT Standard Specifications book (*11*) were evaluated in LMLC mixtures (Table 1), plant (PMLC) mixes (Table 2), and road cores (FMFC) (Table 3). Figure 1 and Figure 2 show aggregate gradations for PG and AR mixtures, respectively. These materials and corresponding field sections were selected in coordination with TxDOT based on available PFC sections constructed in 2006 and 2007.

Table 1. Laboratory (LMLC) Mixtures.

Mixture	Highway	Location	Asphalt Type	OAC (%)	Aggregate Type	Other Materials
US-281-AR	US 281	San Antonio	AC-10 w/16% crumb rubber	8.1	Sandstone Limestone	None
I-35-PG	IH 35	San Antonio	PG 76-22S	6.1	Sandstone Limestone	Lime (1%) Fibers (0.3%)

Table 2. Plant (PMLC) Mixtures.

Mixture	Highway	TxDOT District	Asphalt Type	OAC (%)	Aggregate Type	Other Materials
I-35-PG	IH 35	San Antonio	PG 76-22S	6.1	Sandstone Limestone	Lime (1%) Fibers (0.3%)
US-83-PG	US 83/84	Abilene	PG 76-22S	6.4	Limestone	Lime (1%) Fibers (0.3%)
IH-20-PG	IH 20	Abilene	PG 76-22	6.5	Limestone	Lime (1%) Fibers (0.3%)
IH-30-PG	IH 30	Paris	PG 76-22	6.6	Sandstone	Lime (1%) Fibers (0.3%)

Mixture	Highway	TxDOT District	Asphalt Type	OAC (%)	Aggregate Type	Other Materials
US-59-PG	US 59	Lufkin	PG 76-22	5.9	Granite Limestone	Lime (1%) Fibers (0.3%)
US-59Y-PG	US 59	Yoakum	PG 76-22S	5.8(1)	Limestone	Lime (1%) Fibers (0.3%)
US-281-AR	US 281	San Antonio	AC-10 w/16% crumb rubber	8.1	Sandstone Limestone	None
US-288-AR	US 288	Houston	AC-10 w/17% type II rubber	8.0	Granite Limestone	None
US-290-AR	US 290	Austin	AC-10 w/17 % crumb rubber	8.3	Sandstone	None

Table 3. Cores (FMFC).

Mixture	Highway	TxDOT District	Asphalt Type	OAC (%)	Aggregate Type	Other Materials
I-35-PG	IH 35	San Antonio	PG 76-22S	6.1	Sandstone Limestone	Lime (1%) Fibers (0.3%)
US-83-PG	US 83/84	Abilene	PG 76-22S	6.4	Limestone	Lime (1%) Fibers (0.3%)
IH-20-PG	IH 20	Abilene	PG 76-22	6.5	Limestone	Lime (1%) Fibers (0.3%)
IH-20-PG-TR	IH 20	Abilene	PG 76-22TR	6.2	Limestone	Lime (1%) Fibers (0.3%)
IH-30-PG	IH 30	Paris	PG 76-22	6.6	Sandstone	Lime (1%) Fibers (0.3%)
US-59-PG	US 59	Lufkin	PG 76-22	5.9	Granite Limestone	Lime (1%) Fibers (0.3%)
US-59Y-PG	US 59	Yoakum	PG 76-22S	5.8[1]	Limestone	Lime (1%) Fibers (0.3%)
H-6-PG	SH 6	Houston	PG 76-22 TR	Unknown	Traprock, Limestone	None
I-35-PG-W	IH 35	Waco	PG 76-22 TR	6.0	Limestone Igneous rock	Lime (1%) Fibers (0.4%)
US-281-AR	US 281	San Antonio	AC-10 w/16% crumb rubber	8.1	Sandstone Limestone	None
US-288-AR	US 288	Houston	AC-10 w/17% type II rubber	8.0	Granite Limestone	None
US-290-AR	US 290	Austin	AC-10 w/17 % rubber	8.3	Sandstone	None
I-35-AR	I 35	San Antonio	AC-10 w/17 % type II rubber	8.4	Sandstone, Limestone	None

[1]The design OAC is 6.2. The actual asphalt content used to produce the plant mixture is 5.8%.

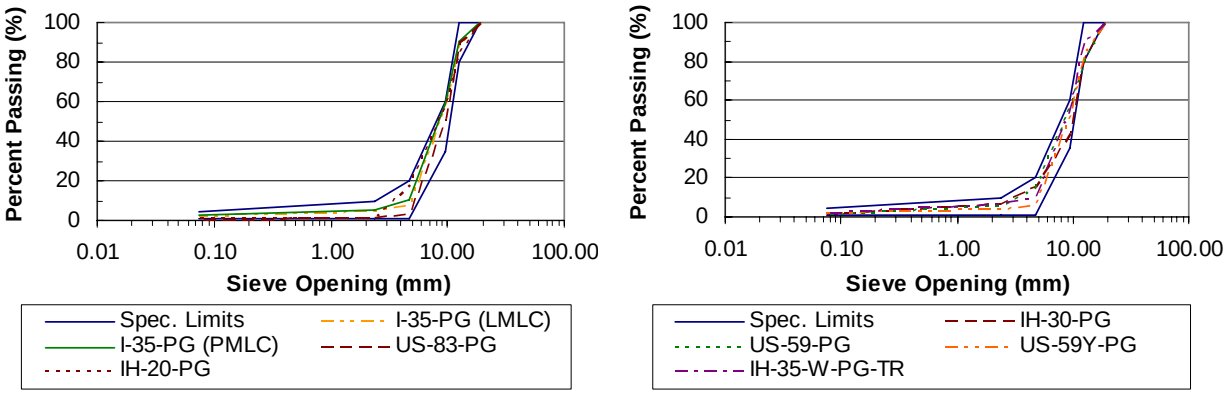

(a) (b)

Figure 1. (a) and (b) Aggregate Gradation for PG Mixtures.

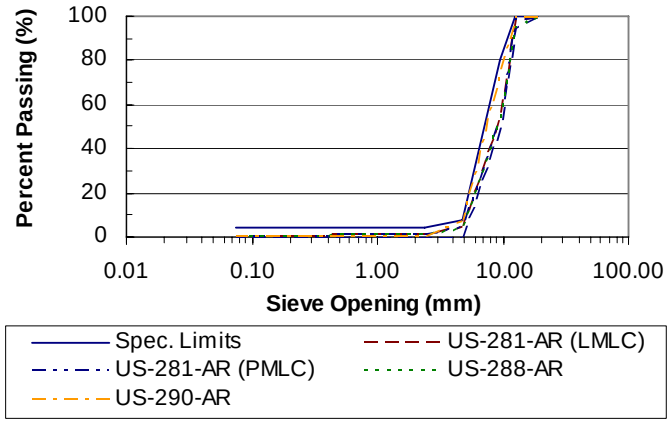

Figure 2. Aggregate Gradation for AR Mixtures.

Researchers developed an extensive laboratory testing program for both I-35-PG and US-281-AR laboratory mixtures to evaluate volumetric, functionality, and durability aspects. The same type of program, but with a reduced number of specimens and testing conditions, was applied to evaluate the US-59Y-PG and US-290-AR plant mixtures. Thus, these four mixtures form the core of the laboratory evaluation conducted for this study. The remaining plant mixtures were subjected to a more specific testing program to complement the evaluation of the four main mixtures (I-35-PG, US-281-AR, US-59Y-PG, and US-290-AR). Subsequent chapters provide details on the specific testing programs.

2.2. SPECIMEN FABRICATION

LMLC specimens for both mixture systems (AR and PG) were mixed at 325°F (163°C) and oven-cured for 2 hours at the compaction temperature (300°F [149°C]). PMLC specimens were compacted at the same temperature, but these specimens were not oven cured in addition to the time required to reheat the mixture to the compaction temperature.

The evaluation of mixture durability required fabricating one particular type of specimen for each test. As these evaluation tests are destructive, replicate specimens were needed to perform the tests on specimens subjected to different conditions and/or tests. Most specimens were compacted using the SGC at an N_{design} value of 50 gyrations (*10*) to dimensions of 6 in. (150 mm) in diameter and either: (1) 4.5 ± 0.2 in. (115 ± 5 mm) in height, (2) 2.4 ± 0.1 in. (62 ± 2 mm) in height, or (3) 2.25 in. (57 mm) in height. Furthermore, some specimens required saw cutting to the final dimensions. LMLC specimens were accepted for use in mixture evaluation if the total AV content was 20 ± 1 percent. In one small experiment this total AV content range was expanded due to practical difficulties in specimen fabrication. For plant mix (PMLC) specimens, the total AV content was controlled to match the AV content targeted for the mix design. In addition, a different level of compaction in terms of N_{design} was also utilized in a small experiment. More details on these small experiments will be provided in the subsequent results chapters.

3. VOLUMETRICS

The current HMA mix design procedure used to determine the OAC for PFC mixtures is based on volumetric properties, primarily total AV content. In addition, the functional and the durability properties of PFC mixtures are closely related to the volumetric properties of these mixtures and have also been associated mainly to the total AV content. This calculated volumetric parameter depends on the bulk specific gravity of the compacted mixture (G_{mb}) and the theoretical maximum specific gravity (G_{mm}) of the mixture. In a compacted HMA mixture, the total AV content, computed as a percent of the total volume, is calculated as follows:

$$Total\ \ AV\ Content = 100\frac{G_{mm} - G_{mb}}{G_{mm}}\ \ (\%) \qquad (1)$$

While the AV calculation is simple, measuring G_{mm} and G_{mb} is difficult for PFC mixtures due to the high asphalt contents, high total AV contents, and the use of modified asphalts.

This chapter describes the activities developed to establish potential improvements for evaluating the volumetric properties of PFC mixtures, and to obtain a better understanding of these properties as a means to promote better mix design procedures and field evaluations of these mixtures. To accomplish these objectives, two methodologies for determining G_{mb} (vacuum and dimensional analysis) and two methodologies for determining G_{mm} values (measured and calculated) were evaluated. The effects of each method on the resulting total AV content and corresponding selection of OAC by weight of mixture are also provided. In addition, the vacuum method and dimensional analysis for calculating water accessible AV content (i.e., proportion of AV in the compacted mixture that are accessible to water) in PFC mixtures are compared. Chapters 4 and 5 compare total AV and water accessible AV with functionality and durability test results to establish the best parameter to use in future functionality and durability evaluations.

Furthermore, X-ray computed tomography (X-ray CT) images obtained from LMLC and PMLC specimens and road cores were scanned and analyzed to provide additional insight into the AV characteristics of these mixtures. Preliminary evaluations of compaction and gradation effects on volumetric characteristics of PFC mixtures were also conducted. The chapter includes the experimental design, followed by a discussion of the results, conclusions, and respective recommendations.

3.1. EXPERIMENT DESIGN

The evaluation of volumetric characteristics included two stages. The first stage involved a major study of G_{mm}, G_{mb} (to compute total AV), and water accessible AV on the I-35-PG and US-281-AR laboratory mixtures and some road cores. The main objectives of this stage were (1) to compare the AV determinations based on both dimensional analysis and the vacuum method with measured and calculated G_{mm} and (2) to establish the water accessible AV for PFC compacted in the laboratory and in the field. Next, an indicative evaluation of the effect of the different methodologies used to determine G_{mm} and G_{mb} on the selection of OAC for the laboratory mixtures studied was performed.

The main objective of the second stage of volumetric testing and analysis was the study of water accessible AV using a procedure associated with dimensional analysis. The US-290-AR and US-59Y-PG plant mixtures and road cores were evaluated using both approaches (dimensional analysis and the vacuum method) to determine both total and water accessible AV.

X-ray CT scanning was performed on LMLC and PMLC specimens and on road cores, and subsequent image analysis determined total and interconnected AV content. The interconnected AV content was compared to the water accessible AV content. Two specimens of each laboratory mixture at each asphalt content and two cores of each location studied were used for volumetric and permeability tests and X-ray CT scans. Similarly, two specimens of each plant mixture were subjected to volumetric determinations, permeability testing, X-ray CT scanning, and the Cantabro test.

The impact of compaction energy on volumetric properties was evaluated using the US-290-AR and US-59Y-PG plant mixtures. For this purpose PMLC specimens of 4.5 ± 0.2 in. (115 ± 5 mm) in height were compacted by applying two different energies with the SGC. The first set of PMLC specimens was compacted applying the number of gyrations required to reproduce the AV content computed for the cores extracted at locations compacted with four and three passes for US-290-AR and US-59Y-PG mixtures, respectively. The second set was compacted applying 50 gyrations, as specified in the current design procedure (*10*).

Finally, a preliminary volumetric evaluation (G_{mm}, G_{mb}, and water accessible AV content) of two particular gradation modifications was performed using the same aggregates and asphalt type used in the I-35-PG mixture. Two specimens were produced using each modified gradation and the current PFC mix design procedure (Tex-204-F Part V) (*10*). The AV contents were

determined using calculated G_{mm} values based on G_{mm} measurements at low asphalt contents (3 to 5 percent).

All of the evaluation methods and tests applied to perform the assessment of PFC volumetrics conducted in this study are described subsequently in this section.

3.1.1. Determination of Bulk Specific Gravity of the Compacted Mixture (G_{mb}) and Water Accessible Air Voids

For PFC mixtures, Tex-207-F Part VI using the vacuum method is required to determine G_{mb} due to the high total AV content of these mixtures and the difficulty of obtaining representative results associated with saturated surface dry measurements of porous samples. Dimensional analysis serves as part of the PFC mix design and quality control processes in the laboratory. Previous research recommended the vacuum method for determining G_{mb} of OGFC (*8, 9, 13*).

In the vacuum method, the Corelok® device was used for double large bag testing (*14*) since initial evaluations using a single bag resulted in frequent puncture problems allowing water to flow into the sealed specimen. The inner bag was 1.5 in. (38 mm) to 2 in. (51 mm) shorter than the external bag to best apply the seal. G_{mb} was calculated as:

$$G_{mb} = \frac{W}{W_b + W - W_{bs,w} - \frac{W_b}{CF}} \quad (2)$$

where W is the mass of the specimen in air (g), W_b is the mass of the bag in air (g), $W_{bs,w}$ is the mass of the sealed bag and the specimen in water (g), and CF represents the double bag correction factor supplied by the manufacturer (*14*). In addition to G_{mb}, water accessible AV content can be calculated by determining the vacuum saturated sample mass in water (W_s) after completing all other measurements. The water accessible AV content may better relate to the functionality and durability of PFC mixtures. Chapters 4 and 5 provide detailed discussion on this topic. Measuring W_s requires: (1) cutting the sealed bag under water and taking it out of the water and (2) allowing access to water until a stable mass is obtained. The minimum saturation time used to determine W_s was 4 minutes, but some mixes required up to 7 minutes before reaching stable saturated weights. This time is mix dependent and requires evaluation for each particular mix. Water accessible AV is then calculated as follows:

$$Accessible\ AV_{vacuum} = \frac{W_b + W - W_{bs,w} - \left(\frac{W_b}{CF}\right) - (W - W_S)}{W_b + W - W_{bs,w} - \left(\frac{W_b}{CF}\right)} * 100 \quad (\%) \tag{3}$$

A second method for determining G_{mb} is known as dimensional analysis; this method requires measuring the mass, height, and diameter of a compacted specimen. This method directly calculates volume assuming that the specimen is a regular cylinder with smooth faces. The dimensional analysis method is simple, inexpensive, and does not require special equipment. Calculating the volume of each specimen involved four diameter and three height measurements using a caliper with a precision of 0.0001 in. (0.00254 mm): two diameter measurements at the top and two at the bottom of the specimen and three uniformly distributed height measurements around the specimen circumference.

Average diameter and height were used to define the volume used in the dimensional G_{mb} calculated as follows:

$$G_{mb} = \frac{\frac{W}{V_{td}}}{\rho_w} \tag{4}$$

where V_{td} is the total volume of the regular cylinder (cm^3), and ρ_w is the density of water (g/cm^3). Dimensions were taken as indicated after allowing the specimens to cool for approximately 15 minutes in the mold after compaction to minimize changes of shape observed in specimens extracted at shorter times. In addition, direct measurement of dimensions was preferred over the height reported by the SGC and the nominal mold diameter, since expansion in the vertical direction (measured after cooling down overnight) was noted based on direct measurement compared to height values reported by the SGC. These differences in height led to total AV content discrepancies up to 3 percent in AR mixtures. Based on the results of this study, diameter measurements at the top, bottom, and center of the specimens are recommended to further improve the accuracy of the total volume.

Water accessible AV content can also be calculated in the dimensional analysis method as follows:

$$Accesible\ AV_{\dim ensional} = \frac{V_{td} - \frac{(W - W_s)}{\rho_w}}{V_{td}} * 100 \quad (\%) \tag{5}$$

where W_s is the saturated sample mass in water.

The dimensional analysis method and the vacuum method differ in the determination of water accessible AV since W_s was redefined for the dimensional procedure as the saturated sample mass in water obtained after direct immersion of the specimen without any vacuum application. However, additional research may be required to establish if a vacuum is required to obtain a representative saturated mass in PFC mixtures and to establish the magnitude of the vacuum that may be needed to obtain saturation without inducing micro-damage in the specimen. The occurrence of this type of damage was stated by Masad et al. (*15*) when studying dense mixtures. This micro-damage will increase the AV connectivity and therefore the measured water accessible AV content. This damage would also negatively affect any subsequent durability evaluation.

3.1.2. Determination of Theoretical Maximum Specific Gravity of the Mixture (G_{mm})

Tex-227-F Theoretical Maximum Specific Gravity of Bituminous Mixtures was the test procedure used to determine G_{mm} at a specific asphalt content (*10*). This measured G_{mm} value is also known as Rice Specific Gravity. In addition, Tex-227-F also includes a second procedure for the calculation of G_{mm} at other asphalt contents assuming a constant effective specific gravity (G_{se}) for the aggregate. For PFC mixtures, direct measurement of G_{mm} is a difficult task given the high asphalt contents generally used, especially for extremely sticky AR mixtures with OAC typically above 8 percent. These characteristics of AR asphalts and in general the high asphalt contents in PFC mixtures lead to loss of asphalt and some fine material throughout the methodology used to directly measure G_{mm}. Thus, a second method of measuring G_{mm} at lower asphalt contents to quantify G_{se} and then calculating the G_{mm} at the actual PFC asphalt contents used for mix design was evaluated.

In this second approach, G_{mm} at asphalt contents of 3.5, 4.0, 4.5 and 5.0 percent were measured for the US-281-AR mixture, while G_{mm} at 3.0, 3.65, 4.0 and 5.15 percent asphalt contents were measured for the I-35-PG mixture. The average G_{se} for each mixture, calculated from the measured G_{mm} values at these low asphalt contents, allowed for calculation of G_{mm} values at the high asphalt contents used in the mix design. Calculation of G_{se} for the proposed

mix design requires the measured asphalt specific gravity (G_b), asphalt content (P_b), and measured G_{mm}:

$$G_{se} = \frac{100 - P_b}{\frac{100}{G_{mm}} - \frac{P_b}{G_b}} \quad (6)$$

The calculated G_{mm} values for the higher asphalt contents (equal to or greater than 6 percent) were then determined as follows:

$$Calculated\ G_{mm} = \frac{100}{\frac{100 - P_b}{G_{se}} + \frac{P_b}{G_b}} \quad (7)$$

Loose mixture samples used for G_{mm} measurement were oven-cured for 2 hours at the compaction temperature [300°F (149°C)]. Afterwards, the mixtures were spread on a clean, nonabsorbent surface in a single aggregate layer to cool to room temperature. Next, the mixture was separated by hand as much as possible into individual particles to minimize inter-particle entrapment of air. The masses needed to measure G_{mm} were established using a metal vibratory pycnometer. All the samples used for measuring G_{mm} were obtained from small batches with masses between 13.2 lb (6000 g) and 15.4 lb (6500 g). Larger batches with masses between 30.8 lb (14,000 g) and 37.5 lb (17,000 g) were used for producing compacted specimens.

3.1.3. Analysis of X-Ray CT Images

X-ray CT images were scanned and analyzed to determine the AV (total and interconnected) distribution of compacted mixture samples of PFC. This analysis was performed on both laboratory compacted specimens and road cores. The X-ray CT system at Texas A&M University acquired digital images using the mini-focus system, which works with an X-ray source of 350 kV.

Figure 3 shows the X-ray system setup that includes as basic components the X-ray source and the detector, with the test specimen placed in between. After the source transmits X-ray radiation with a certain initial intensity, the attenuated intensity of the X-ray after penetrating through the specimen is registered by the detector. Two dimensional images at each specific vertical position of the specimen are created by rotating the specimen 360° with respect to its center (*15*, *16*). In this study, images with a vertical gap of 1 mm were obtained for all the

specimens. In addition, the pixel size was approximately 0.17 mm. Additional details on the principle of operation of the X-ray CT system and image capturing process can be found in Masad et al., 2004 (*16*).

Figure 3. X-ray CT Setup at Texas A&M University.

The image analysis included two stages. The first stage allowed determinations of AV distribution based on the total AV content established using the dimensional analysis, while the second determined the interconnected AV content and distribution based on the results of the first analysis. The first image analysis was executed applying a macro previously developed (*15*) using Image-Pro® Plus. The macro converts the original images to black and white compositions, where black is assigned to the voids and white represents the aggregates and the mastic. This conversion is executed based on a user-input threshold value between 0 and 56,000. Once the user defines the threshold value, the macro assigns a value of zero when the measured gray intensity is less than the indicated threshold (representing the voids), and a value of 256 if the gray intensity is higher than the threshold (representing the aggregates and the mastic). The final threshold was established by matching the total AV content determined using the dimensional analysis and the average of the total AV content computed for the set of analyzed images.

An initial image analysis performed excluding the surface irregularities resulted in low AV contents compared to those calculated applying the dimensional analysis and even those determined using the vacuum method. Although the threshold was modified to adjust for this

discrepancy, the required threshold modifications led to voids contours that did not properly match the voids geometry obtained in the original images. Therefore, the surface irregularities were included in the analysis, which implies assuming a regular circle as surface contour as is also done in dimensional analysis. Since the vacuum method quantifies volume based on an irregular surface, an equivalent diameter could be established for the image analysis and subsequent threshold determination. However, to allow direct comparisons, the image analysis was performed matching the total AV content obtained by the dimensional analysis.

The total AV content of each image (AV_i) and the total AV content of the specimen (AV_s) were computed as follows using a macro previously developed by Masad et al. (*15*) using Image-Pro® Plus:

$$AV_i = \frac{A_{vi}}{A_T} \tag{8}$$

$$AV_s = \frac{\sum_{i=1}^{n} \%AV_i}{n} \tag{9}$$

where A_{vi} is the area of AV in image i, A_T is the cross-sectional area of the image i, and n is the total number of images. The average AV radius ($\bar{r}_i$) in image i is calculated as:

$$\bar{r}_i = \sqrt{\frac{A_{vi}}{\pi M_i}} \tag{10}$$

where M_i corresponds to the number of AVs in each image.

The second stage of image analysis determines the interconnected AV content and distribution using the threshold images obtained after the first image analysis. These black and white images were converted to binary bit files using a macro developed by Masad et al. (*15*). Then, using a FORTRAN-built algorithm (*15*) the binary files were analyzed to determine the connected paths from top to bottom of the specimen. Bit files containing the interconnected AV constitute the output of the algorithm. These bit files were converted back to images using Image-Pro® Plus, and finally the AV content of this final images set is quantified to establish the interconnected AV content.

3.2. COMPARISON AND VARIABILITY OF THEORETICAL MAXIMUM SPECIFIC GRAVITY OF THE MIXTURE

Figure 4 illustrates the differences in the two methods (direct measurement and calculation) for establishing G_{mm}. The average measured G_{mm} corresponds to the average of two or three tests whose difference between individual values meets the maximum difference (0.011) specified by the American Association of State Highway and Transportation Officials (AASHTO) in T 209-05 (*17*) for two properly conducted tests. The discrepancy between the average measured G_{mm} values and the calculated G_{mm} values near the OAC range is significant and shows a horizontal shift between 0.50 and 1.5 percent of asphalt content lost in the G_{mm} measurement process. At asphalt contents lower than 5 percent, the mixture is drier and less cohesive and results in less asphalt loss during the G_{mm} measurement process.

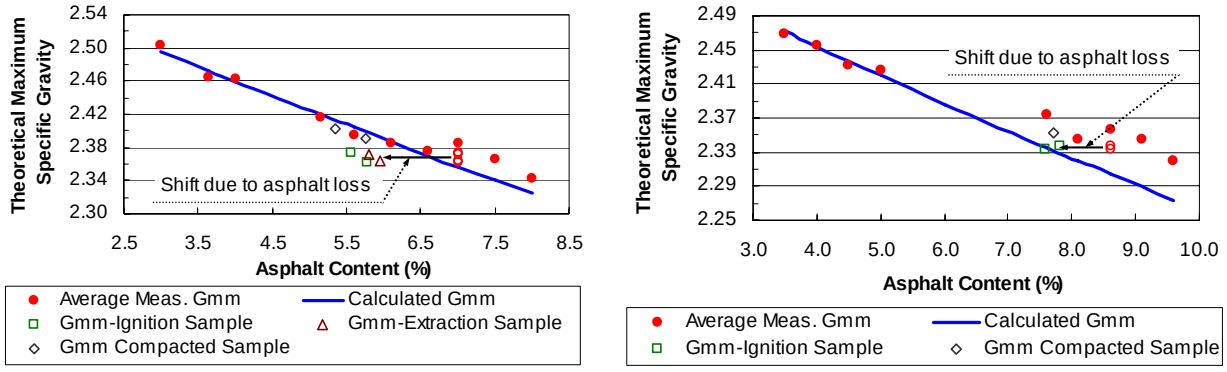

(a) (b)

Figure 4. Theoretical Maximum Specific Gravity (G_{mm}) Comparison for (a) I-35-PG and (b) US-281-AR Mixtures.

To further explore this hypothesis of lost asphalt content, ignition oven (Tex-236-F) (*10*) and extraction (*18*) processes were used to provide alternate measurements of asphalt content on two types of samples: G_{mm} (loose mix) and compacted mixture. Four replicate G_{mm} samples of the I-35-PG mixture produced with a target asphalt content of 7.0 percent were used to establish the final asphalt content after measuring G_{mm}. Two of those samples were subjected to a solvent extraction procedure, and the remaining two samples were evaluated using the ignition oven test. In addition, four replicate G_{mm} samples of the US-281-AR mixture with a target asphalt content of 8.6 percent were also evaluated using the same process. Since the AR extraction procedure

presents difficulties and is still under development, only ignition test data were applied to evaluate the asphalt loss.

The samples of compacted mixture were obtained from two I-35-PG and two US-281-AR compacted specimens randomly selected from different batches prepared with OACs of 6.1 and 8.1 percent, respectively. Smaller samples were split from the compacted specimens. The first split sample was used to determine the asphalt content, while the second sample was utilized to measure G_{mm} and subsequently used to quantify the final asphalt content through the ignition oven test.

The loss magnitudes reported by the ignition oven were adjusted to calculate the final asphalt content reported in Figure 4. AR ash deposited on the oven trays was included in the calculation of AR asphalt content. An additional adjustment was performed to account for partial aggregate ignition. For the I-35-PG mixture, fiber total combustion and partial ignition of aggregate contributed to additional adjustments in the asphalt content determination.

Figure 4 shows the horizontal shifts of measured G_{mm} values from the target binder content due to asphalt losses of 1.2 percentage points on average for G_{mm} samples of the I-35-PG mixture and 0.85 percentage points on average for the same type of samples of the US-281-AR mixture. The shifted measured G_{mm} values are relatively close to the calculated G_{mm} magnitudes. These results provide evidence that the horizontal shift (asphalt loss) accounts for the differences between measured G_{mm} and calculated G_{mm}.

Asphalt content data taken directly from compacted mixtures showed small differences (0.28 and 0.75 percentage points for the I-35-PG mixture and 0.11 and 0.36 percentage points for the US-281-AR mixture) between the target asphalt content and the actual measured asphalt content. These differences show minimal asphalt loss for compacted specimens. Measuring G_{mm} on compacted mixtures resulted in asphalt losses of 0.06 and 0.01 percentage points for the I-35-PG mixture and approximately 0.29 percentage points for the US-281-AR mixture.

Data summarized in Figure 4 also show that the compacted mixture samples require a minimum shift to match the calculated G_{mm} values (which agrees with the minimum loss of asphalt) compared to that encountered for the smaller G_{mm} samples. This is explained by the differences in asphalt content loss between smaller G_{mm} and compacted mixture samples. These differences come from the effect of the batch size (with the compacted mixture batches at least twice as big in weight as the G_{mm} sample batches) that implies less asphalt loss in total

proportion, and from the difference in the degree of mixture handling. The batches used can be representative of the mixture produced for mix design and during field production. Thus, data from this study suggest that both laboratory mix design and field placement density control should be performed using calculated G_{mm} values.

Figure 5 presents G_{mm} values for replicate specimens at different asphalt contents and corresponding standard deviations. Both mixtures exhibit smaller measured G_{mm} variability at low asphalt contents. For the I-35-PG mixture, standard deviations are smaller than 0.0075 at low asphalt contents and as high as 0.012 at high asphalt contents. Likewise, for the US-281-AR mixture standard deviations range between 0.003 and 0.006 at low asphalt contents. Standard deviations were significantly larger, between 0.015 and 0.02, for this mixture at high asphalt contents. These results provide additional rationale for recommending calculation of G_{mm} based on an average G_{se} value evaluated at low asphalt contents.

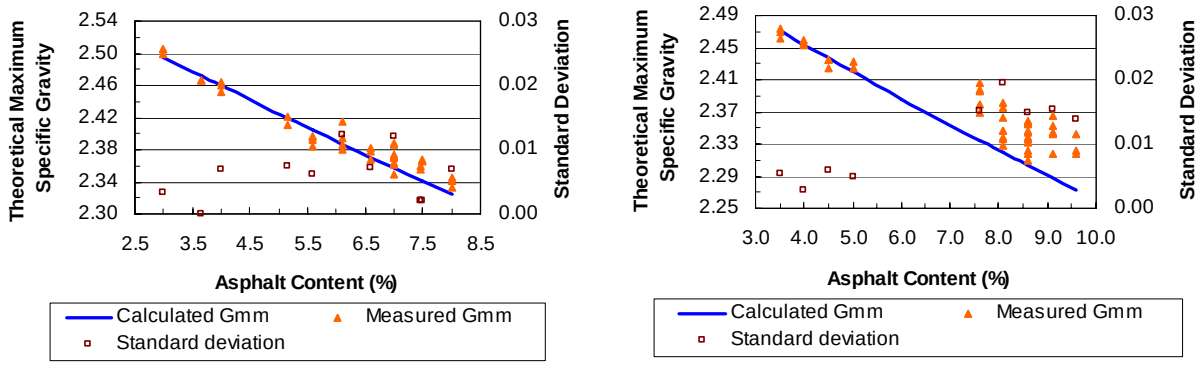

Figure 5. Theoretical Maximum Specific Gravity (G_{mm}) Variability for (a) PG and (b) AR Mixtures.

3.3. TOTAL AIR VOIDS CONTENT

Figure 6 and Figure 7 illustrate the differences in the two G_{mb} methods (vacuum and dimensional analysis) for calculating total AV content. For both mixtures, higher total AV contents resulted from dimensional analysis as compared to those from the vacuum method. A linear fit for both methods is shown in Figure 6. Former research by Watson et al. (*9*) stated a similar relationship between dimensional analysis and the vacuum method. For both mixture

systems, the R^2 value is larger for the total AV determination based on calculated G_{mm} values compared to that obtained from measured G_{mm} values.

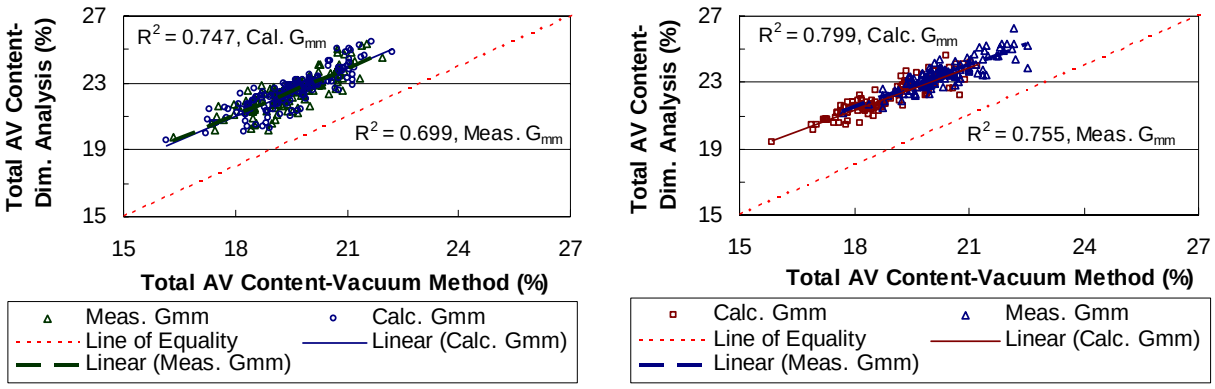

(a) (b)

Figure 6. Comparison of Dimensional and Vacuum Method Total Air Voids Content for (a) I-35-PG and (b) US-281-AR Laboratory Mixtures.

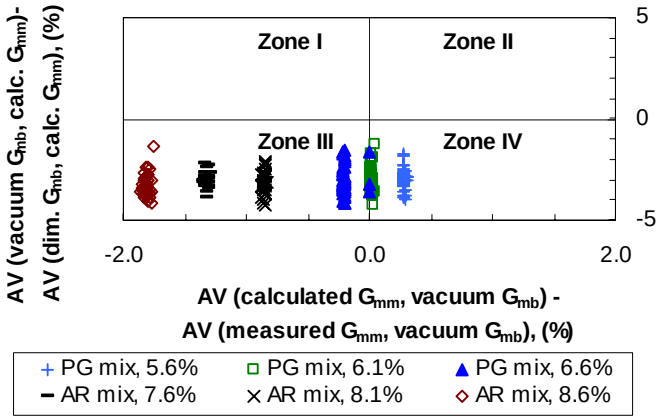

Figure 7. Total Air Voids Content Comparison Based on G_{mb} and G_{mm} Calculations for I-35-PG and US-281-AR Laboratory Mixtures.

Figure 7 defines four zones to distinguish the differences in total AV content when the dimensional and vacuum methods are used to determine G_{mb} and when the AV computation is based on measured and calculated G_{mm} values. Zones III and IV contained all data presented in Figure 7 for different asphalt contents. These results imply that in all cases the total AV contents determined from dimensional analysis are higher than those obtained from the vacuum method, and that in most cases the total AV content obtained from calculated G_{mm} values are less than

those established based on measured G_{mm} values. Figure 4 highlighted these same results where the calculated G_{mm} values were less compared to the measured G_{mm} values thus providing higher densities and therefore lower total AV contents.

When comparing the vacuum and dimensional analysis methods in Figure 7, the difference in total AV content ranges from 1 to 4 percentage points. For plant mixtures and road cores differences between 2.5 and 4.8 percentage points and between 2.6 and 6.7 percentage points, respectively, were found based on data collected in this study. In previous research, Watson et al. (*9*) reported differences of approximately 2 percentage points on specimens prepared in the laboratory. The basic discrepancy between both methods relates to the surface voids. The calculation for dimensional analysis includes all surface voids, whereas the vacuum method partially includes them because the bag partially follows the surface voids with depth once the vacuum sealing process is applied.

When comparing the methods used to determine G_{mm}, Figure 7 shows that for the US-281-AR mixtures evaluated in this study, the total AV contents obtained using the calculated G_{mm} values are 0.8 to 1.8 percentage points lower than those obtained using measured G_{mm} values. For the I-35-PG mixture these differences are lower where higher total AV contents were obtained using calculated G_{mm} values for the lowest asphalt content. However, the variability in measuring G_{mm} provides an explanation for these contrasting results. In general, at asphalt contents higher than 7 percent, the differences in total AV content induced by the G_{mm} methods increase since obtaining accurate G_{mm} measurements becomes more difficult, and the loss of asphalt (horizontal shift in Figure 4) at these high asphalt contents induces higher differences between measured G_{mm} and calculated G_{mm} values.

3.4. ADDITIONAL VARIABILITY IN TOTAL AIR VOIDS CONTENT FOR COMPACTED SPECIMENS

In addition to variability introduced in the determination of G_{mm} and G_{mb} and differences introduced by different determination methods, the compaction process and the handling of hot compacted specimens influence the volumetric properties of laboratory compacted specimens of PFC, probably even more than in dense-graded HMA. Table 4 summarizes the average total AV content and respective standard deviations obtained per batch for two types of specimens compacted in the laboratory to evaluate functionality and durability. Specimens with identical

asphalt contents were produced targeting different total AV contents, which implies different weights of compacted mixture since the number of gyrations in the SGC was fixed at 50 according to the current design specification (*10*). The relationship between the target AV content (or in other words the mixture weight) and the total AV content is not always linear, as the data for an asphalt content of 8.6 percent shows.

Table 4. Variability of Total AV Content for US-281-AR Laboratory Mixture.

Specimen	Asphalt Content, %	Target AV SGC, %	Total No of Specimens	Average of Total AV, %	Stand. Dev. of Total AV
4.5 in. (114 mm)	7.6	18.5	3	18.9	0.57
	7.6	18.5	4	18.4	0.29
	7.6	18.5	4	19.3	0.38
	7.6	19.5	3	21.3	0.57
	7.6	19.5	3	18.7	0.46
	8.1	20.0	3	19.4	0.26
	8.1	20.0	3	18.3	0.27
	8.1	22.0	2	20.0	0.92
	8.1	22.0	4	19.5	0.08
	8.1	22.0	4	19.3	0.51
	8.1	22.0	2	18.3	0.07
	8.1	22.5	3	19.3	1.05
	8.1	22.5	3	19.1	0.06
	8.6	25.0	3	19.6	0.50
	8.6	25.0	4	18.3	0.93
	8.6	25.5	4	19.3	0.95
	8.6	25.5	3	19.3	0.22
	8.6	26.0	3	17.3	0.50
	8.6	26.0	4	18.2	0.53
2.25 in. (57 mm) and 2.4 in. (61 mm)	7.6	21.0	2	23.2	0.07
	7.6	21.0	2	21.7	1.48
	8.1	24.0	2	19.6	0.28
	8.1	24.0	2	21.4	0.07
	8.1	26.0	2	23.2	0.42
	8.1	26.0	2	21.2	0.49
	8.6	21.5	2	20.2	1.48
	8.6	21.5	2	20.0	0.49

Note: 1. The total AV content was computed using calculated G_{mm} and G_{mb} measured by applying the vacuum method; 2. Height tolerances were 4.5 ± 0.2 in. (115 ± 5 mm), 2.4 ± 0.1 in. (62 ± 2 mm), or 2.25 in. (57 mm).

The total AV content of shorter specimens exhibited more variability than those obtained for larger specimens 4.5 in. (115 mm) in height conventionally used for mix design (the coefficients of variation are 0.030 and 0.016, respectively, for the smaller and larger specimens), although the variability is large enough to change the selected OAC based exclusively on total AV content. In addition, the larger variability in the shorter specimens led to greater difficulty fabricating replicates of these shorter specimens compared to the production of larger specimens.

This evaluation provides evidence of an additional source of variability involved in the selection of OAC related to the particular characteristics of PFC mixtures. Although average values of total AV content computed from two replicate specimens compacted at each asphalt content are included for current PFC mix design (*10*) to reduce the random error, additional research may be required to better include this variability source into the mix design procedure.

3.5. EFFECTS ON OPTIMUM ASPHALT CONTENT (OAC) SELECTION

Based on the results in Figure 7, the use of measured G_{mm} values and the vacuum method to determine G_{mb} values may result in substantial changes in OAC and/or in a significant portion of specimens fabricated being rejected for subsequent mixture testing due to total AV contents outside the specification (18-22 percent). This conclusion depends on the assumption that the calculated G_{mm} values and the dimensional analysis method provide the best methods to determine total AV contents in PFC.

Figure 8 shows the impact of the method used to determine G_{mm} and G_{mb} on the OAC calculation for both I-35-PG and US-281-AR mixtures when a design total AV content of 20 percent is used. Actual mix design data required for evaluating the relationships between measured G_{mm}, calculated G_{mm}, and G_{mb} established using both dimensional analysis and the vacuum method were not available for these mixtures. Therefore, Figure 8 provides only an indication of the possible effect on OAC based on actual design data (measured G_{mm} and G_{mb} using the vacuum method for the I-35-PG mixture and measured G_{mm} and G_{mb} by dimensional analysis for the US-281-AR mixture) and the average AV differences calculated based on the data set presented in Figure 6 and Figure 7.

The impact of the G_{mb} method in both mixtures is significant. In fact, when the G_{mb} method is changed (with respect to that used for the mix design), the OAC becomes undefined for both mixtures since the total AV content is higher than 22 percent or less than 18 percent, which implies the necessity of gradation modifications or changing fiber content to meet AV requirements.

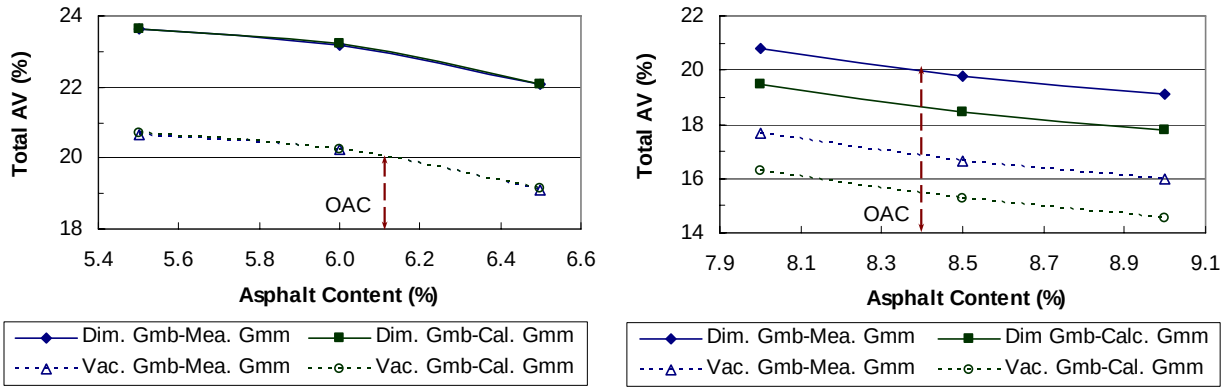

(a) (b)

Figure 8. Impact of Volumetric Parameters on Optimum Asphalt Content Selected at 20 Percent Total Air Voids Content for (a) I-35-PG and (b) US-281-AR Laboratory Mixtures.

The procedure used to determine G_{mm} has more of an impact on the AR mixture as compared to the PG mixture. In fact, no modification is indicated on the OAC established in the original design for the I-35-PG mixture. Conversely, the use of calculated G_{mm} values for the US-281-AR mixture leads to total AV contents that do not allow defining an OAC at a total AV content of 20 percent. Since the minimum asphalt content specified for AR mixtures is eight percent, these results imply the necessity of modifying the aggregate gradation to meet the AV requirement. This analysis does not account for the variability in total AV content associated with determinations on replicate specimens.

3.6. WATER ACCESSIBLE AIR VOIDS CONTENT

Data presented in Figure 9 suggest the existence of a linear relationship between the water accessible AV content (computed by applying the vacuum method) and total AV content (determined using the vacuum method for G_{mb} and calculated G_{mm} values). Corresponding ratios of water accessible AV content to total AV content are above 100 percent for a significant subset of these data. This can be partially explained by the fact that the total AV content of all LMLC specimens fabricated at a specific asphalt content were calculated using constant G_{mm} magnitudes that correspond to those shown in Figure 4. These constant magnitudes were adopted because of the large number of batches needed to fabricate the required number of specimens that made it impractical to measure G_{mm} for each batch. In other words, the variability of G_{mm}

measurements at both low and high asphalt contents will induce some variability in total AV content calculations.

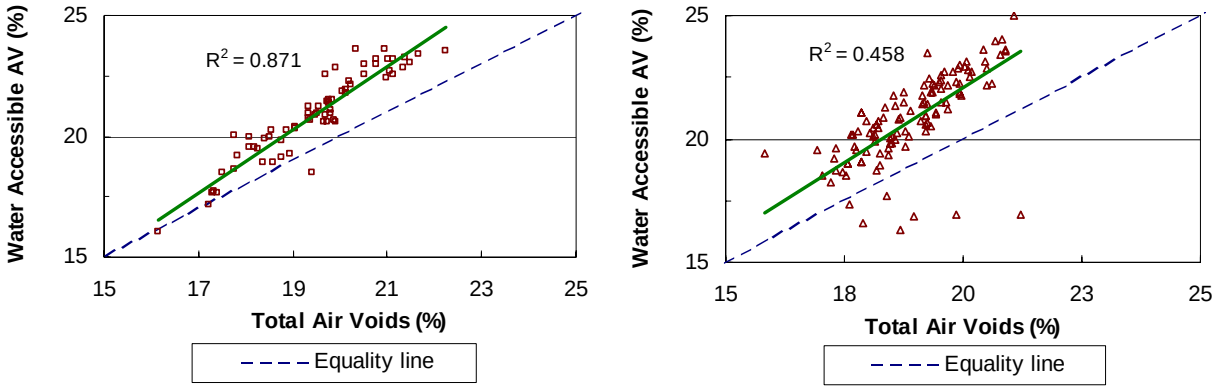

(a) (b)

Figure 9. Comparison of Water Accessible and Total Air Voids Content for (a) I-35-PG and (b) US-281-AR Laboratory Mixtures.

Since the variability of G_{mm} determinations at low asphalt contents is smaller than that obtained at the OAC, higher reliability is expected from the void ratios obtained from calculated G_{mm} values. Moreover, the large water accessible AV contents obtained using the vacuum method may be related to micro-damage induced in the specimen when it is subjected to a vacuum during the testing process. Previous research (*15*) suggested this as a possibility during vacuum saturation of dense-graded mixture specimens.

In addition, a correction for the water accessible AV calculations of the laboratory mixtures was required to discount the weight of the bag from the saturated weight since the bag was kept in the water during the measurement of that weight. The correction factor (bag specific gravity) provided by the manufacturer was used to perform that correction. However, direct measurements executed to compare the saturated weight obtained with and without bag and the calculated saturated weight obtained after discounting the weight of the bag did not lead to consistent results. This fact shows inaccuracies in the bag specific gravity values, which constituted an additional factor contributing to generate unusual high AV ratios (over 100 percent) for the laboratory mixture specimens.

Figure 10 shows the relation of water accessible and total AV content for both types of plant mixtures (AR and PG) and both G_{mb} determination methods (vacuum and dimensional

analysis.) This data set provided more consistent evaluations for water accessible AV magnitudes and their relation to total AV, leading to ratios of water accessible to total AV smaller than 100 percent as presented in Figure 11a. In addition, Figure 11b illustrates the same ratio for road cores of both mixture systems (AR and PG).

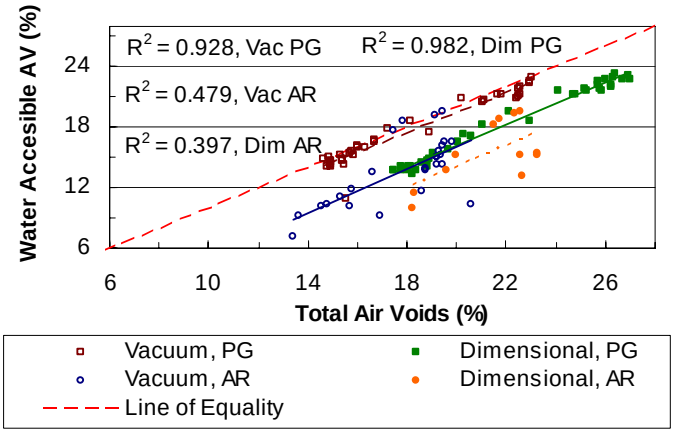

Figure 10. Comparison of Water Accessible Air Voids Content and Total Air Voids Content for Plant Mixtures.

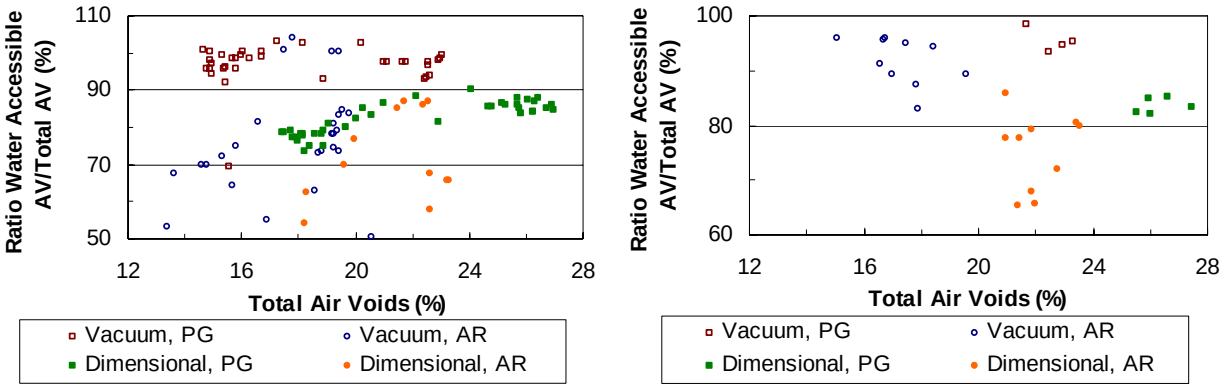

(a) (b)

Figure 11. Ratio of Water Accessible Air Voids Content to Total Air Voids Content for (a) Plant Mixtures and (b) Road Cores.

AV (water accessible and total) contents evaluated on PMLC specimens by applying both methods (dimensional analysis and the vacuum method) also showed a linear relationship (Figure 12). As reported for LMLC specimens in Figure 6, total AV contents obtained from

dimensional analysis are higher than those computed from dimensional analysis for PMLC specimens. However, the water accessible AV contents were closer to the equality line. The water accessible AV content and the total AV content evaluated on road cores by using either dimensional analysis or the vacuum method showed preliminary evidence of a linear relationship.

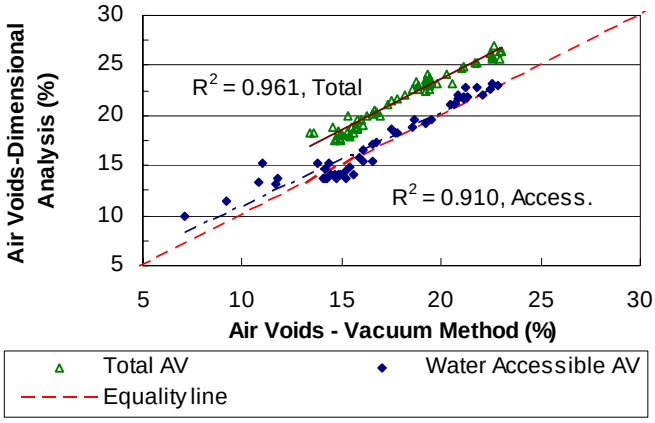

Figure 12. Comparison of Air Voids Content Measured Using the Vacuum Method and Dimensional Analysis for Plant Mixtures.

Based on the evaluation of laboratory and plant mixtures and road cores, the following aspects can be highlighted:

- A linear relationship can be established between the water accessible and the total AV contents. This relationship was defined using both the dimensional analysis and the vacuum method and it is better defined for PG mixtures than for AR mixtures.
- Most of the AV present in the mixture are water accessible. The dimensional analysis ratios of water accessible AV to total AV were between 70 and 90 percent for most of the plant mixtures specimens and road cores, while ratios between 80 and 100 percent were found using the vacuum method.
- In general, for both plant mixtures and road cores, higher water accessible AV to total AV ratios were obtained for PG mixtures compared to those obtained for AR mixtures.
- Approximately equal water accessible AV content values were reported from dimensional analysis compared to those calculated using the vacuum method for PMLC specimens, but for road cores the water accessible AV content values computed using dimensional analysis were

in some cases higher than those calculated based on the vacuum method. These differences are related to the smaller hydrostatic saturated mass and the higher total volume obtained by dimensional analysis (since no vacuum is applied).

- Smaller differences between the dimensional analysis and the vacuum method were obtained in terms of water accessible AV than those established using total AV.

3.7. TOTAL AND INTERCONNECTED AIR VOIDS BASED ON ANALYSIS OF X-RAY CT IMAGES

Figure 13 shows one gray scale image and the outputs obtained after processing it. The first output corresponds to the black and white image obtained after applying the threshold required to reproduce the total AV content computed with dimensional analysis, and the second output corresponds to the black and white image obtained after the analysis of interconnected AV performed as described in Section 3.1.3. This last analysis was conducted without including the voids in contact with the surface.

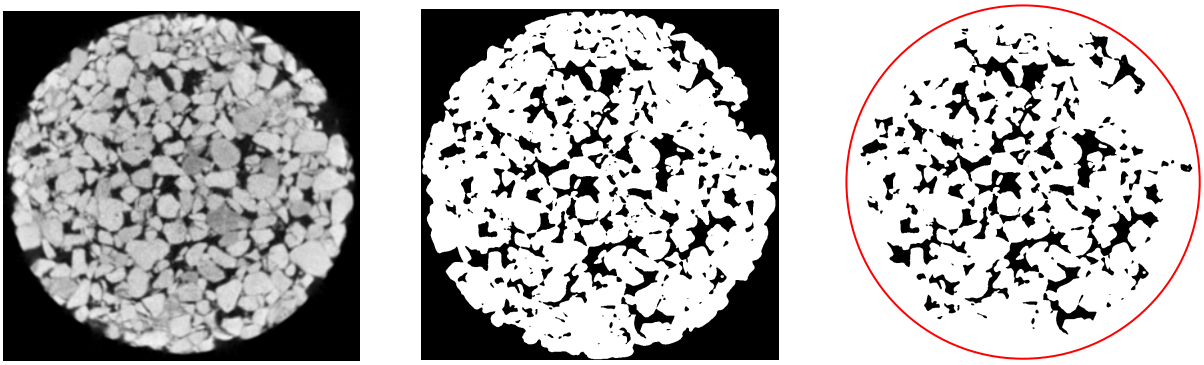

(a) (b) (c)

Figure 13. X-ray CT Image Analysis (a) Original Grayscale Image, (b) Black and White Image after Threshold and (c) Black and White Image after Interconnected AV Analysis.

The comparison of the total and water accessible AV calculated based on both the vacuum method and dimensional analysis and the interconnected AV content calculated based on the analysis of X-ray CT images for the main mixtures (I-35-PG, US-59Y-PG, US-281-AR, and US-290-AR) used to study the volumetric properties is presented in Table 5. This comparison reveals that for most of the specimens interconnected AV values were smaller compared to the water accessible AV values. Two aspects can account for this discrepancy: (1) while the water

accessible AV computation includes the AV that are accessible from all surfaces of the cylindrical specimen, the interconnected AV are computed including only the voids connected from the top to the bottom surface, and (2) the computation of interconnected AV may be underestimated because the voids connected to the surface were not included in the image analysis.

Table 5. Comparison of Total, Water Accessible, and Interconnected Air Voids for PMLC Specimens.

Mix	Specimen	Vacuum, Total AV (%)	Vacuum, Accessible AV (%)	Dimensional Total AV (%)	Dimensional Accessible AV (%)	Total AV (X-Ray CT) (%)	Interconnected AV (X-Ray CT) (%)
I-35-PG	I35-C1D1	15.7	15.4	18.9	14.9	19.0	13.1
	I35-C2D1	16.0	16.1	19.1	15.5	19.0	14.2
US-59Y-PG	59Y-50C1D1	15.0	14.1	18.0	13.7	15.9	10.3
	59Y-50C2D1	15.8	15.2	18.6	14.5	17.1	11.1
	59Y-15C1D1	23.1	22.9	26.3	22.9	26.5	17.3
	59Y-15C2D1	22.6	22.0	25.7	22.1	25.7	16.8
US-281-AR	281-C1D1	17.5	17.6	21.5	18.3	21.5	15.0
	281-C2D1	17.8	18.5	21.7	18.9	21.8	15.2
US-290-AR	290-50C2D1	15.8	11.8	19.6	13.7	20.1	15.1
	290-50C1D2	15.3	11.0	20.0	15.3	19.4	15.1
	290-12C1D2	19.8	16.5	23.3	15.3	23.0	18.1
	290-12C1D1	19.4	14.2	23.0		23.3	17.1

Figure 14 and Figure 15 show the distribution of total and interconnected AV for PMLC specimens of the US-59Y-PG and US-290-AR mixtures, respectively. The PMLC specimens correspond to two replicates compacted at 50 gyrations of the SGC and two replicates compacted by applying 10 and 12 gyrations to reproduce the average total AV content computed using dimensional analysis for corresponding road cores. The PMLC specimens compacted by applying different energies and the replicates compacted by applying the same energy consistently showed higher AV contents at the top and bottom portions, with a characteristic AV distribution resembling a “C” shape, that can be related to the restriction imposed by the top and bottom surfaces of the SGC during compaction. Substantial differences (i.e., up to 12 percentage points) between the central and the top and bottom portions of this kind of specimens were observed for both total and interconnected AV. This heterogeneous AV distribution may affect

durability and functionality evaluations (including both drainability and noise reduction capacity characteristics) performed on PFC specimens compacted using the SGC.

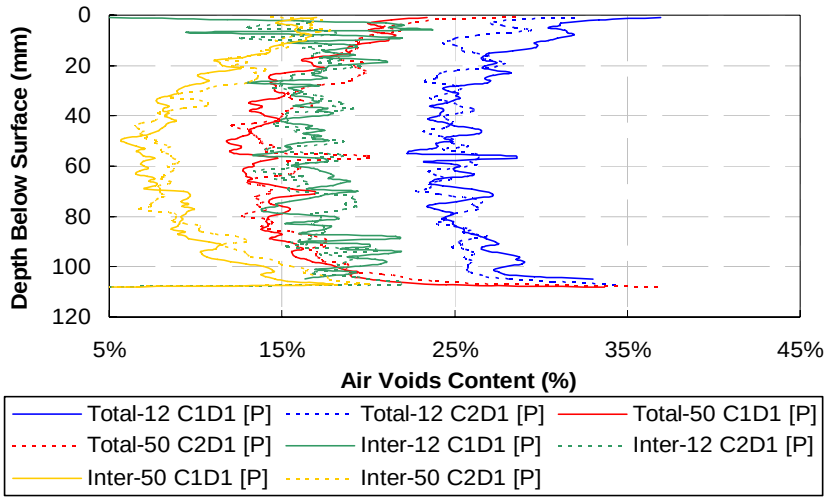

Figure 14. Total and Interconnected Air Voids Distribution for PMLC Specimens and Road Cores of the US-59Y-PG Mixture.

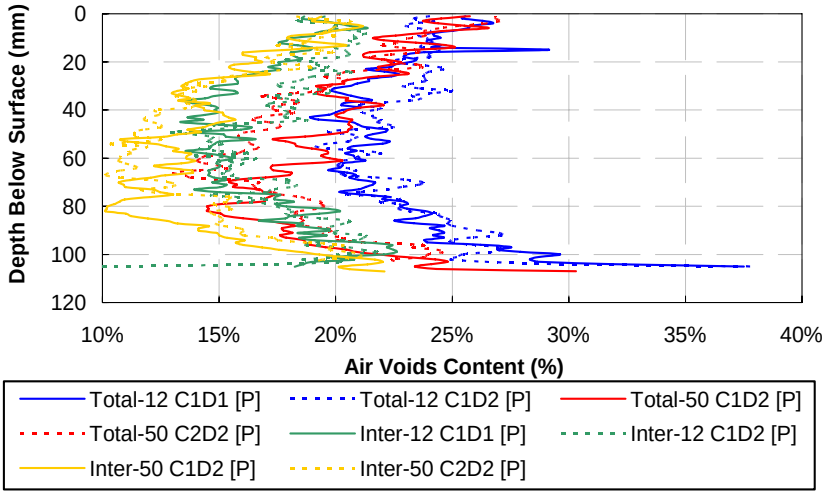

Figure 15. Total and Interconnected Air Voids Distribution for PMLC Specimens of the US-290-AR Mixture.

Figure 16 shows the distribution of total and interconnected AV for the road cores of both the US-59Y-PG and US-290-AR mixtures. The approximate offset formed by the total and the interconnected AV distributions for both the PMLC specimens and the road cores shown in

Figure 14 to Figure 16 suggest that these parameters are directly proportional. On the other hand, the AV distributions shown in Figure 16 suggest that the field compaction process generates a decreasing AV content with the maximum AV content at the pavement surface. The comparison shown in Figure 17 for road cores and PMLC specimens compacted at small energies indicates that the distribution and total AV content of road cores are approximately reproduced at the top an bottom portions of the SGC compacted specimens, but there is not adequate coincidence at the central third of these specimens, which can limit functionality and durability evaluation conducted using these compacted specimens.

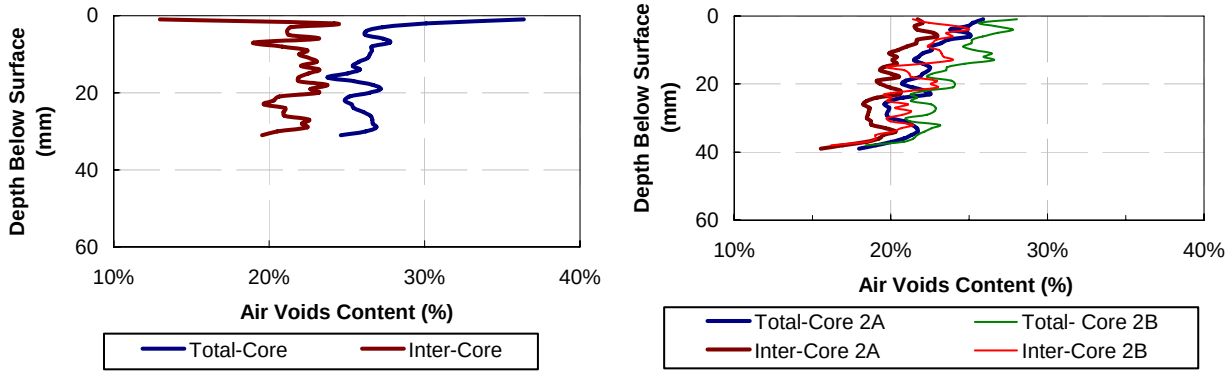

(a) (b)

Figure 16. Total and Interconnected Air Voids Distribution for Road Cores of the (a) US-59Y-PG and (b) US-290-AR Mixture.

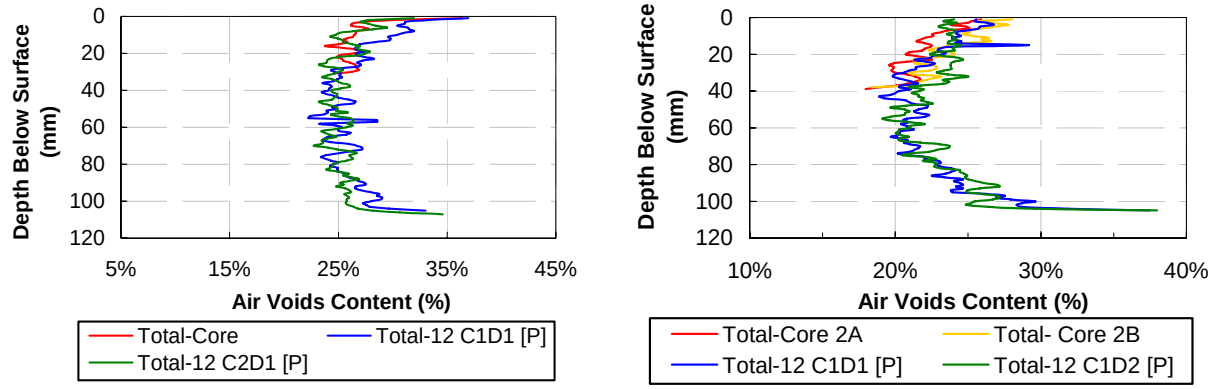

(a) (b)

Figure 17. Comparison of Air Voids Distributions for PMLC Specimens and Road Cores of the (a) US-59Y-PG and (b) US -290-AR Mixtures.

3.8. COMPACTION EFFECTS

One mixture fabricated with each binder system (PG and AR) was evaluated in both field and laboratory conditions to assess the impact of the compaction energy on AV content, functionality, and durability of PFC mixtures. This section discusses the methodology applied and results obtained for AV content, and those corresponding to functionality and durability are included in Chapters 4 and 5.

An initial comparison of AV content between mixtures placed in the field (based on the evaluation of road cores) and PMLC specimens provided evidence that in general, higher AV were obtained in the field compared to those computed for specimens compacted in the laboratory (Figure 18). While most of the AV contents of the PMLC specimens are between the AV design range (18 to 22 percent), the AV for road cores in general were higher than 25 percent. Minimizing these AV differences would provide higher reliability in terms of the expected performance of the mixture in the field, since not only the selection of the OAC is based on the total AV content, but also the functionality and the durability of the mixture depend on the AV content as will be discussed subsequently in Chapters 4 and 5.

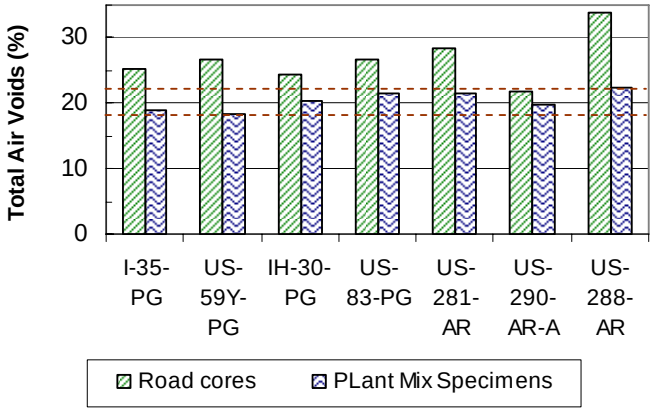

Figure 18. Comparison of Air Voids Content of Plant Mix Specimens and Road Cores.

To further explore the effect of compaction on PFC mixtures, PMLC specimens of US-290-AR and US-59Y-PG mixtures were produced in two groups differentiated by the energy applied by the SGC during compaction. The first group was compacted using 50 gyrations as currently required by the TxDOT design procedure (*10*), whereas the number of gyrations

required to obtain the same AV content established for the road cores was applied to the second group of specimens. For both US-290-AR and US-59Y-PG plant mixes, the energy required to reproduce the field total AV content corresponded to 12 to 15 gyrations, but most of the specimens were compacted applying 15 gyrations. According to the criterion suggested by NCAT (7), specimens compacted at 15 gyrations achieved stone on stone contact. At this number of gyrations, at least 70% of the total reduction in high generated during compaction was obtained. The volumetric characteristics of both sets of specimens were then determined and reported in Figure 19. These specimens were subsequently used to perform durability and functionality tests as described in Chapters 4 and 5.

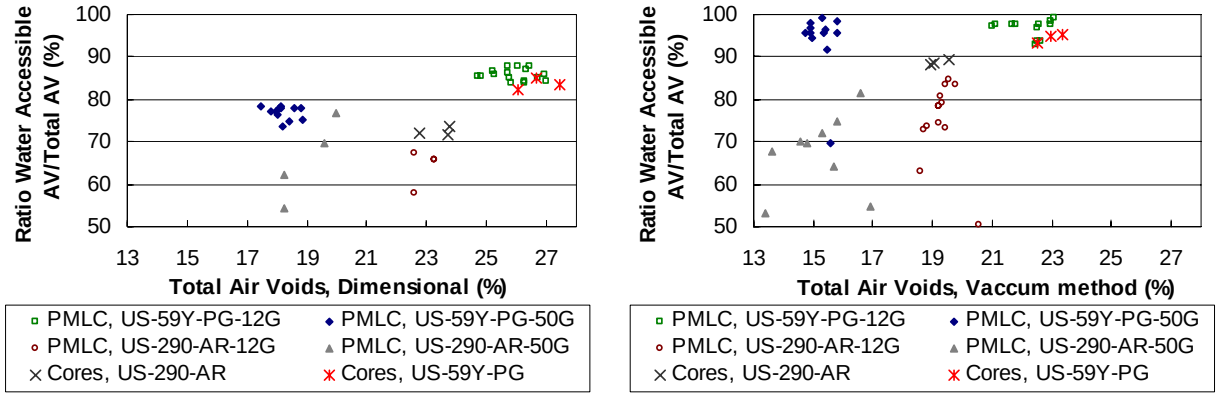

(a) (b)

Figure 19. Compaction Energy Effect on Air Voids Content Evaluated Using (a) Dimensional Analysis and (b) Vacuum Method.

Reducing the energy of compaction to 15 gyrations of the SGC induced a substantial change in the AV content, and modifications can also be expected in the internal structure of these mixtures. For the US-59Y-PG mixture both the total AV content and the ratio of water accessible to total AV obtained in the field were reproduced in the laboratory by decreasing the compaction energy, which may indicate that equivalent internal voids structures were obtained by both the field and the laboratory compaction processes. However, for the US-290-AR mixture, the total AV content was reproduced using 15 gyrations of the SGC, but smaller ratios of water accessible to total AV were obtained for the PMLC specimens, indicating some discrepancies in the internal structures of the laboratory and field compacted mixtures. While the application of 50 gyrations led to the reduction of total AV compared to those specimens

obtained with 15 gyrations, the ratio of water accessible to total AV showed approximately a constant magnitude for both compaction energies.

3.9. GRADATION EFFECTS

Materials used to conduct the volumetric evaluation of finer PFC mixtures are presented in Table 6. Both 6F and 9F mixtures were fabricated using the same aggregate and asphalt used in the I-35-PG mixture to facilitate the comparison of results with a mixture previously characterized in the laboratory. Figure 20 shows the gradations of these mixtures. Researchers selected these gradations to evaluate the feasibility of including finer materials in PFC mixtures.

Table 6. Fine PFC Mixtures.

Mixture	Asphalt Type	Asphalt Content (%)	Aggregate Type and Proportions	Other Materials
6F	PG 76-22S	6.0	Sandstone (49.5%) Limestone (49.5%)	Lime (1%) Fibers (0.3%)
9F	PG 76-22S	6.5	Sandstone (49.5%) Limestone (49.5%)	Lime (1%) Fibers (0.3%)

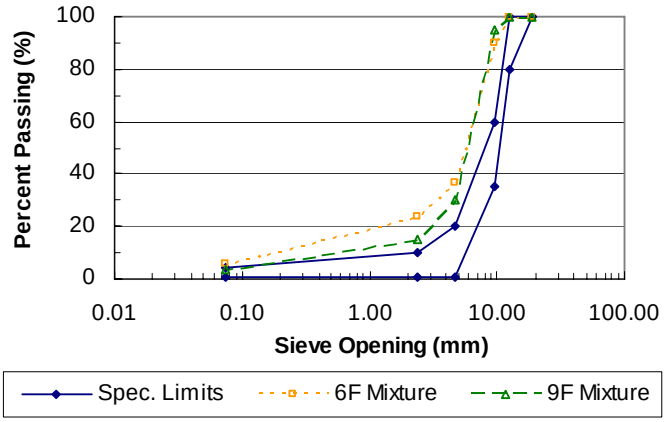

Figure 20. Gradations of Fine PFC Mixtures.

Results of total and water accessible AV of compacted specimens are presented in Table 7. The weight of these specimens was calculated to obtain total AV contents (after compaction) in the range of 20 to 22 percent using dimensional analysis. Results presented in Table 7 provide evidence on the impact of these gradation modifications since the AV contents were less than 50 percent of the target AV contents. Given these low AV contents, no additional functionality or

durability tests were conducted to further evaluate these mixtures. Additional modifications may be evaluated in future research based on the 9F mixture gradation to reduce both sand and filler contents to increase the AV content.

Table 7. Average Air Voids Contents for Fine Mixture Specimens.

Mixture	Total AV, Vacuum	Water Accessible AV, Vacuum	Total AV, Dimensional	Water Accessible AV, Dimensional
6F	5.1	2.3	7.0	3.5
9F	10.3	9.9	13.2	9.2

3.10. SUMMARY AND RECOMMENDATIONS

Based on the results and discussion presented, the following conclusions are offered:

- The laboratory measurement of G_{mm} at the asphalt content design range for use in the mix design may produce an asphalt content that is not optimum. The procedure explained in this chapter to calculate the G_{mm} values at the asphalt content design range based upon G_{mm} measurements for samples produced at lower asphalt contents (i.e., 3.5 to 4.5 percent) was shown to be more reliable for PFC mix design. The magnitude of the discrepancies between measured G_{mm} and calculated G_{mm} values at the asphalt content design range may lead to significant differences in the total AV content and thus the selected OAC.
- The methodology for calculating G_{mm} has several advantages: the variability of G_{mm} from replicate samples is reduced, producing and handling mixtures in the laboratory is straightforward, and most importantly, there is less asphalt loss and the results are more accurate. Therefore, calculating G_{mm} provides more insight into the mixture structure in terms of total AV content calculations for mix design and volumetric evaluation purposes in both the laboratory and the field.
- The selection of the method used for measuring G_{mb} (comparing dimensional analysis and the vacuum method) impacts not only the OAC selection, but in many cases also the design of the mixture aggregate gradation and the fibers content, since the total AV content differences obtained using these methods may be as high as 5 percentage points. Additional variability of

total AV content obtained in replicate compacted specimens used for mix design may also influence the selection of the OAC.

- The main difference between dimensional analysis and the vacuum method for calculating G_{mb} corresponds to the selection of the reference surface to quantify the surface voids. While the dimensional analysis includes all of the surface voids (i.e., the specimen is assumed as a regular cylinder), in the vacuum method the shape of the bag surrounding the specimen dictates the volume of surface voids that are included. Thus, a high stiffness bag will lead to volume determinations from the vacuum method similar to those computed using the dimensional analysis. On the other hand, the main difference between dimensional analysis and vacuum method for calculating water accessible AV corresponds to the application of vacuum (no vacuum is applied in dimensional analysis as proposed) and subsequent measurement of the specimen saturated weight.
- Dimensional analysis performed as described in this chapter to determine both total and water accessible AV (compared to the vacuum method) is simpler, faster, and less expensive. The required equipment is readily available, and additional testing supplies are not needed. Environmental disposal of the vacuum bags is also not required. In addition, data obtained by dimensional analysis (i.e., total AV content) can be directly used as input to analyze computerized images from X-ray CT scanning to perform advanced durability and functionality analyses. These reasons support the selection of the dimensional analysis over the vacuum method to measure G_{mb} in PFC mixtures. No data are available to statistically compare the variability of computations based on these methods. Therefore, this variability was not included in this analysis.
- The water accessible AV evaluation performed using both the vacuum method and a methodology proposed for dimensional analysis showed that most of the AV present in the mixture are water accessible and that a linear relationship can be established between the water accessible and the total AV contents. Approximately equal water accessible AV content values were reported from dimensional analysis compared to those calculated using the vacuum method. In addition, for both plant mixtures and road cores, higher water accessible AV to total AV ratios were obtained for PG mixtures compared to those obtained for AR mixtures. Additional research is required to evaluate the most appropriate method to quantify the saturated mass of the specimens used to compute water accessible AV.

- Volumetric parameter determination influences OAC selection, fibers content, and the design of mixture aggregate gradation. These changes directly affect both mixture functionality (permeability and noise reduction capacity) and durability. Therefore, mix design should also require a durability evaluation.
- Important differences in total AV contents for specimens compacted in the laboratory (PMLC) and in the field (road cores) were determined. Minimizing these AV differences would provide higher reliability in terms of the expected performance of the mixture in the field, since not only the selection of the OAC is based on the total AV content, but also the functionality and the durability of the mixture depend on the AV content as subsequently discussed in Chapters 4 and 5. Since the current design practice for selecting the OAC is based only on volumetric mixture properties, field reproduction of densities should be required as a minimum parameter of quality control related to mixture compaction. On the contrary, current practice in most agencies does not include field density as a mixture placement requirement for PFC and similar mixtures.
- Future research can define alternative gradation(s) for PFC mixtures allowing the use of finer granular materials while retaining high AV contents. The inclusion of higher proportions of filler and better filler combinations should also constitute an important aspect for future research.

The following recommendations are provided based on the conclusions and analysis developed from data gathered during this study:

- Utilize dimensional analysis for determining both G_{mb} (total AV) and water accessible AV of PFC mixtures.
- Measure G_{mm} at two low asphalt contents (i.e., 3.5 and 4.5 percent are suggested) to determine the average G_{se} of the aggregate, then calculate G_{mm} at the actual asphalt content at the design range for establishing total AV content.
- Include durability mixture testing in PFC mix design in addition to volumetric criteria.
- Specify density requirements for field compaction activities.

4. FUNCTIONALITY

PFC functionality includes both permeability and noise reduction capacity, which are related among other variables to AV characteristics. Unfortunately, the AV content decreases during service as a consequence of clogging. Therefore, in the absence of cleaning activities, the initial permeability, and so the initial capacity to reduce hydroplaning and splash and spray, and noise reduction capacity are expected to decrease such that at the end of the functional life (when the functional characteristics are lost) PFC behaves as a dense-graded HMA.

Determination of the drainability of PFC in the laboratory and in the field is useful not only to provide high initial drainability but also to evaluate mixture field performance by comparing the evolution of this parameter during the functional life. This chapter describes results from laboratory permeability tests and field water flow tests conducted to characterize PFC drainability in the laboratory and in the field, respectively, the relationship of the parameters obtained, and the best way for incorporating drainability evaluations for PFC mix design and construction. The drainability tests conducted are related to the AV evaluated through the vacuum method, dimensional analysis, and analysis of images obtained from X-ray CT scans.

4.1. EXPERIMENTAL DESIGN

Permeability tests were conducted in the laboratory in accordance with American Standard of Testing and Materials (ASTM) PS 129-01 (*19*). This test was also suggested by NCAT to evaluate permeability of OGFC as an optional parameter to determine during the mix design process (*7*). The permeability test is performed on a vacuum saturated sample using a falling head permeameter with a flexible wall to establish the water permeability based on the application of Darcy's law. For that purpose, the elapsed time t (registered in seconds) required to reach a defined change in head across the specimen is recorded and the corrected coefficient of water permeability at 20°C (68°F), k_{20} (cm/s), is calculated as:

$$k_{20} = \frac{al}{At} \ln\left(\frac{h_1}{h_2}\right) R_T \tag{11}$$

where a is the cross section of test tube (cm^2); l corresponds to the specimen thickness (cm); A is the cross section of specimen (cm^2); h_1 is the initial head (cm); and h_2 is the final head (cm), and

R_T is the correction factor to adjust for changes in water viscosity at temperatures different than 20°C (68°F). For each sample, at least eight measurements of elapsed time were performed in each test to guarantee saturation, and the final time measured was used in the computation of the water coefficient of permeability (*19*).

Both laboratory compacted specimens and field road cores were tested for permeability after determining their volumetric properties and X-ray CT scanning. Since the water accessible AV determinations were proposed at an intermediate stage of the project, water accessible AV determinations using dimensional analysis are not available for the entire set of specimens and road cores used for permeability evaluation. Therefore, some subsequent analyses are performed using water accessible AV measured using either dimensional analysis or the vacuum method to try to get the maximum benefit from the collected data.

Permeability tests were executed once on two compacted specimens of each plant mixture and in all the road cores extracted from the field sections, with a minimum of three road cores per field section. This approach was used given the higher variability in the AV content of road cores compared to that of the laboratory compacted specimens. In addition, the permeability of the I-35-PG and US-281-AR laboratory mixtures was determined once on three replicate specimens for each asphalt content (i.e., 5.6, 6.1, and 6.6 percent and 7.6, 8.1 and 8.6 percent, respectively) used to fabricate these mixtures. The permeability values reported in subsequent sections correspond to the individual values established per specimen.

Preparation of the road cores for testing included subjecting them to low temperature (40°F [4.4°C]) for a minimum period of 24 hours and then saw cutting to separate the PFC layer from the entire HMA core. This methodology minimized any closure of AV during the sawing process, which was especially critical for AR mixture road cores. Although maximum care was taken in this process, partial sealing of AV was observed at the bottom of some AR and PG mixture road cores that may affect permeability results. AV closure was not encountered with PMLC and LMLC specimens, which could occur as a consequence of draindown in these specimens.

Field evaluations of drainability were conducted according to the Tex-246-F (*10*) procedure. The test evaluates the time required to discharge a given volume of water channeled into the pavement surface with the use of a variable charge outflow meter 6 in. (152 mm) in diameter. This time corresponds to the water flow value (WFV), expressed in seconds. Although

the WFV is not a coefficient of permeability, this time of discharge is a useful parameter to compare the drainage performance of different mixtures or that of a specific mixture in different compaction conditions, stages, or project locations. Table 8 indicates the mixture, highway project, and location where WFVs were measured. In addition, repeated determinations of WFV were performed for the US-290-AR mixture to evaluate the effect of repeated flow (i.e., possible saturation effect) on the WFV.

Table 8. Locations and Mixtures Selected for Evaluations of Water Flow Value.

Mixture	Highway	Location
I-35-PG	IH 35	San Antonio, Tx
US-59Y-PG	US 59	Yoakum, Tx
IH-30-PG	IH 30	Paris, Tx
US-59-PG	US 59	Lufkin, Tx
H-6-PG-TR	SH 6	Hempstead, Tx
I-35-AR	I 35	San Antonio, Tx
US-281- AR	US 281	San Antonio, Tx
US-290-AR	US 290	Paige, Tx
US-288-AR	US 288	Houston, Tx

Drainability was evaluated with a field and laboratory assessment of the compaction energy effect on the US-290-AR and US-59Y-PG mixtures. First, the effect of the total number of static roller passes (including the passes made by the finish roller) on the WFV was established in the field for these mixtures. Then, road cores were taken at the same locations (compacted with four and six passes) where the WFV was evaluated for the US-290-AR mixture, and at the location (compacted with three passes) where the WFV was measured for US-59Y-PG mixture. The laboratory evaluation included permeability measurements on PMLC specimens and the extracted road cores. PMLC specimens of 4.5 ± 0.2 in. (115 ± 5 mm) in height were compacted by applying two different energies with the SGC. The first set of PMLC specimens were compacted applying the number of gyrations required to reproduce the AV content computed for the road cores extracted at locations compacted with four and three passes for US-290-AR and US-59Y-PG mixtures, respectively. The second set was compacted applying 50 gyrations as specified in the current design procedure (*10*).

Two LMLC specimens of each asphalt content (i.e., 5.6, 6.1, and 6.6 percent for the I-35-PG mixture and 7.6, 8.1, and 8.6 percent for the US-281-AR mixture) used to evaluate the laboratory mixtures and two road cores at each location evaluated were cored to 4 in. to prepare them for noise measurements. These measurements were conducted at the University of Texas under TxDOT Project 0-5185 "Noise Level Adjustments for Highway Pavements in TxDOT." Respective results will be included in the reports produced from TxDOT Project 0-5185.

4.2. EVALUATION OF LABORATORY CHARACTERIZATION OF DRAINABILITY

The relationship of water permeability and AV established for PMLC specimens is shown in Figure 21 with the respective linear fits for each data set. Table 9 presents the coefficients of correlation between water permeability values and total and water accessible AV calculated using both the vacuum method and dimensional analysis. The differences between the permeability values of both PG and AR mixtures and the comparison of the coefficients of correlation obtained when the data for each mixture are analyzed independently and when they are combined shows the importance of independently analyzing the data for each type of mixture.

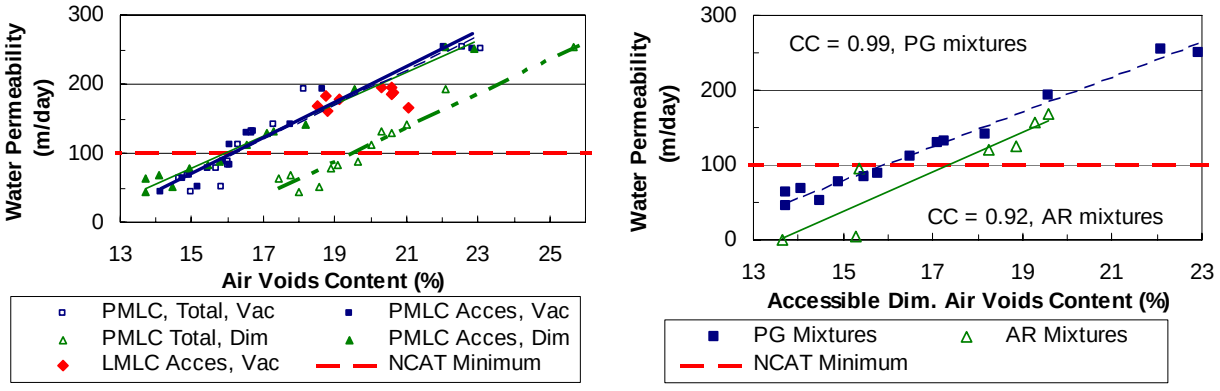

(a) (b)

Figure 21. Comparison of Air Voids Content and Water Permeability for (a) PG Plant Mixtures and (b) PG and AR Plant Mixtures.

Table 9. Coefficients of Correlation for Air Voids Content and Permeability.

Data Set	Total AV, Vacuum	Water Accessible AV, Vacuum	Total AV, Dimensional	Water Accessible AV, Dimensional
AR and PG plant mixtures (combined data)-PMLC	0.77	0.97	0.74	0.94
PG plant mixtures-PMLC	0.95	0.98	0.98	0.99
AR plant mixtures-PMLC	0.65	0.99	0.59	0.92
I-35-PG laboratory mixture-LMLC	0.41	0.45	0.53	-
US-281-AR laboratory mixture-LMLC	0.59	0.83	0.26	-
PG road cores	-	-	-0.36	-
AR road cores	0.52	0.33	0.90	-

This fact corroborates the importance of analyzing the mixtures produced with each type of asphalt (i.e., PG and AR) as a system with different properties. In addition, the coefficients of correlation presented in Table 9 for laboratory compacted specimens (i.e., PMLC and LMLC) suggest that for these type of specimens the water accessible AV are better related to the water permeability compared to the total AV. Comparable coefficients of correlation were established for both dimensional analysis and the vacuum method, which provides additional rationale to recommend dimensional analysis over the vacuum method given the advantages described previously.

Figure 21b shows the relationship and the linear fit established for water permeability and water accessible AV computed by dimensional analysis. Although additional data will more accurately define this relationship for AR mixtures, the data gathered suggest the same tendency presented for PG mixtures. Furthermore, for both plant and laboratory compacted specimens the data set presented in Figure 21 show higher permeabilities for the PG mixtures compared to those of AR mixtures. However, the average permeability values (evaluated on two PMLC specimens) in three out of six PG plant mixtures were less than 100 m/day (328.1 feet/day), which is the minimum permeability suggested by NCAT (7). For the AR mixtures, one out of three mixtures had permeabilities below the minimum recommended.

Based on the linear fit obtained for the relationships between permeability and AV content, the minimum permeability suggested by NCAT can be achieved by ensuring minimum

water accessible AV contents measured by dimensional analysis of 16 and 17.5 percent for PG and AR mixtures, respectively. If the total AV content computed by dimensional analysis is used, the minimum AV contents correspond to 19.5 and 22 percent for PG and AR mixtures, respectively. However, given the high variability in AR mixture results this total AV content is only indicative for this type of mixture. These results agree with previous research performed by NCAT (*9*) which concluded that the minimum AV content evaluated using dimensional analysis should be 20 percent (18 percent for the vacuum method) to obtain a minimum permeability of 100 m/day (328.1 feet/day) in OGFC.

These results also suggest that the design of PG-PFC mixtures should ensure an approximate minimum of 20 percent in total AV content when using dimensional analysis, which excludes the lower portion of the current design range (i.e., 18-22 percent). In the case of AR mixtures a higher AV magnitude may be required but there are not enough data to recommend a minimum value. The relationships of permeability and AV content in Figure 21 provide rationale for controlling AV content.

Although limited data are available regarding the impact of asphalt content on mixture permeability, the analysis of the average permeability values based on three replicate specimens for each asphalt content used in the laboratory mixtures (Table 10) suggest that this variable does not have a major influence on permeability. The differences in permeability at different asphalt contents that can be computed based on the data reported in Table 10 may be attributed to the test variability or most probably to differences in AV contents (Figure 21a provides a general idea about the possible impact of AV content for the I-35-PG mixture).

Table 10. Permeability Values for Laboratory Mixtures.

Laboratory Mixture	Asphalt Content (%)	Average Permeability (m/day)	Average Water Accessible AV, Vacuum Method (%)
I-35-PG	5.6	191.4	20.5
	6.1	179.7	19.3
	6.6	168.3	19.7
US-281-AR	7.6	224.9	22.5
	8.1	218.7	22.0
	8.6	210.3	22.4

The comparison of AV content and water permeability for PMLC specimens and road cores is shown in Figure 22a. As stated previously, permeability values established for laboratory compacted specimens show a defined tendency as the AV content increases. On the contrary, permeability values and AV contents determined for road cores do not present the same tendency established for laboratory compacted specimens. Although the coefficient of correlation for the AR mixture road cores was 0.90 (Table 9), the slope of the respective linear fit is not comparable to that defined for laboratory compacted specimens, which implies that important differences in mixture properties impact the establishment of minimum required AV contents to ensure minimum permeabilities. Data for PG mixture road cores showed poor coefficient of correlation (–0.36) as illustrated by the high dispersion of the data set presented in Figure 22a, which does not allow a relationship between minimum AV content and a minimum permeability value for the field conditions represented by the road cores.

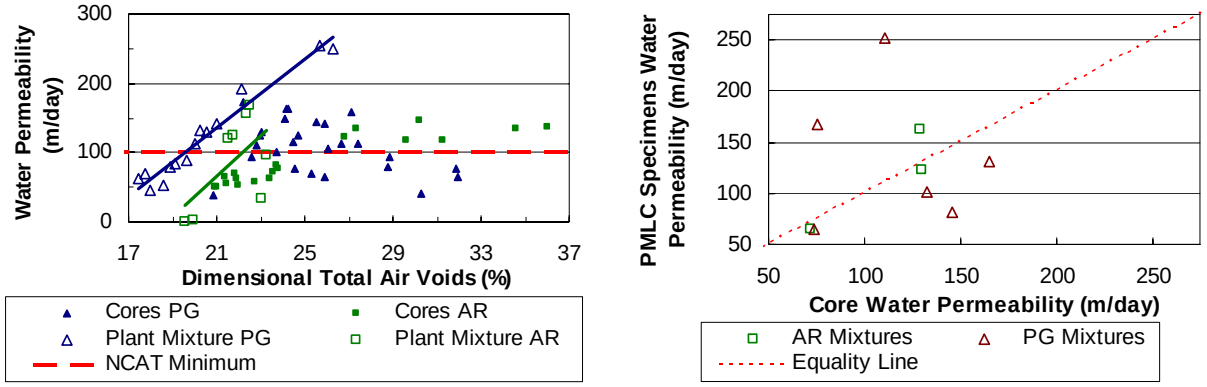

(a) (b)

Figure 22. (a) Comparison of Air Voids Content and Water Permeability and (b) Comparison of Water Permeability for Road Cores and Plant Mixture Specimens.

Although maximum care was taken in cutting the road cores, some AV sealing was observed at the bottom of a few AR and PG mixture road cores which may affect the laboratory permeability results. This aspect was not a problem for measuring permeability on LMLC or PMLC specimens. Therefore, most of the values contained in the data set presented in Figure 22a are accurate and validates the conclusion that specimens compacted using the SGC exhibit higher permeability than those compacted in the field at the same AV content. This conclusion is in agreement with the results presented by Masad (*16*) when comparing asphalt mixtures with

AV contents up to approximately 15 percent. Masad (*16*) stated that these differences in permeability can be related to discrepancies in the AV distribution induced by dissimilarities between the compaction methods applied in the laboratory and in the field. Since current practice does not specify density in the field as a compaction requirement (*1*), limited control is applied at present on the final AV content of the mixture and its homogeneity, which may generate significant differences in final AV contents and internal distribution.

Figure 22b shows the relationship of average permeabilities measured for both road cores and PMLC specimens. The differences are partially related to discrepancies in the total AV content of road cores and laboratory compacted specimens. For all the mixtures studied, higher AV contents were computed for road cores than for PMLC specimens, which in principle should lead to higher permeabilities for the road cores if the AV structures of road cores and PMLC specimens are comparable. However, data presented in Figure 22b do not substantiate that expectation and provide evidence of difficulties encountered in establishing a direct relationship between the permeabilities measured for road cores and those computed for laboratory compacted specimens. Permeability results measured on specimens and road cores from US-59Y-PG and US-290-AR mixtures corroborate this conclusion. For these two mixtures, PMLC specimens were compacted modifying the energy applied by the SGC to the number of gyrations required to reproduce the AV content established for the road cores. Table 11 summarizes both the total AV content computed using dimensional analysis and permeability values and illustrates the differences in permeability that substantiate the same conclusion.

Table 11. Water Permeability Comparison for Specimens Compacted in the Laboratory and in the Field.

Laboratory Mixture	Road Cores Total AV	PMLC Total AV	Road Cores Permeability (m/day)	PMLC Permeability (m/day)
US-59Y-PG	26.6	26.3	113.5	250.3
	27.4	25.7	111.7	254.3
	26.0	-	106.5	-
US-290-AR	23.8	23.3	76.6	95.1
	23.7	23.0	80.5	34.2
	22.7	-	58.3	-

4.3. EVALUATION OF FIELD CHARACTERIZATION OF DRAINABILITY

Results of repeated determinations of WFV for the US-290 project are summarized in Table 12. These WFV were used to evaluate the effect (i.e., possible mixture saturation) of repeated measurements in the same location. The WFV were measured twice at four locations compacted with one to four static roller passes and seven consecutive times in a location compacted with six passes. Data summarized in Table 12 provided evidence of the minimum impact of repeated tests on the WFV. The coefficient of variation for the values established at the location compacted with six passes corresponds to 2.3 percent. Therefore, subsequent WFV values correspond to averages of two individual measurements.

Table 12. Results of Repeated Determinations of Water Flow Value.

Number of Passes	Water Flow Value (s)	Number of Passes	Water Flow Value (s)
1	8.2	6	25.1
1	8	6	25.7
2	9.9	6	25.9
2	10	6	25.4
3	14.4	6	25.1
3	14.4	6	26.2
4	18.2	6	26.7
4	19		

The variability of water permeability values measured on replicate road cores and the corresponding WFVs determined in the field (i.e., average of two consecutive measurements) are shown in Figure 23a. The average water permeability values for the same set of road cores are compared to the WFVs in Figure 23b. The analysis of the data from both types of mixtures (i.e., PG and AR) was kept independent due to the same reasons described for analyzing the laboratory characterization of drainability. The variability encountered in data reported in Figure 23 is associated with both variability of the permeability test (not established as part of this study) and differences in permeability due to changes in the AV content of the road cores. The second aspect is believed to induce most of the variability as differences in total AV content between 0.4 and 4.9 percentage points were registered.

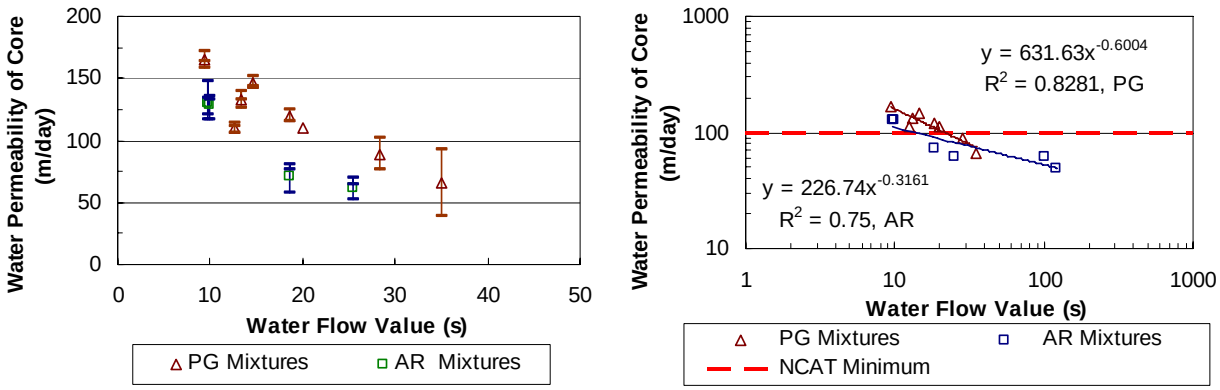

(a) (b)

Figure 23. Comparison of Water Flow Value and Water Permeability Based on (a) Individual Test Results (Variability) and (b) Average Values.

The linear fits shown in Figure 23b suggest the existence of a good correlation between the water permeability measured for road cores in the laboratory and the WFV determined to evaluate field drainability in PFC. Laboratory permeability values and field water flow times measured using the L.C.S permeameter, a device with an operation principle similar to that of the equipment used to measured the WFV, showed adequate correlation according to evaluations performed in Spain on similar PA mixtures *(20)*.

Few data were available in this study for long WFVs (i.e., longer than 35 seconds) to better define the actual tendencies as the drainability decreases in PFC mixtures. Additional data can substantially modify the degree of correlation reported. For example, when the WFVs of 101 and 122 seconds are not included in the AR mixture data set, the R^2 coefficient increased to 0.98 and the slope of the fit line is similar to that defined for the PG mixtures. The type of correlation may also require modification to adjust for the values obtained at reduced drainability conditions.

The linear fits shown in Figure 23b led to WFVs of 21.5 and 13.3 seconds to ensure the minimum permeability value recommended by NCAT *(7)* (i.e., 100 m/day [328.1 feet/day]) in PG and AR mixtures, respectively. However, there are other variables such as gradation, compaction level, and pavement age that may be contributing to the differences shown between the PG and AR mixtures. Test method Tex-246 *(10)* recommends a maximum WFV of 20 seconds for newly constructed PFC mixtures. The correlations between the WFV and the laboratory water permeability conducted on road cores from the same locations (as shown in Figure 23) indicate that, in general, the current recommended value of 20 seconds for WFV

correlates to the 100 m/day laboratory permeability recommended by NCAT. Thus, these data support the current maximum WFV of 20 seconds as recommended in Test Method Tex-246 *(10)*.

An additional attempt to compare field and laboratory drainability evaluations was made by relating the water permeability values measured on PMLC specimens and respective WFVs. The coefficients of correlation calculated for the data sets shown in Figure 24 are -0.237 and -0.905 for the PG and AR mixtures, respectively. Additional data are required to better define the existence of this relationship, which may be used to define the minimum permeability values required on PMLC specimens to ensure the minimum WFVs established using a relationship like that presented in Figure 23b. However, the lack of comparability of the AV contents currently obtained in the field and in the laboratory is an important limitation to establishing this type of relationship.

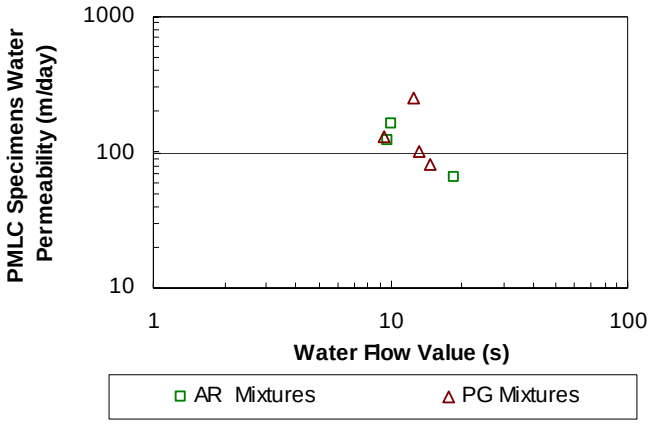

Figure 24. Comparison of Water Flow Values and Water Permeability for PMLC Specimens.

The water permeability values and the water accessible AV content measured on both LMLC and PMLC specimens showed a high coefficient of correlation, which would suggest the possibility of controlling the permeability of PFC mixtures through the evaluation of AV contents in the field. However, the lack of a defined relationship between the water permeability values computed for road cores and their AV contents may imply a limitation to ensure permeability by checking AV content. Alternatively, available data suggested that the relationship of water permeability for road cores and WFV could be used to determine a

minimum WFV for each type of mixture (i.e., PG and AR) associated with the minimum desired water permeability value.

Additional data are required to define the relationship for each mixture. However, the control of WFV in the field cannot be the only criterion applied during construction as lack of compaction may become a problem while pursuing more drainable mixtures by modifying the compaction energy. Deficient compaction works directly against mixture durability, as explored in the next chapter.

4.4. COMPACTION EFFECTS ON DRAINABILITY

Results for the field drainability evaluation performed to assess the effect of the compaction energy are shown in Figure 25. In Figure 25, the reported total number of static roller passes includes the passes made by the finish roller. The tendencies of the curves and the differences in AV content (average values obtained from three road cores in each case using dimensional analysis) shown in Figure 25 suggest that the WFV is mixture dependent. In fact, the field mixture drainability can change as a function of aggregate gradation, asphalt content, fiber content (for PG mixtures only), aggregate shape properties, compaction temperature, and characteristics of the compaction equipment, among others.

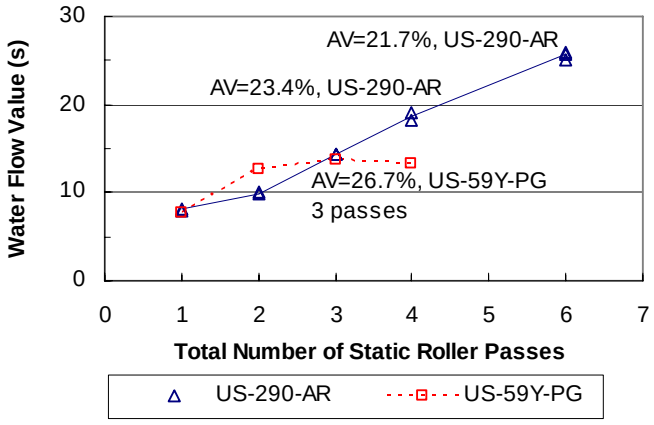

Figure 25. Effect of Field Compaction Pattern on Water Flow Number.

PFC mixtures are typically compacted by applying three to four passes with a flat-wheeled static roller, which according to the evaluation performed on the extracted road cores leads to AV contents between 22.7 and 27.4 percent for the US-59Y-PG and US-290-AR

mixtures. These magnitudes are considerably higher than the design AV content range (18 to 22 percent). However, high AV contents, even up to 36 percent, were found as shown in Figure 22a. This fact motivated the laboratory evaluation of volumetric, drainability, and durability characteristics in PMLC specimens compacted at two different energies (i.e., 12 to 15 and 50 gyrations) for both the US-59Y-PG and US-290-AR mixtures. With the application of these energies, the mix design procedure and the field AV content were reproduced for both mixtures. The results of water permeability measured on these PMLC specimens are shown in Figure 26.

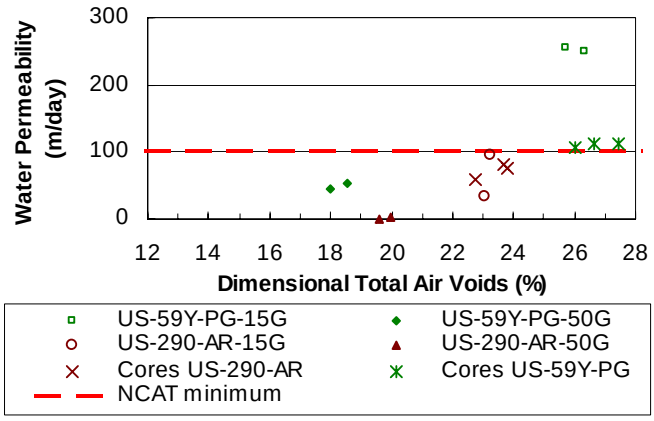

Figure 26. Effect of Laboratory Compaction Energy on Water Permeability.

As previously indicated from the comparison of PMLC specimens and core permeabilities, at similar AV contents permeabilities were generally higher for laboratory compacted specimens compared to those computed for road cores. The complete loss of drainability encountered for the US-290-AR specimens compacted at 50 gyrations constitutes a remarkable aspect of this evaluation. Although the AV content of these specimens are right in the middle of the current AV design range, the permeability substantially decreases to the point of practically losing the distinctive drainage properties in these specimens. Similarly, the US-59Y-PG mixture reduces its permeability by approximately 80 percent when the number of gyrations is increased from 15 to 50.

4.5. SUMMARY AND RECOMMENDATIONS

The following conclusions are stated based on the analysis of field and laboratory data gathered for this study:

- The study of drainability data suggested that its analysis should be performed independently for AR and PG mixtures.
- Although the water permeability values (i.e., measured in the laboratory using a falling head permeameter) determined for both LMLC and PMLC specimens showed a high coefficient of correlation with both total and water accessible AV content, the same parameters evaluated on road cores showed poor correlation. In addition, at similar AV contents, laboratory compacted specimens exhibited higher water permeability values than road cores. These facts suggest a limitation to the adoption of a minimum water permeability value to establish a minimum AV content during mix design and control of AV content in the field as a way to guarantee minimum field permeability.
- The correlations between the WFV and the laboratory water permeability conducted on road cores from corresponding field locations indicate that, in general, the current recommended value of 20 seconds for WFV correlates to the 100 m/day laboratory permeability recommended by NCAT. Thus, the current maximum WFV of 20 seconds as recommended in Test Method Tex-246 (*10*) is supported by the data in this study. Additional data are required to define the relationships distinguishing AR mixtures from PG mixtures and to define relationships for poorly draining mixtures (i.e., WFV longer than 35 seconds). The control of WFV in the field should not be the only criterion applied during construction because insufficient compaction may also contribute to a lack of mixture durability as explored in the next chapter.
- Since all of the PFC mixtures in Texas have been in service for a maximum of approximately three years, no data regarding long-term performance in terms of drainability were available for this study. This aspect requires future assessment to establish the actual functional life of PFC mixtures and possible maintenance actions required to extent the functional life (i.e., technical and economical appraisal of cleaning techniques versus the nonintervention alternative, or different gradation combinations, for example). Future research should also be directed to define an analytical model for calculating permeability as a function of the mixture characteristics to better estimate this property in PFC mixtures.
- The evaluation of road cores and PMLC specimens proved that the energy of compaction has a substantial effect on the mixture drainability through modifications of the AV content and its distribution.

The following recommendations are stated based on the conclusions and analysis presented in this chapter:

- Conduct evaluations of drainability in the field as described in Test Method Tex-246-F to guarantee adequate initial mixture drainability properties in the field.
- Limit the maximum WFV to 20 seconds for both AR and PG mixtures as currently recommended in Test Method Tex-246.
- Conduct additional research to define relationships between WFV and laboratory water permeability performed on road cores for each mixture system (PG and AR) and to define relationships for poorly draining mixtures (i.e., WFV longer than 35 seconds).
- Specify density requirements for field compaction in addition to the control of WFV in the field.

5. DURABILITY

Many agencies select the OAC in PFC and OGFC based on volumetric mixture properties. This design practice guarantees mixture functionality, but it only accounts for durability indirectly in terms of accessibility to air and water that may cause excessive aging or moisture damage, respectively. This second characteristic is a main concern for PFC and OGFC performance because the primary distress causing failure in these mixtures is raveling. This type of distress can be associated with aging of asphalt, inadequate compaction or insufficient asphalt content, mixture segregation, and asphalt softening generated by oil and fuel drippings in areas where car accidents have occurred (*1*).

At present an analytical model is not available to evaluate PFC performance in terms of durability, and important work also remains in terms of assessing the aging potential of PFC mixtures and the resulting impact on durability. Phenomenological approaches used to evaluate durability in these mixtures include TSR, Hamburg Wheel-Tracking test (HWTT), and Cantabro Loss test (Cantabro). The TSR is used only in Switzerland and was also proposed by NCAT to design new generation OGFC (*7, 9*). Denmark uses the HWTT for permanent deformation assessment of PA; and Australia, South Africa, and some European countries use the Cantabro test to design PA mixtures (*1*). The Cantabro test was also recommended by NCAT for OGFC mix design (*7, 9*).

This chapter describes the activities performed to evaluate different tools that could be applied to assess the durability of PFC mixtures in the laboratory with a special interest in mixture moisture susceptibility, aging potential, and permanent deformation. The durability evaluations were limited to laboratory determinations because field data on long-term performance in terms of durability were not available at this time. Since all of the PFC mixtures in Texas have been in service for a maximum of approximately three years, future assessment is required to establish the actual service life of PFC mixtures, failure mechanisms, and their relationship with laboratory evaluations.

First, this chapter presents a preliminary evaluation of the current tests used for PFC mix design (draindown and boiling test) and the results from a first trial application of the TSR for mix design purposes. Subsequently, an evaluation of three durability tests (Cantabro, HWTT, and the Overlay Test [OT]) to establish their potential application in PFC mix design and

laboratory performance evaluations is presented. In addition, a preliminary evaluation of the compaction effects on durability conducted by applying these three tests is summarized.

Surface free energy measurements on asphalt and aggregate and calculations of work of adhesion were also performed on materials selected to develop a complete characterization of the laboratory mixtures (I-35-PG and US-281-AR) and the two main plant mixtures (US-59Y-PG and US-290-AR) utilized in the comprehensive evaluation of volumetric properties, functionality, and durability (based on Cantabro, HWTT, and OT.) Finally, based on the durability information gathered from this extensive testing program, a comparison of AR and PG mixture systems is provided. The chapter includes the experimental design, discussion of the results, and conclusions and respective recommendations.

5.1. EXPERIMENTAL DESIGN

This section presents the experimental design developed to evaluate the durability of PFC mixtures in the laboratory, which includes mix design and materials selection, descriptions of the tests used for mixture evaluation, specimen fabrication, and laboratory conditioning and testing.

5.1.1. Current Tests for PFC Mix Design

The TxDOT mix design process currently includes volumetric determinations, draindown (Tex-235-F) (*10*), "boiling" test (Tex-530-C), and Cantabro test (Tex-245-F), which is conducted at present for informational purposes only (*12*). These tests were executed for the laboratory mixtures to evaluate potential problems of asphalt draindown in representative PG and AR mixtures and to obtain a preliminary assessment of moisture damage, respectively. Each of these tests was performed at three different asphalt contents: OAC and OAC ± 0.5 percent. Only limited draindown testing was performed because the initial draindown evaluation did not reveal any problems for AR or PG mixtures at any binder content. The "boiling" test was also not performed on additional mixtures since the assessment of alternative methodologies for evaluating moisture damage was the main objective to improve this aspect in mix design.

5.1.2. Additional Tests for Mixture Performance Evaluation

Researchers used the Cantabro test, the HWTT, and the OT to evaluate the performance of PFC mixtures in the laboratory. In addition, a preliminary evaluation of the application of the tensile strength ratio (TSR) was performed. The following sections present details related to materials, test procedures, specimen fabrication, laboratory conditioning, and laboratory testing.

Material Selection. Both mixture systems that include different asphalts (AR and PG) and other materials as defined in the TxDOT specifications and corresponding aggregate gradations were evaluated. Table 13 provides details of the materials used for each mixture included in this evaluation. Aggregate gradations for these PG and AR mixtures are shown in Figure 1 and Figure 2, respectively.

Table 13. Mixture Descriptions.

Mixture	Highway	Location	Asphalt Type	OAC (%)	Aggregate and Proportion (%)	Other Materials
US-281-AR	US 281	San Antonio, Tx	AC-10 w/ 16% crumb rubber	8.1	Sandstone[1], 50 Limestone[2], 50	None
US-290-AR	US 290	Paige, Tx	AC-10 w/ 17 % crumb rubber	8.3	Sandstone[1], 100	None
I-35-PG	IH 35	San Antonio, Tx	PG 76-22S	6.1	Sandstone[1], 52 Limestone[2], 47	Lime (1%), fibers (0.3%)
US-59Y-PG	US 59	Yoakum, Tx	PG 76-22S	5.8	Limestone[2], 100	Lime (1%), fibers (0.3%)

[1]The same sandstone was used in all three mixtures. [2]The limestone used in the I-35-PG and US-59Y-PG mixtures is the same and is similar to that used for the US-281-AR mixture.

Tests Used for Mixture Performance Evaluation. This section presents a brief description of the main aspects related to the tests used to evaluate PFC mixtures. The Cantabro test provides an indirect evaluation of mixture cohesion, resistance to disintegration, and aggregate interlock (*21*). Although the test was originally proposed on dry specimens, since 2001 the Spanish have required the Cantabro test for specimens in both dry and wet conditions. The moisture conditioned test was introduced as a way to evaluate aggregate-binder combinations with poor adhesion, and the effect of low quality fillers, which were identified as responsible for accelerated mixture deterioration (i.e., raveling) (*3*).

The Cantabro test was performed by placing SGC compacted specimens 4.5 in. (115 mm) in height into the Los Angeles (LA) abrasion machine without any abrasive load. The initial mass of the specimens (W_o) was compared to its final mass (W_f), obtained after applying 300 revolutions (after approximately 10 minutes, since the machine rotates at a speed of 30 to 33 revolutions per minute) in the LA abrasion machine, to calculate the Cantabro loss as follows:

$$\text{Cantabro loss}\,(\%) = \frac{W_o - \left(W_f - \left(W_d - W_o\right)\right)}{W_o} * 100 \qquad (12)$$

where W_d is the weight of the specimen after drying to eliminate water trapped during measurements associated with water accessible AV. The Cantabro loss specification used in Spain for high traffic highways corresponds to a maximum of 20 and 35 percent loss in dry and wet conditions, respectively (*1*). Research conducted by NCAT also recommended limiting the Cantabro loss evaluated in dry condition to 20 percent (*9*).

Since PFCs are relatively new mixtures in Texas, long-term performance data (i.e., mixture resistance to disintegration under field service conditions) are not yet available. However, based on previous research (*3*) that concluded that the Cantabro loss test was suitable to evaluate the resistance to disintegration (i.e., raveling) in the laboratory of similar PA mixtures with appropriate correlation to field performance, the Cantabro loss test was used to evaluate the durability of different PFC mixtures in the laboratory.

Texas has used the HWTT since 2000 for all types of HMA mixtures as a tool for evaluating rutting and moisture damage susceptibility. The HWTT was conducted by applying a repeated load of 158 lb force (705 N) on two trimmed SGC molded specimens using a 1.85 in. (47 mm) wide steel wheel that rolls back and forth on the surface of the specimens while they are immersed in a water bath at 122°F (50°C). Rut depths were measured during the test at 11 different positions along the wheel path, and the average rut depth from the three central measurements was reported. Each HWTT required an average time of 5 hours to perform for the mixtures evaluated. The minimum number of passes, at 0.5 in. (12.5 mm) rut depth tested at 122°F (50°C), specified for dense-graded HMA fabricated using PG 76-XX asphalt corresponds to 20,000 (*11*).

The OT was conducted using the Texas Transportation Institute (TTI) Overlay Tester. For this test, the specimen is glued on two metallic plates, one that is mobile and one that is fixed. The Overlay Tester operates in a controlled-displacement mode (constant maximum

displacement of 0.025 in. [0.62 mm]) to induce horizontal movement in the mobile plate to simulate the opening and closing of joints or cracks in old pavements beneath an overlay. The test is conducted at 77°F (25°C), with a load rate of 10 seconds per cycle and a repeated load applied in a cyclic triangular waveform. For the mixtures studied, an average time of 2 hours was required to perform the OT. The cracking life (expressed as number of cycles) was calculated by applying a modified version of the load reduction method suggested by Zhou et al. (*22*). In this study, the average of the 93 and 80 percent load reduction levels for the first and the second load cycles, respectively, was used to establish the cracking life for PFC mixtures. The second cycle was included to take into account possible distortions in the first load cycle due to differences in the setting of the plates and induction of residual stresses. The pass/fail criterion proposed in previous research for dense-graded HMA corresponds to 300 cycles (*22*).

The TSR constitutes an indication of the loss of strength generated by moisture conditioning, and it is calculated as the ratio of the average indirect tensile strength of moisture conditioned specimens and the average indirect tensile strength of unconditioned specimens. Four unconditioned and four moisture conditioned specimens were used to obtain the average dry and wet indirect tensile strengths, respectively. The specimens used were similar to those produced for the Cantabro test. The minimum TSR specified by most agencies for dense-graded HMA varies between 70 and 80 percent (*23*), and the minimum TSR suggested by NCAT for OGFC mix design is 80 percent evaluated using SGC specimens subjected to one freeze/thaw cycle (*7, 9*).

While the Cantabro test, the OT, and the TSR may be used to define a minimum asphalt content that limits mixture fracture and disintegration, the HWTT can establish a maximum asphalt content that minimizes permanent deformation issues.

Specimen Fabrication. Table 14 presents the parameters utilized to fabricate specimens for the Cantabro test, the HWTT, and the OT, and the methods applied to determine G_{mb} to subsequently calculate the total AV content, which was utilized as parameter of compaction control. Specimens for the TSR (LMLC) were produced using only I-35-PG laboratory mixture. The durability mixture evaluation required fabricating one particular type of specimen for each test, except for TSR and Cantabro, which use the same type of specimen. As these evaluation tests are destructive, replicate specimens were needed to perform the tests on specimens

subjected to different conditions and/or tests. All specimens were compacted using the SGC at an N_{design} value of 50 gyrations (*10*) to dimensions of 6 in. (150 mm) in diameter and 4.5 ± 0.2 in. (115 ± 5 mm) in height for the TSR and the Cantabro test, 2.4 ± 0.1 in. (62 ± 2 mm) in height for the HWTT, and 2.25 in. (57 mm) in height for the OT. Furthermore, OT specimens required saw cutting to the final dimensions and shape as indicated in Tex 248-F (*10*). Thus, the control of AV content for the OT specimens was based on AV content after cutting.

Table 14. Parameters and Evaluation Methods for Fabrication of Durability Specimens.

Mixture	Specimen Type	Asphalt Content (%)	Design AV Content (%)	G_{mb} Measuring Method	Conditioning of Cantabro Loss Test Specimens
US-281-AR	LMLC	OAC, OAC±0.5	20±1	Double bag vacuum	Dry, temperature, wet, and aged 3 and 6 months[1]
US-290-AR	PMLC	OAC	20±1	Dimensional analysis	Dry, wet, and temperature
I-35-PG	LMLC	OAC, OAC±0.5	20±1	Double bag vacuum	Dry, temperature, wet, and aged 3 and 6 months[1]
US-59Y-PG	PMLC	OAC	20+1	Dimensional analysis	Dry, temperature, wet, and aged 3 and 6 months

[1] Specimens with AV contents between 15 and 25 percent were also produced for testing in a dry condition to evaluate the impact of the AV content on the Cantabro loss.

The initial range of total AV content (19 to 21 percent) selected for Cantabro test specimens was modified to 18-21 percent for specimens compacted at the highest asphalt content for the I-35-PG and US-281-AR mixtures due to practical difficulties encountered in producing replicate specimens within the initial AV range. To reproduce the mix design, the production of PMLC specimens from the US-290-AR and US-59Y-PG and all other plant mixtures was controlled through dimensional analysis. For these mixtures, the compaction process was controlled to try to obtain AV contents equal to those defined in the respective mix designs. Although the amount of material to compact was successively modified (using dimensional analysis to calculate the approximate total AV content immediately after compaction), researchers encountered difficulties in reproducing the design AV content for most of the plant mixtures. In general, smaller total AV contents were obtained compared to those reported as target values for mix design.

The total AV content of HWTT and OT specimens was also 20 ± 1 percent, but the HWTT was also performed using specimens with lower and higher AV contents. The production

of short compacted specimens for the HWTT and the OT was particularly difficult due to the higher variability encountered in the total AV content of these specimens compared to that of those 4.5 in. (115 mm) in height as previously reported in Section 3.4.

Laboratory Conditioning. The specimens utilized for determination of TSR were conditioned according to the procedure indicated in Tex-531-C. However, the specimens were frozen after filling the plastic bag to the top with water instead of adding only 0.3 oz (10 mL) of additional water into the bag. This modification ensured saturation of the specimens during the freezing process since water drains out while the specimens are taken out from the equipment used for vacuum saturation and placed into the plastic bags. One freeze-thaw cycle was applied following recommendations from previous research for moisture conditioning of PFC samples for determination of TSR (*9*).

Cantabro tests were performed on compacted specimens subjected to five different conditioning processes (dry, wet, temperature, and 3 and 6 months aging). The dry and wet conditioning processes were selected to evaluate the mixture response in its original state (dry-no aging) and after inducing moisture damage using controlled laboratory conditions. The dry conditioning consisted of drying the specimens (after saturation to measure water accessible AV) for a minimum time of 24 hours using forced ventilation at room temperature (77°F [25°C]). The wet conditioning required keeping the specimens for 24 ± 0.5 hours in a water bath with a constant temperature of 140°F (60°C), and then drying the specimens for 24 ± 0.5 hours using forced ventilation at room temperature (*24*).

The temperature conditioning process allowed assessing the material response at low temperature when the asphalt becomes stiffer and more susceptible to brittle fracture and thus, to raveling. The temperature conditioning was similar to the dry conditioning, but instead of testing after drying, the specimens were first placed in a cool room at 37.4°F (3°C) for a minimum time of 24 hours. Since the LA abrasion machine does not have temperature control, some variability was induced due to differences in ambient temperature. Differences of approximately 8 to 15°F (4.4 to 8.3°C) between initial and final temperatures were measured during testing. Finally, to investigate the potential impact of binder aging on the loss of cohesion of PFC mixtures, compacted specimens were subjected to accelerated aging for 3 and 6 months in a temperature-controlled room at 140°F (60°C) with free heated air circulation.

Since the HWTT is performed with wet specimens, no special conditioning was applied after measuring G_{mb} and cutting the specimens to their final shape as indicated in Tex-242-F (*10*). After cutting and determining G_{mb} for the OT specimens, these specimens were dried at room temperature for a minimum time of 24 hours under forced ventilation before testing.

Laboratory Testing Procedures. Two replicate TSR tests at each of three different asphalt contents were performed according to Tex-531-C (*10*). The HWTT with two replicate specimens and the OT with four replicate specimens were conducted as defined for dense-graded HMA mixtures in Tex-242-F and Tex-248-F, respectively *(10)*. The Cantabro tests were conducted as described in Tex-245-F (*10*) using four replicate specimens for each condition and asphalt content. However, the evaluation of the impact of AV content on the Cantabro loss included between 7 and 17 specimens per asphalt content.

5.1.3. Compaction Effects on Durability

The effects of compaction energy on durability were determined using PMLC specimens from both US-290-AR and US-59Y-PG mixtures. As described in Section 3.8, an attempt to reproduce the compaction condition achieved in the field was made by reducing the number of gyrations applied by the SGC to obtain the same AV content in both road cores and PMLC specimens. Twelve to fifteen gyrations were required in the SGC to reproduce the field AV contents of both mixtures. In addition, specimens compacted according to the energy specified (i.e., 50 gyrations of the SGC) by the current TxDOT design procedure were produced for both mixtures. These specimens were evaluated using HWTT, OT, and the Cantabro test using the same testing and conditioning processes as described previously.

5.1.4. Surface Free Energy Measurements

Material selection. All of the asphalts used to fabricate the plant mixtures evaluated in this study (Table 15) were subjected to surface free energy testing using unaged samples. The two procedures (filtering and chemical extraction) indicated in Table 15 to obtain unaged AR samples are discussed subsequently. Table 16 presents the aggregates subjected to surface free energy testing. These aggregates include those that were used to fabricate the four PFC

mixtures (I-35-PG, US-59Y-PG, US-281-AR, and US-290-AR) utilized in the main laboratory characterization program.

Table 15. Asphalts Tested for Surface Free Energy Using Unaged Samples.

Mixture	Highway	Asphalt Type
I-35-PG	I-35	PG 76-22S
IH-20-PG	IH 20	PG 76-22
IH-20-PG-TR	IH 20	PG 76-22 TR
IH-30-PG	IH 30	PG 76-22
US-59-PG	US 59	PG 76-22
US-59Y-PG	US-59	PG 76-22S
US-281-AR[1]	US-281	AC-10 w/16% type II rubber
US-288-AR[2]	US 288	AC-10 w/17% type II rubber
US-290-AR[2]	US 290	AC-10 w/17% crumb rubber

[1]Sample prepared by both filtering and chemical extraction methods. [2]Sample prepared by filtering.

Table 16. Aggregates Tested for Surface Free Energy.

Aggregate	Quarry	PFC Mixture
Limestone	Colorado Materials	I-35-PG, US-59Y-PG
Sandstone	Brownlee	I-35-PG, US-281-AR, US-290-AR
Limestone	Hanson, New Braunfels	US-281-AR
Sandstone	Smith/Buster	I-30-PG

Surface Free Energy, Tests Used to Measure Surface Free Energy Components and Calculation of Work of Adhesion. From the thermodynamic point of view, the surface free energy of a material is the amount of work required to create a unit area of new surface of that material in vacuum. According to the Good-Van Oss-Chaudhury (*25*) theory, based on the source of intermolecular forces the surface free energy can decompose into three separate components. These components correspond to: monopolar acidic, Γ^{+}; monopolar basic, Γ^{-} (these two terms define the polar component Γ^{AB}), and Lifshitz-van der Waals or apolar component, Γ^{LW}. The surface free energy, Γ, of a given material is computed according to Equation 13, which was applied to calculate the surface energy of asphalts and aggregates.

$$\Gamma = \Gamma^{LW} + 2\sqrt{\Gamma^{+}\Gamma^{-}} = \Gamma^{LW} + \Gamma^{AB} \tag{13}$$

Surface free energy components for asphalts and aggregates were determined using the Wilhelmy Plate (WP) method and the Universal Sorption Device (USD), respectively. The WP method allows computing the contact angle of a probe liquid on the asphalt surface. Thin glass plates (50 mm by 24 mm by 0.15 mm thick), coated with a thin asphalt film, are immersed and withdrawn from a probe liquid at very slow and constant speed while suspended from an accurate balance that registers the loading force for the immersion and receding processes. Using the forces measured during the advancing and receding processes, advancing and receding contact angles are calculated, respectively. The advancing (or wetting) and receding (or dewetting) contact angle determinations are used to compute two separate sets of surface free energy components. Equation 14, derived from the analysis of forces for the measurement setup, is used to calculate the contact angle (θ):

$$\cos\theta = \frac{\Delta F + V_{im}(\rho_L - \rho_{air})g}{P_t \Gamma_L} \tag{14}$$

where, ΔF is the force measured with the balance, V_{im} is the volume of the immersed plate, ρ_L is the density of the probe liquid, ρ_{air} is the density of the air, g is the local acceleration of gravity, P_t is the perimeter of the asphalt coated plate, and Γ_L is the total surface energy of the probe liquid.

By using the equation proposed by Good, van Oss and Chaudhury (*26*) (Equation 15), the contact angle of a probe liquid, *L*, in contact with a solid, *S*, is related to the surface energy components (Γ^{LW}, Γ^{+}, and Γ^{-}) of the liquid and the solid as follows:

$$W_{L,S}^{a} = \Gamma_L(1+\cos\theta) = 2\sqrt{\Gamma_S^{LW}\Gamma_L^{LW}} + 2\sqrt{\Gamma_S^{+}\Gamma_L^{-}} + 2\sqrt{\Gamma_S^{-}\Gamma_L^{+}} \tag{15}$$

where $W_{L,S}^{a}$ represents the work of adhesion. Determination of the contact angles of a particular asphalt with at least three known probe liquids will allow obtaining a system of linear simultaneous equations based on Equation 15. The solution of this system unknowns will render the magnitudes of the surface free energy components of the asphalt (represented in this case by Γ_S^{LW}, Γ_S^{+}, and Γ_S^{-}). The five liquids used in this study increased the calculation reliability. Table 17 presents the surface free energy characteristics of these probe liquids (*27*). The surface energy measurements were performed according to the procedure described in detail by

Hefer et al. (*27*), and the liquids included in the final calculation of asphalt surface free energy were screened as suggested by Hefer et al. (*27*) using a plot of $\Gamma_L(\cos\theta)$ versus Γ_L.

Table 17. Surface Free Energy Characteristics of Probe Liquids at 20°C (ergs/cm^2).

Liquid	Γ_L	Standard Deviation	Γ_L^{LW}	Γ_L^+	Γ_L^-
Water	72.8	0.2	21.8	25.5	25.5
Glycerol	64.0	0.3	34.0	3.92	57.4
Formamide	58.0	0.2	39.0	2.28	39.6
Ethylene glycol	48.0	0.2	29.0	1.92	47.0
Methylene fodide[1]	50.8	0.1	50.8	0.0	0.0

[1]Also known as diiodomethane.

The surface energy of the aggregates is indirectly determined using the USD based on the gas adsorption characteristics of three probe vapors. The work of adhesion (W_a) of the probe vapor (V) on a solid (aggregate) (S) and their surface energy components are related as indicated by Equation 16.

$$W_a = 2\sqrt{\Gamma_S^{LW}\Gamma_V^{LW}} + 2\sqrt{\Gamma_S^+\Gamma_V^-} + 2\sqrt{\Gamma_S^-\Gamma_V^+} \tag{16}$$

where the surface energy components (Γ_i^j) are defined as previously indicated. In addition, this work of adhesion can be quantified in terms of the equilibrium spreading pressure of the probe vapor on the solid surface (π_e) and the surface free energy of the probe vapor (Γ_V) as:

$$W_a = \pi_e + 2\Gamma_V \tag{17}$$

Equations (16) and (17) lead to:

$$\pi_e + 2\Gamma_V = 2\sqrt{\Gamma_S^{LW}\Gamma_V^{LW}} + 2\sqrt{\Gamma_S^+\Gamma_V^-} + 2\sqrt{\Gamma_S^-\Gamma_V^+} \tag{18}$$

The computation of the spreading pressure is conducted by applying Equation 19 and using the adsorption isotherm of the amount of solvent adsorbed versus relative pressure at constant temperature determined using the USD.

$$\pi_e = \frac{RT}{A}\int_0^{p_0}\frac{n}{P}dP \tag{19}$$

where, R is universal gas constant, T is absolute temperature, A is the specific surface area of the aggregate, n is the mass of the adsorbed vapor on the aggregate surface, and P is the vapor

pressure of the probe vapor. The specific surface area of the aggregate is also calculated using the USD through the application of the Brunauer, Emmett, and Teller (BET) equation (*28*).

Therefore, the aggregate surface free energy can be computed by solving a system of three linear equations of the form of Equation 18. For this purpose, the aggregate must be tested with three different known probe vapors in the USD. Table 18 introduces the characteristics of the probe vapors used in this study.

Table 18. Surface Free Energy Characteristics of Probe Vapors (ergs/cm^2).

Vapor	Γ_v	Γ_v^{LW}	Γ_v^+	Γ_v^-
Distilled water	72.60	21.60	25.50	25.50
n-hexane	18.40	18.40	0.00	19.60
MPK	24.70	24.70	0.00	0.00

Once the surface energy components of both asphalt and aggregate are quantified, the work of adhesion between these two materials (dry condition) is computed as:

$$W_{AS}^{dry} = 2\sqrt{\Gamma_A^{LW}\Gamma_S^{LW}} + 2\sqrt{\Gamma_A^{+}\Gamma_S^{-}} + 2\sqrt{\Gamma_A^{-}\Gamma_S^{+}} \quad (20)$$

Adhesive work of adhesion between asphalt and aggregate in the presence of water is computed by applying Equation 21.

$$W_{ASW}^{wet} = 2\begin{bmatrix} -\sqrt{\Gamma_A^{LW}\Gamma_W^{LW}} - \sqrt{\Gamma_S^{LW}\Gamma_W^{LW}} + \sqrt{\Gamma_A^{LW}\Gamma_S^{LW}} + \Gamma_W^{LW} \\ -\sqrt{\Gamma_W^{+}}\left(\sqrt{\Gamma_A^{-}} + \sqrt{\Gamma_S^{-}} - \sqrt{\Gamma_W^{-}}\right) \\ -\sqrt{\Gamma_W^{-}}\left(\sqrt{\Gamma_A^{+}} + \sqrt{\Gamma_S^{+}} - \sqrt{\Gamma_W^{+}}\right) + \sqrt{\Gamma_A^{+}\Gamma_S^{-}} + \sqrt{\Gamma_A^{-}\Gamma_S^{+}} \end{bmatrix} \quad (21)$$

The wetting and dewetting surface free energy components are used to compute corresponding wetting and dewetting works of adhesion, respectively. According to Lytton (*29*) the dewetting work of adhesion should be used to predict fracture, and the wetting work of adhesion can be used to predict healing in asphalt concrete mixtures. In addition, the nonpolar component of the wetting work of adhesion, W^{LW}, is inversely related to the short-term healing rate, while the polar component, W^{AB}, is directly related to the long-term healing rate. Furthermore, the total amount of healing directly relates to the ratio of the polar to the nonpolar component of the wetting work of adhesion, W^{AB}/W^{LW} (*29*).

The magnitude of the work of adhesion is positive in the absence of water on the interface and typically negative when water is present at the interface. While the positive values indicate resistance to fracture and capacity to heal, the negative magnitudes show that the water will promote debonding along the interface since it will adhere more strongly to the aggregate surface (*29*).

Specimen Fabrication and Laboratory Conditioning. The procedures followed for specimen fabrication, laboratory conditioning, and testing using the WP method and the USD corresponded to those described by Lytton et al. (*28*) for surface energy measurements of asphalts and aggregates. Additional information on surface energy fundamentals, equipment, and detailed tests procedures are also illustrated by Lytton et al. (*28*). This section describes the specific procedures required to fabricate asphalt slides to test using the WP method.

The application of the WP method requires the use of thin uniform films of asphalt that are obtained by coating thin glass slides with hot asphalt. Initial trials to fabricate and test this type of slide fabricated with AR asphalt proved impossible in terms of obtaining uniform films, and corresponding results showed a lack of consistency in the contact angles measured on AR slides given the size of rubber particles adhering to the slide surface. In fact, particles approximately 1/8 in. (3.2 mm) in size or larger were observed on this type of slides. Consequently, two procedures were evaluated to obtain representative AR samples to fabricate the required slides.

The first procedure corresponds to chemical extraction of the AR. The procedure applied was the same used to obtain AR asphalt samples for chemical testing as described in Chapter 6. The second procedure was performed by heating the AR to the mixing temperature (325°F [163°C]) and filtering it on a No. 80 sieve while the binder was kept at high constant temperature inside an oven. Figure 27 shows slides prepared with original and filtered AR.

Figure 27. Asphalt Rubber Slides Prepared with Original Asphalt Rubber (Left) and Asphalt Rubber Filtered on Sieve 80 (Right).

The chemical extraction allows obtaining only the base asphalt cement since the rubber is completely extracted, whereas the filtering process keeps the fine fraction of rubber particles which may constitute the main component modifying the asphalt response. Incidentally, slides prepared using the PG76-22-TR (i.e., IH-20-PG-TR asphalt) asphalt showed an adequate profile. Therefore, there was no need to prepare these samples as described for the AR samples. To improve the smoothness of the slide profile, all of them were placed in the oven for 20 to 60 seconds at the mixing temperature. The subsequent surface energy results reported were determined using samples obtained from the filtering process. This process was preferred since less time is required to obtain the samples, the finer portion of the rubber is retained, and there is no uncertainty related to modifications of the asphalt chemical properties during the chemical extraction.

5.2. DRAINDOWN AND BOILING TEST RESULTS

Table 19 summarizes the results of the draindown and boiling tests performed on laboratory mixtures. The current TxDOT specification for draindown corresponds to a maximum of 0.2 percent, which was not reached by any of the specimens tested. Although a minimum evidence of draindown was identified in the AR mixture, calculated draindown values were well

below the required specification. The use of fibers in PG mixtures proved effective in the laboratory mixture evaluated at different asphalt contents. Since the interviews conducted with selected TxDOT district personnel (*1*) or the mix design gathered for the plant mixtures evaluated did not reveal concerns regarding draindown issues in PFC mixtures, this aspect was not further investigated.

Table 19. Draindown and Boiling Test Results for Laboratory Mixtures.

Mixture	Binder Content (%)	Fibers Content (%)	Lime Content (%)	Draindown (%)	Stripping-Boiling Test (%)
I-35-PG	5.6	0.3	1.0	0.0	0.0
	6.1	0.3	1.0	0.0	0.0
	6.6	0.3	1.0	0.0	0.0
US-281-AR	7.6	0.0	0.0	0.06	0.0
	8.1	0.0	0.0	0.07	0.0
	8.6	0.0	0.0	0.04	0.0

The laboratory mixtures evaluated did not show any evidence of stripping after the boiling test. This test was performed for indicative purposes only and no additional efforts were done to determine its applicability in mix design since the impact of moisture damage was evaluated using the Cantabro loss test, the HWTT, and calculations of work of adhesion, as presented subsequently.

5.3. EVALUATION OF CANTABRO LOSS TEST RESULTS

Data presented in Figure 28 and Figure 29 show the Cantabro tests results at different conditions and binder contents for both laboratory mixtures. The Cantabro loss comparison presented in Figure 30 includes results from specimens compacted using 50 gyrations (50G) and 15 gyrations (15G) applied by the SGC, which permitted obtaining similar AV contents for all four mixtures and allowed direct comparison of these mixtures.

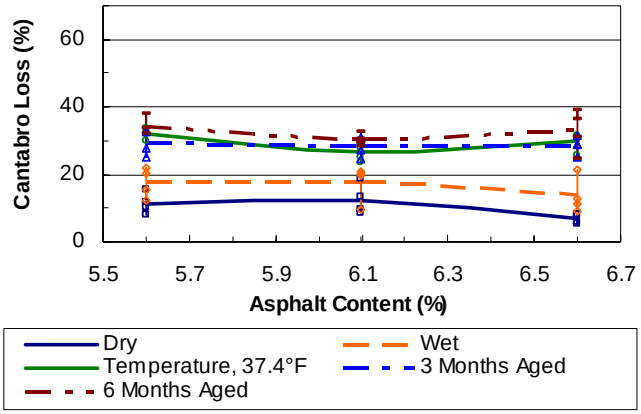

Figure 28. Average Cantabro Loss for Different Conditioning Processes in I-35-PG Mixture.

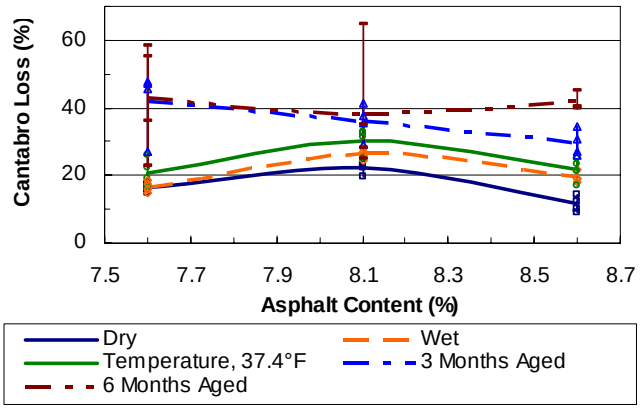

Figure 29. Average Cantabro Loss for Different Conditioning Processes in US-281-AR Mixture.

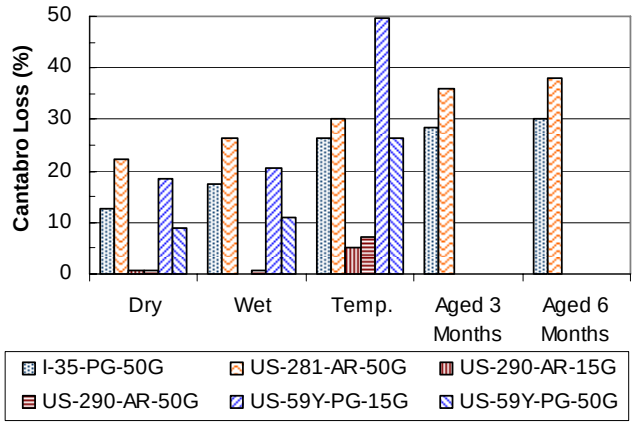

Figure 30. Cantabro Loss at Optimum Asphalt Content (OAC) for Different Conditioning Processes.

Table 20 summarizes the average AV content for mixtures compared in Figure 30. Data corresponding to wet and aged specimens (3 and 6 months) for the US-290-AR mixture fabricated by applying 12 to 15 gyrations are not presented in Figure 30 because these specimens disintegrated during the conditioning processes at high temperature (140°F [60°C]). This aspect is specifically discussed further in Section 5.6.

Table 20. Average Total Air Voids Content (Vacuum Method) of Specimens Tested for Cantabro Loss.

Mixture	Dry (%)	Wet (%)	Temperature (%)	Aged 3 months (%)	Aged 6 months (%)
I-35-PG-50 G (LMLC)	20.2	19.8	19.7	20.0	19.8
US-281-AR-50G (LMLC)	19.6	19.6	19.6	20.0	19.8
US-290-AR-15G (PMLC)	19.3	19.9	19.2	19.2	18.7
US-290-AR-50G (PMLC)	15.5	14.8	16.4	-	-
US-59Y-PG-15G (PMLC)	22.8	23.0	22.5	22.4	22.6
US-59Y-PG-50G (PMLC)	15.4	14.9	15.4	14.6[1]	14.8[1]

[1]One specimen was tested; two and four specimens were tested for PMLC and LMLC mixtures, respectively.

Cantabro loss data presented in Figure 28, Figure 29, and Figure 30 suggest that for the mixture systems studied, the Cantabro test was sensitive to changes in chemical and viscoelastic properties of the binder. Although quantification of fundamental properties related to those

changes is not provided, the Cantabro test offered an indirect indication of the potential impact of those changes on the PFC mixture resistance to disintegration, which has been associated with mixture durability and resistance to abrasion (*3*). In addition, for the mixtures included in this study the Cantabro test indicated that the properties of the aggregate may have a greater influence on the mixture performance evaluated in the laboratory than the binder does. This result agrees with the findings reported by Molenaar et al. (*30*) on the relative importance of the mixture composition parameters assessed using Artificial Neural Networks analysis applied to PA. Furthermore, as discussed subsequently, the Cantabro loss values showed a direct relationship with water accessible AV content, and thus provided an indication of the importance of the volumetric properties on the durability of PFC mixtures. The following subsections provide further discussion of these general conclusions.

Despite these positive results, the trends and the variability in Cantabro loss values obtained for the mixtures systems included in this study suggest that the Cantabro test may not provide enough sensitivity to be selected as a definitive tool for selecting the OAC of PFC mixtures based on durability. However, the Cantabro test is a simple and quick test that may be useful as an initial screening tool for selecting material combinations to include in more advanced testing toward selection of the OAC.

5.3.1. Effect of Different Conditioning Processes on Cantabro Loss and Selection of Optimum Asphalt Content

Statistically different Cantabro loss values were obtained for specimens tested after applying different conditioning processes used to induce modifications in the binder chemical properties (i.e., through moisture conditioning and aging) and viscoelastic properties (i.e., through temperature conditioning). This result suggests that the Cantabro test was sensitive to the changes induced to alter mixture resistance to disintegration. However, when each mixture system was analyzed independently based on both the average and the variability of the Cantabro loss, the impact of asphalt content on the mixture resistance to disintegration cannot be accurately evaluated. This fact suggests that the Cantabro test may not provide enough sensitivity to be selected as a definitive tool for selecting the OAC of PFC mixtures.

An important impact of asphalt aging on mixture resistance to disintegration was observed when comparing the Cantabro loss obtained in dry condition and that established after

3 and 6 months of aging. However, for the I-35-PG mixture (Figure 28) and for the US-281-AR mixture specimens (Figure 29) tested after 3 and 6 months of aging consistently resulted in small differences. This finding may indicate a decreasing rate of aging with time and/or the existence of an initial jump in aging that occurred after a short time as suggested by Glover et al. (*31*) in former research on asphalt durability. To better understand aging in these PFC mixtures, physical and chemical properties were measured on asphalt recovered from Cantabro test specimens after testing. Chapter 6 contains the results of this additional analysis.

The coefficient of variation (COV) of the Cantabro test values was approximately 0.20 for the US-281-AR mixture and between 0.10 and 0.39 for the I-35-PG mixture. These magnitudes are comparable to those obtained in the HWTT and smaller than those calculated for the OT results as subsequently presented. Results from t-tests at a 95 percent significance level conducted using the Cantabro loss data at the OAC showed for the US-281-AR mixture that the average loss in the dry condition is statistically different from that in the other conditions (wet, temperature, and 3 and 6 months aged). The same conclusion is valid for the I-35-PG mixture, except that the average loss in the dry and wet conditions are statistically equivalent at a 95 percent significance level.

5.3.2. Effect of Material Quality on Cantabro Loss

Comparison of the results presented in Figure 31 illustrates the impact of different material combinations on the mixture resistance to disintegration evaluated using Cantabro loss. The US-290-AR and US-281-AR mixtures were produced with the same type of binder and their OAC differs by 0.3 percentage points, but the aggregate composition was substantially different (Figure 31). The differences in the Cantabro loss values in dry and temperature condition for these two mixtures are mainly related to the effect of the type of aggregate on mixture resistance to disintegration as discussed subsequently. The same comparison can be established when comparing the I-35-PG and US-59Y-PG mixtures, which were fabricated with similar asphalts and their OAC differs by 0.3 percentage points, but again the aggregate composition was different.

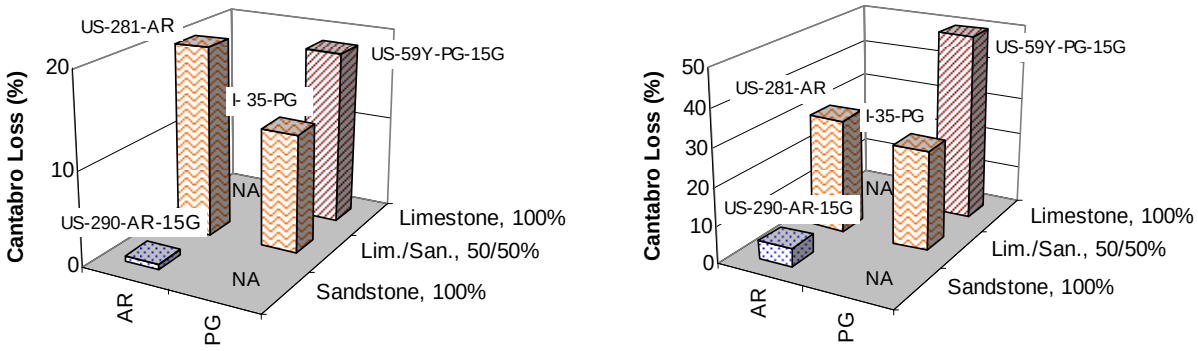

(a) (b)

NA: Information is not available.

Figure 31. Cantabro Loss Comparison at Optimum Asphalt Content (OAC) for (a) Dry and (b) Temperature Conditioned Specimens.

The differences in Cantabro loss may be partially related to differences in water accessible AV content as discussed in the next section. However, the influence of this parameter in this comparison is believed to be minimized as the AV contents of the specimens were similar according to data provided in Table 20. In addition, although the compaction energies were different in order to reach similar AV contents in specimens of diverse mixtures, the fact that most of the compaction is completed (i.e., stone on stone contact was achieved and at least 70% of the total reduction in high generated during compaction was obtained) with 15 gyrations of the SGC permits the comparison of the Cantabro loss as discussed. Thus, the differences in Cantabro loss can be related at least to two other mechanisms: (1) aggregate breakage during compaction and (2) asphalt-aggregate interaction.

First, higher Cantabro loss values are expected as the mixture become more prone to disintegration due to the presence of unbonded aggregate particles produced by crushing. Direct observation of both laboratory compacted specimens and road cores cut in the laboratory showed evidence of aggregate crushing induced by compaction (Figure 32). This phenomenon affected mainly the soft limestone used in the mixtures studied. Watson et al. *(8)* also reported aggregate breakage of OGFC induced by compaction. Specimens compacted by applying 30 and 60 gyrations of the SGC exhibited similar breakdown.

Figure 32. Aggregate Breakage Due to Compaction (I-35-PG Mixture).

Second, the reduced Cantabro loss in the US-290-AR and I-35-PG mixtures compared to that computed for the US-281-AR and US-59Y-PG mixtures, respectively, can most likely be associated with a better interaction (higher work of adhesion) between aggregate and asphalt in the US-290-AR and I-35-PG mixtures, which contain aggregates of comparatively higher quality. Additional research performed to evaluate the surface energy of the aggregates and asphalts used in these four mixtures and respective calculations of work of adhesion in both wet and dry conditions do not show a defined relationship between work of adhesion and Cantabro loss. As discussed in Section 5.7.2, another parameter related to the mechanical response of the mixture is required to fully explain the mixture response.

Since the aggregate composition and the water accessible AV contents are approximately equal for the US-281-AR and the I-35-PG mixtures, the magnitude of the differences in Cantabro loss between these specific mixtures (Figure 31) shows that the type of binder also plays a role in the mixture resistance to disintegration and therefore possibly to raveling. Finally, comparing the differences in Cantabro loss of the four mixtures integrated in Figure 31, leads to the conclusion that the influence of aggregate type is greater than that of the binder. Dissimilarities in gradation between AR and PG mixture systems may also be related to the differences in Cantabro loss of these two types of mixtures, although this aspect may be indirectly reflected in the Cantabro loss through AV content and the effect of different OAC in these mixtures.

Figure 33 shows the average Cantabro loss values measured for plant mixture specimens and respective average total AV contents computed using the vacuum method. These average Cantabro loss values were obtained from two specimens in each case except by those corresponding to the IH-20-PG wet conditioned mixture and IH-30-PG temperature conditioned mixture, which are results based on one available specimen. Due to differences in AV contents, the Cantabro loss values shown in Figure 33 were not directly compared to those presented in Figure 31. However, the comparison of data presented in Figure 33 illustrates similar tendencies to those shown in Figure 31, except for the values determined for the I-35-PG and US-59Y-PG mixtures. The inversion of Cantabro loss values of these mixtures can be related to the variability of this parameter.

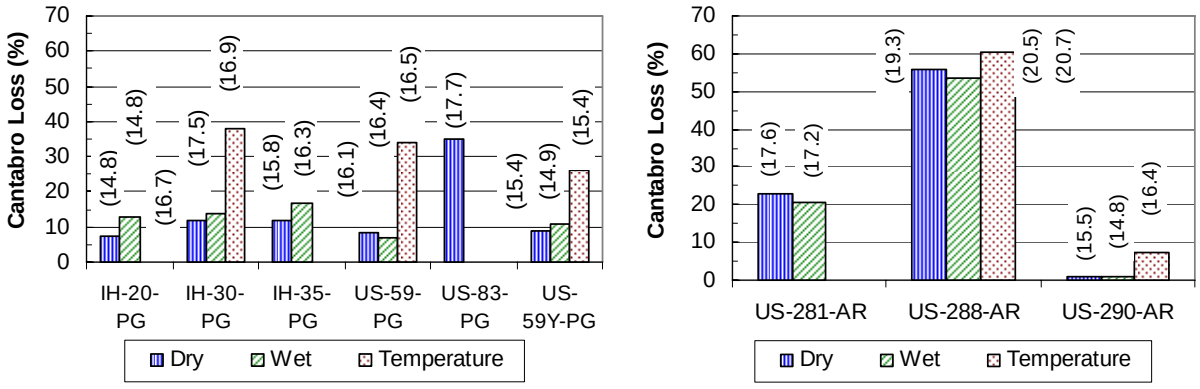

Figure 33. Cantabro Loss of Plant Mixture Specimens for (a) PG and (b) AR mixtures.

The comparison of the Cantabro loss values shown in Figure 33, for mixtures compacted at similar total AV contents and fabricated with different aggregates (Table 2) but similar AR and PG asphalts in each of these mixture groups, illustrates the effect of these variables as discriminated by the Cantabro test. The subsequent discussion provides additional rationale for: (1) the possibility of using the Cantabro test as an initial screening tool for selecting the best material combinations to include in more advanced testing toward selection of the OAC as previously discussed and (2) the relative importance of asphalt and aggregate in the mixture resistance to disintegration evaluated in the laboratory.

The comparison of the Cantabro loss obtained for the US-83-PG, IH-20-PG, and US-59Y-PG mixtures, fabricated using limestone from thee different sources and similar PG

asphalts, illustrates the important impact of each particular combination of materials on the mixture resistance to disintegration. In this case, differences in both asphalt and aggregate material properties may explain the substantial differences in Cantabro loss of these mixtures that have similar compositions.

On the other hand, the effect of two aggregate combinations can be observed by comparing the Cantabro loss values (i.e., resistance to disintegration) of the I-35-PG and US-59-PG mixtures constructed with sandstone and limestone and granite and limestone, respectively. Similarly, Cantabro loss values ordered by increasing magnitude for the AR mixtures (Figure 33b) were reported for the US-290-AR, US-281-AR, and US-288-AR mixtures, which contain sandstone, sandstone and limestone, and granite and limestone, respectively. These results again show the effect of specific materials combinations in terms of Cantabro loss values.

5.3.3. Effect of Air Voids Content on Cantabro Loss

In addition to the impact of the combination of materials, the Cantabro loss in both mixture systems (PG and AR) showed a direct relation with AV content, which is in agreement with previous research on the impact of density and corresponding AV content on field performance of PA and OGFC. In Spain, inadequate compaction has been identified as one of the causes of rapid failure (i.e., raveling) of PA mixtures (*3*), and Huber concluded that OGFC is more susceptible to raveling than dense-graded HMA when low densities are obtained (*32*). Figure 34 shows the coefficients of correlation (CC) obtained for Cantabro loss and AV content. The Cantabro loss values showed a better relationship with water accessible AV content than with total AV content. Water accessible AV as connected pathways of mixture discontinuities can initiate mixture disintegration if they act as potential interconnected fracture paths. Data shown in Figure 34 provide rationale for recommending evaluation of PFC durability in terms of water accessible AV content instead of total AV content.

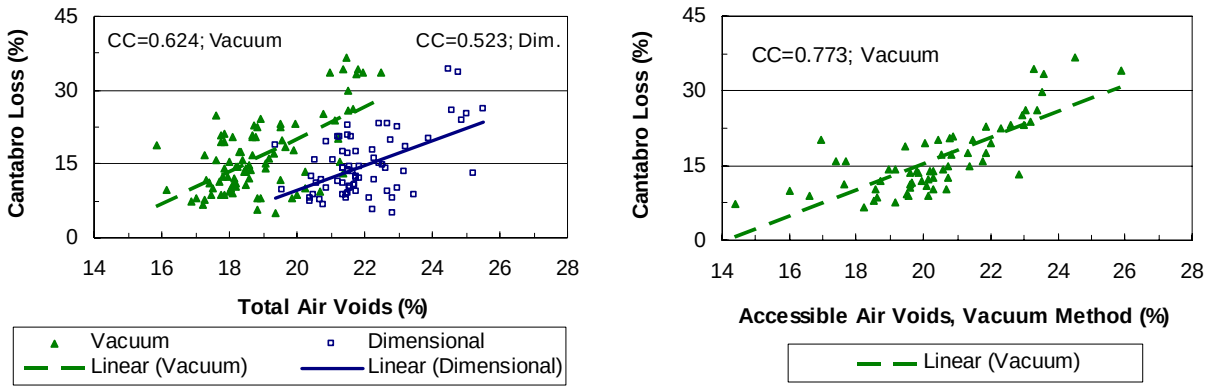

(a) (b)

Figure 34. Cantabro Loss (Dry Condition) Compared to Total Air Voids (a) and Water Accessible Air Voids (b) for I-35-PG and US-281-AR Mixtures.

5.4. EVALUATION OF HAMBURG WHEEL-TRACKING TEST AND OVERLAY TEST RESULTS

Figure 35a shows the rut depth and respective COV determined for the I-35-PG and US-59Y-PG mixtures after applying 20,000 load cycles in the HWTT, and Figure 35b shows the number of cycles required to reach a rut depth of 12.5 mm and respective COV for the US-281-AR and US-290-AR mixtures. These different types of testing are defined in Tex-242-F for rut resistant mixtures (Figure 35a) and for mixtures more susceptible to rutting (Figure 35b). The average values obtained for the I-35-PG mixture define the expected tendency corresponding to higher rut depths as the asphalt content increases, whereas the US-281-AR data do not indicate the same trend. However, in these two cases the variability plays an important role in the results and makes it difficult to assess the impact of asphalt content on the rut resistance of these mixture systems. These results agree with previous studies that indicate that the variability in the HWTT results should be included in evaluating dense-graded HMA (*33*). Data collected in this study suggest that a COV of approximately 0.15 is a representative value, although extreme values of 0.57 and 0.02 suggest that this index can vary substantially.

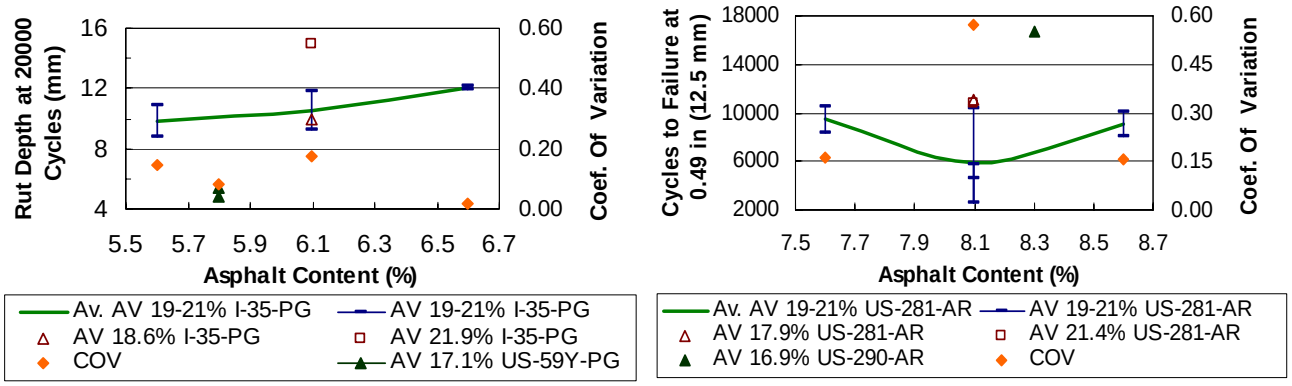

(a) (b)

Figure 35. Hamburg Wheel-Tracking Test Results for (a) I-35-PG and US-59Y-PG and (b) US-281-AR and US-290-AR Mixtures.

The impact of AV content on HWTT results is not completely defined, most likely due to the variability in the testing results. For example, the US-281-AR mixture specimens with AV contents of 17.9, 19.8, and 21.4 percent showed similar numbers of cycles to failure. However, the smaller AV content of specimens from the US-59Y-PG and US-290-AR mixtures (compared respectively to their PG and AR counterpart) may explain the improved performance of the US-59Y-PG and US-290-AR mixtures in the HWTT. Additional data are required to establish rutting resistance as a function of AV content in PFC mixtures.

The cracking life values (expressed as number of cycles to failure) and respective COV obtained from the OT are shown in Figure 36. While the I-35-PG mixture data represent the expected tendency (longer cracking life should be obtained as the asphalt content increases), the US-281-AR mixture may reflect the improvements that a higher asphalt content should offer. Substantially higher COV were obtained with the OT data, especially for the AR mixture system, as compared to the HWTT and the Cantabro test data. Data gathered as part of this study suggest that a COV of approximately 0.30 is a representative value, although extreme magnitudes of 0.78 and 1.17 for the AR mixtures suggest that this index can vary substantially for the OT. This variability is expected to contribute substantially to any conclusions drawn from the data.

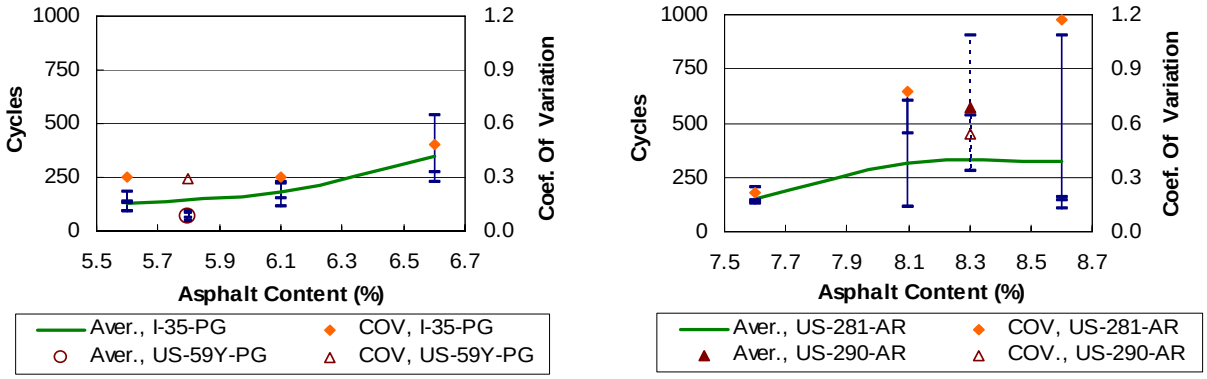

(a) (b)

Figure 36. Overlay Test Results for (a) I-35-PG and US-59Y-PG and (b) US-281-AR and US-290-AR Mixtures.

The impact of total AV content on cracking life is shown in Figure 37. This data set provides evidence of a poor relationship between these variables for the PFC mixtures studied. The high variability of the cracking life values determined for both the laboratory and the plant mixtures is an additional element that impedes establishment of the response of the mixture in terms of AV content and cracking life. The amount, distribution, but probably most important, the ratio of voids size to sample dimensions (6 in. [150 mm] long by 3 in. [75 mm] wide by 1.5 in. [38 mm] high) probably have an important impact on the variability of the cracking life values because the voids may be large enough to influence the development of cracking during the test.

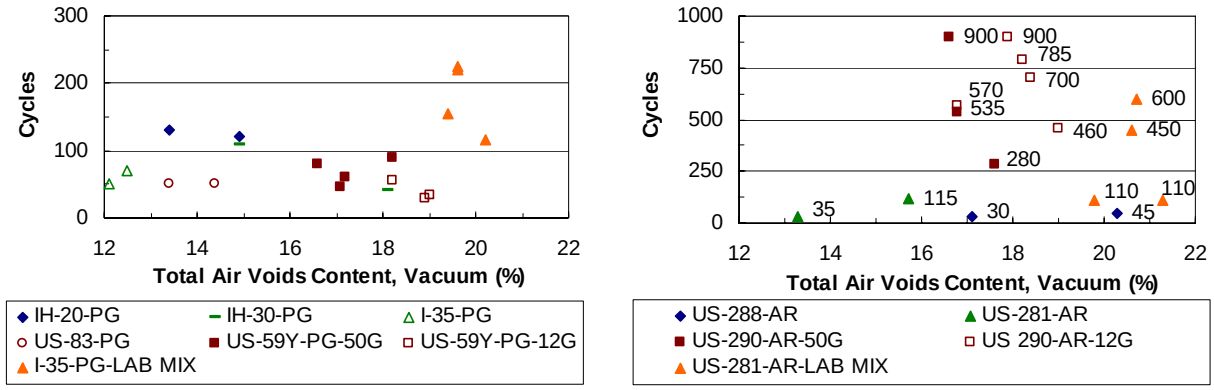

(a) (b)

Figure 37. Comparison of Overlay Test Results for (a) PG and (b) AR Plant Mixtures.

5.5. EVALUATION OF TENSILE STRENGTH RATIO RESULTS

Figure 38 shows the results of the moisture susceptibility evaluation for the I-35-PG mixture performed using two replicate tests at each asphalt content. These data show that the tendency defined for the TSR for this particular mixture does not clearly define an OAC. The number of specimens required to perform the test (eight for each mixture), the time involved to complete the test, and the lack of a conclusive tendency as a function of asphalt content did not motivate additional efforts to further evaluate the applicability of this test for PFC mix design purposes.

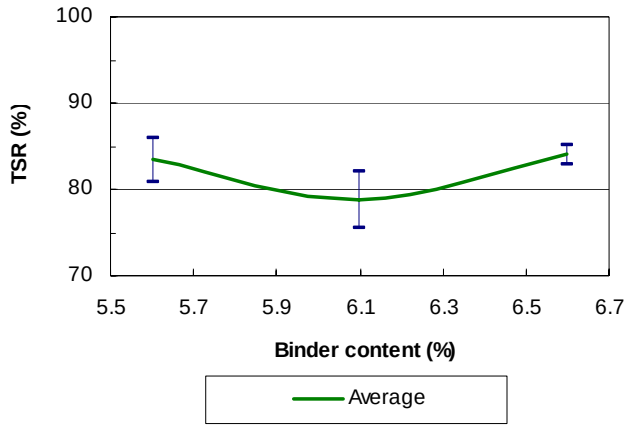

Figure 38. Tensile Strength Ratio for I-35-PG Laboratory Mixture.

5.6. COMPACTION EFFECTS ON DURABILITY

Researchers evaluated the impact of the compaction energy on durability in the laboratory through HWTT, OT, and Cantabro tests performed on specimens compacted at both 15 and 50 gyrations of the SGC (denoted as 12G and 50G, respectively). The Cantabro loss values determined on specimens produced at these two different compaction energies for both the US-290-AR and US-59-PG plant mixtures are shown in Figure 39a. Data corresponding to wet specimens for the US-290-AR mixture fabricated by applying 15 gyrations are not included because these specimens disintegrated during the water conditioning processes (i.e., immersion at 140°F [60°C]). However, specimens compacted at 50 gyrations and subjected to the same

conditioning process did not show this type of premature failure. US-290-AR specimens fabricated by applying both 12 and 50 gyrations disintegrated after aging at 140°F (60°C) for less than one month. The mixture shape adopted by the failed specimens (Figure 39b) suggested that the material failed by creep when the asphalt viscosity was reduced due to the increased temperature.

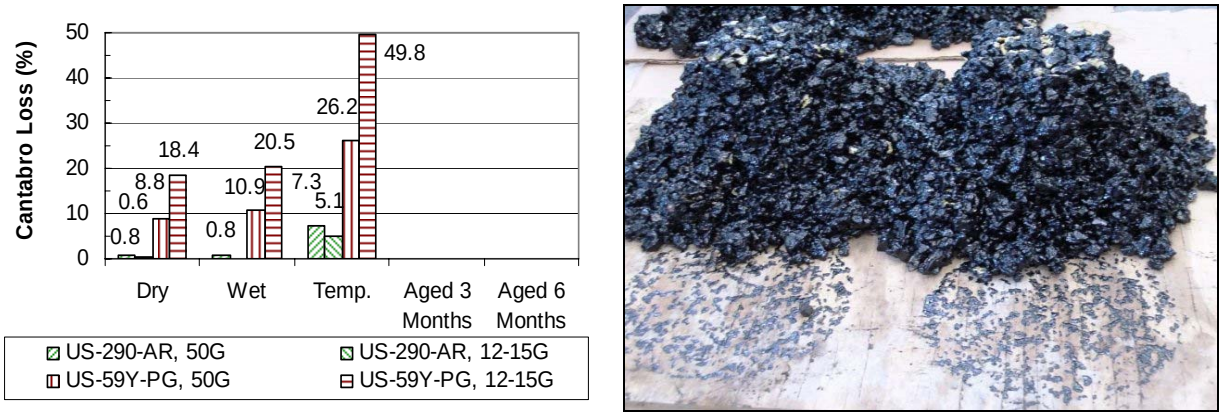

(a) (b)

Figure 39. (a) Effect of Compaction Energy on Cantabro Loss and (b) US-290-AR Mixture Failure at High Temperature (140°F [60°C]).

The occurrence of the same type of failure in specimens compacted at both 15 and 50 gyrations can be related to an excess of asphalt that facilitates the creep mechanism. An indication of the high binder content is the asphalt deposit observed where the specimens were originally located for the aging process (bottom of Figure 39b). This type of asphalt accumulation, which can correspond not only to the asphalt present at the specimen surface but probably also to draindown, was not observed in any other PFC mixture subjected to the same conditions. The draindown evaluation performed as part of the US-290-AR mix design provided by TxDOT did not show draindown susceptibility. The described failure occurred in laboratory conditions (i.e., unconfined compacted mixture), and at present there is no direct indication of stability problems in the field. However, this case should be evaluated to establish if stability problems are later revealed in the field.

The US-59Y-PG mixture exhibited a 100 percent increase in Cantabro loss when the energy of compaction was reduced to reproduce the AV content achieved in the field. This response indicates an important reduction of the mixture resistance to disintegration, and was

consistently observed for dry, wet, and temperature conditioned specimens. On the other hand, smaller Cantabro loss values were obtained for the US-290-AR mixture specimens compacted at 15 gyrations and tested in both dry and low temperature conditions, compared to specimens compacted at 50 gyrations.

These results showed a reduced influence of AV content on the response of the US-290-AR mixture at low and at room temperatures, which is expected since at these temperatures the relatively high amount of asphalt bonding the granular particles benefits the resistance to disintegration, but at high temperature the effect is reversed as the high asphalt content can lubricate the particle contacts and reduce the mixture stability. At low and room temperatures, the proper asphalt-aggregate interaction in this mixture is an important additional factor that positively impacts the resistance to disintegration and reduces the Cantabro loss values as discussed in Section 5.7. The response of the mixtures studied preliminarily suggests that for those mixtures with poor aggregate-asphalt interaction the mixture AV content has a more pronounced effect on the mixture resistance to disintegration.

HWTT results presented in Table 21 indicate a substantial improvement in rut resistance for the PFC mixtures studied and compacted at 50 gyrations compared to that determined on specimens compacted at 12 gyrations. Ultimately, these results provide evidence of the importance of controlling the AV content to guarantee adequate permanent deformation performance for a particular mixture. The improvement in mixture performance will be a result of the reduced deformability of mixtures that have fully developed stone-on-stone contact.

Table 21. Effect of Compaction Energy on Hamburg Wheel-Tracking Test Results.

Mixture	Asphalt Content	Comp. Energy (SGC Gyrations)	Average Total AV Content, Vac. Method	Cycles to Failure @ 12.5 mm	Rut Depth @ 20000 Cycles (mm)
US-290-AR	8.3	12	19.9	7550	-
		50	16.9	16700	-
US-59Y-PG	5.8	12	22	-	11.41
		12	22.3	-	8.96
		50	17.6	-	4.82
		50	16.2	-	5.43

OT results shown in Figure 40 indicate the effect of compaction energy on cracking life. For the US-59Y-PG mixture, cracking life is extended as specimens are fully compacted at 50

gyrations. This result can be related to the improvement of the fracture properties obtained in a less deformable mixture. The results obtained for the US-290-AR mixture did not exhibit this same tendency. Taking into account the variability, the cracking life determined for specimens compacted at 50 gyrations can be equal or even less than that calculated for specimens produced by applying 12 gyrations. The high variability and the lack of defined trends in the results obtained for the AR mixture system evaluated at different compaction levels and different asphalt contents (Figure 36b) might be an indication of the limitations of the OT to capture the response of this particular material.

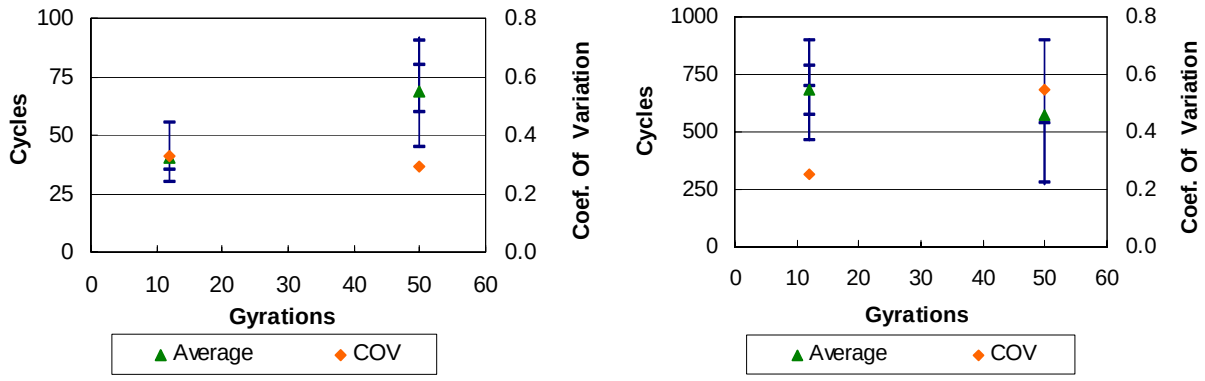

(a) (b)

Figure 40. Effect of Compaction Energy on Cracking Life for (a) US-59Y-PG and (b) US-290-AR Mixtures.

5.7. EVALUATION OF RESULTS OF SURFACE FREE ENERGY AND WORK OF ADHESION CALCULATIONS

Table 22 presents the components and total surface free energy of the aggregates tested, and Table 23 and Table 24 show the same parameters for asphalts computed based on receding and advancing contact angles, respectively. The surface energy of aggregates with similar origins (in this case two limestones and two sandstones) showed important differences in their components related basically to discrepancies in the polar component. The results for the five asphalts classified as PG-76-22 showed that although these materials have the same PG classification, their surface free energy components are different, which induce diverse responses in terms to work of adhesion (related to fracture and healing properties) with the aggregate.

Similar conclusions are valid for the three AR asphalts studied; particularly regarding the differences encountered in the wetting surface free energy components (related to their healing capacity).

Table 22. Components and Total Surface Free Energy of Aggregates (ergs/cm^2).

Aggregate	PFC Mixture	Γ	Γ^{LW}	Γ^{AB}	Γ^+	Γ^-
Limestone	I-35-PG, US-59Y-PG	73.82	49.48	24.34	0.34	433.59
Sandstone	I-35-PG, US-281-AR, US-290-AR	144.67	54.16	90.51	2.84	721.22
Limestone	US-281-AR	95.53	45.17	50.36	1.33	474.99
Sandstone	I-30-PG	94.77	41.46	53.31	1.17	607.45

Note: Γ = total surface free energy, Γ^{LW} = Lifshitz-van der Waals component or non polar component, Γ^{AB} =acid-base component or polar component, Γ^+ = acid component, Γ^- = base component.

Table 23. Components and Total Surface Free Energy of Unaged Asphalts Based on Receding Contact Angles (Dewetting-Fracture).

Mixture	Asphalt	Γ (ergs/cm^2)	Γ^{LW}	Γ^{AB}	Γ^+	Γ^-
I-35-PG	I-35-PG-76-22	40.14	40.13	0.02	0.00	10.37
IH-20-PG	IH-20-PG-76-22	39.07	32.03	7.04	0.53	23.19
IH-20-PG-TR	IH-20-PG-76-22TR	33.56	8.65	24.91	5.08	30.55
IH-30-PG	IH-30-PG-76-22	50.77	39.89	10.87	1.71	17.24
US-59-PG	US-59-PG-76-22	44.27	41.81	2.45	0.07	21.59
US-59Y-PG	US-59Y-PG-76-22	42.05	40.85	1.20	0.06	6.16
US-281-AR	US-281-AR, filtered[1]	40.87	39.53	1.34	0.03	14.52
US-288-AR	US-288-AR, filtered[1]	44.73	41.23	3.50	0.31	9.74
US-290-AR	US-290-AR, filtered[1]	39.01	33.09	5.92	0.47	18.75

[1]Sample prepared by filtering the AR on sieve No. 80

Table 24. Components and Total Surface Free Energy of Unaged Asphalts Based on Advancing Contact Angles (Wetting-Healing).

Mixture	Asphalt	Γ (ergs/cm^2)	Γ^{LW}	Γ^{AB}	Γ^{+}	Γ^{-}
I-35-PG	I-35-PG-76-22	10.98	8.27	2.71	1.83	1.00
IH-20-PG	IH-20-PG-76-22	11.95	6.68	5.27	3.26	2.13
IH-20-PG-TR	IH-20-PG-76-22TR	8.34	6.60	1.74	3.42	0.22
IH-30-PG	IH-30-PG-76-22	20.51	20.12	0.39	0.17	0.23
US-59-PG	US-59-PG-76-22	11.74	8.49	3.25	2.64	1.00
US-59Y-PG	US-59Y-PG-76-22	18.53	17.85	0.68	0.15	0.75
US-281-AR	US-281-AR, filtered[1]	16.96	15.55	1.41	0.21	2.42
US-288-AR	US-288-AR, filtered[1]	14.42	12.37	2.04	0.92	1.14
US-290-AR	US-290-AR, filtered[1]	10.15	4.74	5.41	4.56	1.61

[1]Sample prepared by filtering the AR on sieve No. 80

The IH-20-PG-76-22TR asphalt containing tire rubber showed the smallest dewetting total surface free energy which suggests the lowest resistance to fracture. In addition, it was the only asphalt that exhibited a dewetting polar component higher than the nonpolar component. However, the wetting surface free energy components (associated with the healing ability) exhibit the typical response with a higher nonpolar component as compared to the polar component. Therefore, the healing ability does not seem to be substantially different compared to that of the PG-76-22 asphalts.

In summary, asphalt groups with similar rheological properties exhibited different fundamental material properties in terms of surface energy. Combining these asphalts with aggregates of diverse origin may yield substantially different responses for the asphalt-aggregate interaction and the corresponding mixture performance. Some additional differences may emerge as aging progresses in the field and modifies the surface free energy components of the asphalt. The higher variability observed for the PG asphalts compared to that obtained for the AR asphalts is most probably related to the higher diversity of asphalt sources employed to produce PG asphalts. The three AR asphalts studied were modified asphalts fabricated using the same asphalt source.

Since the I-35-PG-76-22 and US-281-AR asphalts were produced using the same asphalt source, the comparison of their surface free energies illustrated the effect of the respective modifications with polymer and with AR. In terms of dewetting surface free energy the change is

minimal, which implies approximately equivalent fracture resistance for both asphalts when interacting with the same aggregate. However, important differences were determined for the wetting surface free energy, thus changing the healing capacity of the PFC mixture. Less short-term healing capability is expected from this AR asphalt as compared to this PG asphalt because of the higher nonpolar wetting, Γ^{LW}, component calculated for the AR asphalt. In addition, less long-term healing ability is expected from the AR asphalt given the smaller polar component, Γ^{AB}.

In summary, comparable fracture resistance would be expected for mixtures fabricated with these AR and PG asphalts and the same aggregate, but the AR asphalt would have less healing ability. Therefore, better performance may be expected for this PG mixture, although as discussed in detail by Lytton et al. (*28*), other factors related to the aggregate gradation and properties of the asphalt and mixture can also influence mixture performance. In addition, the comparison presented previously assumed that both asphalts were produced using asphalt from comparable production batches, but data did not prove this aspect. Different production batches can lead to important differences in asphalt surface free energy values. For example, an evaluation of surface free energy conducted on samples taken in 2006 and 2007 for the PG-76-22 asphalt used in the I-35-PG mixture showed a difference of 40 percent in the wetting total surface free energy.

5.7.1. Work of Adhesion

The adhesive dewetting and wetting works of adhesion for both dry and wet conditions and corresponding dry to wet works of adhesion ratios (ER_1) are presented in Table 25 and Table 26, respectively. Higher ER_1 values indicate asphalt-aggregate combinations less sensitive to moisture damage because these values correspond to the minimum work of adhesion in wet condition that implies less thermodynamic potential for water to cause debonding.

Table 25. Adhesive Dewetting Work of Adhesion for Both Dry and Wet Conditions.

Mixture	Aggregate	Work of adhesion-dry W_{AS}^{dry} (ergs/cm^2)			Work of adhesion- wet W_{ASW}^{wet} (ergs/cm^2)			$ER_1 = \left\lvert \frac{W_{AS}^{Dry}}{W_{ASW}^{wet}} \right\rvert$
		W_{AS}^{dry}	$W_{AS}^{dry,LW}$	$W_{AS}^{dry,AB}$	W_{ASW}^{wet}	$W_{ASW}^{wet,LW}$	$W_{ASW}^{wet,AB}$	
I-35-PG	Limestone	93.0	89.1	3.9	-135.0	7.9	-142.9	0.69
I-35-PG	Sandstone	104.2	93.2	11.0	-198.8	9.0	-207.8	0.52
US-59Y-PG	Limestone	102.9	89.9	12.9	-120.6	8.1	-128.8	0.85
IH-30-PG	Sandstone	154.9	81.3	73.5	-133.6	5.8	-139.5	1.16
US-281-AR	Limestone	101.0	84.5	16.5	-146.9	6.6	-153.6	0.69
US-281-AR	Sandstone	114.8	92.5	22.3	-195.5	8.7	-204.2	0.59
US-290-AR	Sandstone	136.0	84.7	51.3	-179.7	5.8	-185.6	0.76

Table 26. Adhesive Wetting Work of Adhesion for Both Dry and Wet Conditions.

Mixture	Aggregate	Work of adhesion-dry W_{AS}^{dry} (ergs/cm^2)			Work of adhesion- wet W_{ASW}^{wet} (ergs/cm^2)			$ER_1 = \left\lvert \frac{W_{AS}^{Dry}}{W_{ASW}^{wet}} \right\rvert$
		W_{AS}^{dry}	$W_{AS}^{dry,LW}$	$W_{AS}^{dry,AB}$	W_{ASW}^{wet}	$W_{ASW}^{wet,LW}$	$W_{ASW}^{wet,AB}$	
I-35-PG	Limestone	98.0	40.5	57.6	-88.9	-8.5	-80.4	1.10
I-35-PG	Sandstone	118.5	42.3	76.1	-143.5	-9.6	-133.9	0.83
US-59Y-PG	Limestone	76.7	59.4	17.3	-111.7	-2.1	-109.6	0.69
IH-30-PG	Sandstone	79.0	57.8	21.3	-146.2	-0.6	-145.5	0.54
US-281-AR	Limestone	76.4	53.0	23.4	-129.7	-3.0	-126.7	0.59
US-281-AR	Sandstone	87.7	58.0	29.6	-180.8	-3.9	-176.9	0.48
US-290-AR	Sandstone	151.0	32.0	118.9	-115.1	-13.4	-101.7	1.31

The comparison of the I-35-PG-76-22 and US-281-AR asphalts is further discussed subsequently in terms of the work of adhesion computed for the combination of these asphalts and sandstone, which was the same in both the I-35-PG and US-281-AR mixtures. The dry dewetting work of adhesion is higher for the AR asphalt as compared to that for the PG asphalt, but in a wet condition this parameter has approximately the same magnitude. The relationship of these works of adhesion expressed as the ER_1 ratio suggests better performance for the AR-sandstone combination in terms of fracture resistance.

On the other hand, the analysis of the wetting work of adhesion for the same combinations in both dry and wet conditions provides evidence of better short- and long-term healing abilities and higher total amount of healing for the PG-sandstone combination. As stated by Lytton (*29*), since longer times elapse between successive load applications (resting periods) compared to those of load applications generated by transient loads, healing response has an

important effect on mixture performance. The combination of fracture and healing responses may substantiate better performance for the PG-sandstone combination compared to that expected for the AR-sandstone combination, but as indicated in the previous section, other factors need to be taken into account to fully predict mixture performance.

The evaluation of the work of adhesion for the AR-sandstone combination of mixture US-290-AR (fabricated with the same sandstone in the I-35-PG and US-281-AR mixtures) shows that in this case the AR combination has an even better fracture resistance and healing ability compared to those of the PG-sandstone combination for the I-35-PG mixture and the AR-sandstone combination for the US-281-AR mixture. The comparisons previously stated and data provided in Table 25 and Table 26 provide evidence for the possibility of selecting the best material combinations to maximize the performance of the mixture and illustrate the difficulties encountered in judging the quality of individual component materials (aggregates or asphalts) instead of conducting this judgment based on a comparison of the interaction determined for different material combinations.

5.7.2. Relationship of Cantabro Loss and Bond Strength

Figure 41 and Figure 42 show the comparison of work of adhesion in both dry and wet conditions and Cantabro loss for the main plant and laboratory mixtures and for the plant mixture specimens. Although the work of adhesion values in a wet condition are all negative, they were plotted as positive magnitudes to facilitate the comparison with the Cantabro loss.

These comparisons do not show a defined relationship between work of adhesion and Cantabro loss, which impedes explaining the mixture resistance to disintegration based only on the asphalt-aggregate interaction. This is a consequence of the fact that the work of adhesion does not capture the entire complexity of the mixture response. For example, the stress-strain response, which can be modified not only by the asphalt properties but also by the asphalt content and the aggregate gradation, is not integrated. This fact provides evidence of the necessity of generating a design procedure based on an analytical model that combines both physical and chemical properties of the PFC mixture.

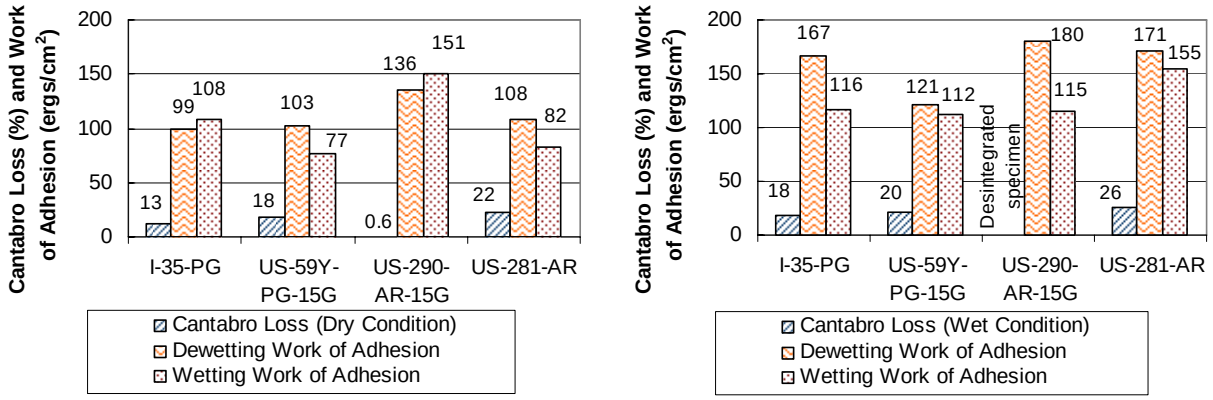

(a) (b)

Figure 41. Cantabro Loss and Work of Adhesion Comparison in (a) Dry Condition and (b) Wet Condition for the Main Laboratory and Plan Mixtures.

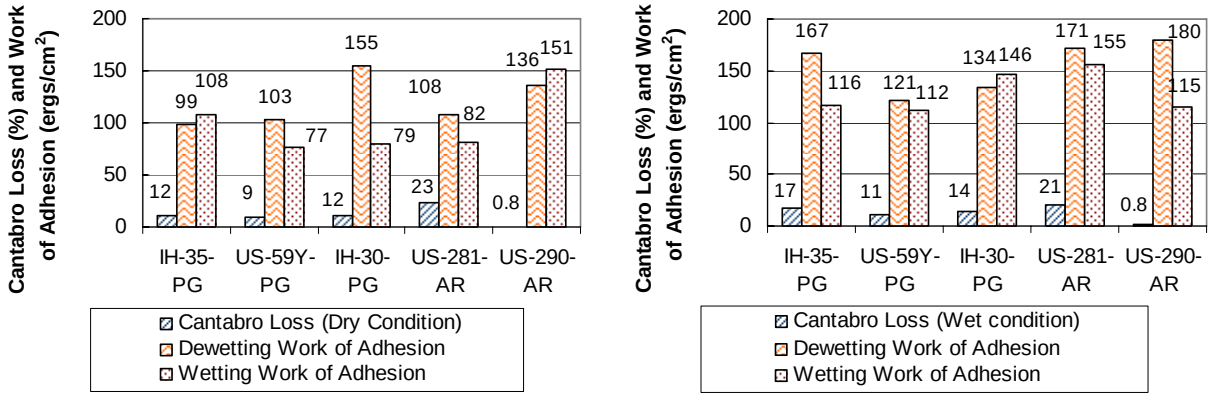

(a) (b)

Figure 42. Cantabro Loss and Work of Adhesion Comparison in (a) Dry Condition and (b) Wet Condition for Plant Mixtures.

At present, for PFC mixtures there is not any analytical performance model available that incorporates the work of adhesion, or any other fundamental material property, to predict mixture performance (i.e., durability life). The results exposed in this and in previous sections for the evaluation of different durability tests show the necessity of this analytical model to overcome the limitations of the phenomenological approaches that govern PFC mixture evaluation and design and to incorporate advanced characterization tools as part of the PFC analysis.

5.8. COMPARISON OF ASPHALT RUBBER AND PERFORMANCE GRADE MIXTURE SYSTEMS

AR and PG mixture systems are compared in this section based on the previous durability evaluation. The comparison of both mixture systems was established based on data gathered for the I-35-PG and US-281-AR laboratory mixtures due to their similarity in aggregate composition and AV contents. At the OAC established from volumetric mixture properties (6.1 and 8.1 percent for the I-35-PG and US-281-AR mixtures, respectively) and for all Cantabro conditions except low temperature, the I-35-PG mixture exhibited smaller Cantabro losses as compared to the US-281-AR mixture (Figure 28 and Figure 29). This result could be an indication of better resistance to disintegration of the PG mixture system, assuming the same aggregate is used.

However, the ratios of Cantabro loss established for the I-35-PG mixture (Figure 43) indicate that the proportional impact of the conditioning processes, which may represent the modification that the binder properties can experience in the field, is higher for the PG mixture system compared to the AR mixture system. The ratios of temperature to dry Cantabro loss shown in Figure 43 suggest that the effect of low temperature on the Cantabro loss could be higher in PG mixtures than in AR mixtures. This result may have an important impact on the mixture response to disintegration in the field when temperature decreases and the binder becomes stiffer.

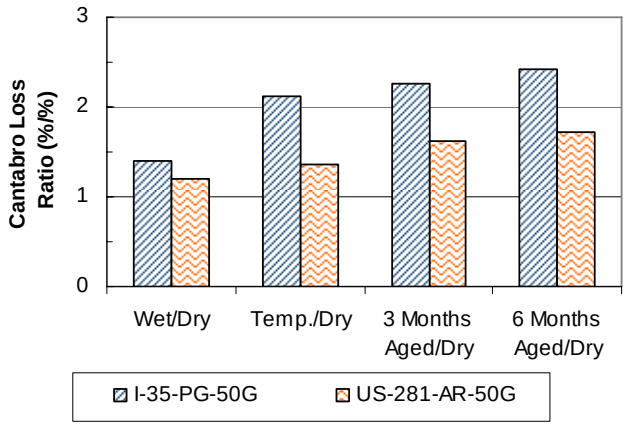

Figure 43. Cantabro Ratio at Optimum Asphalt Content (OAC) for Different Conditioning Processes.

A comparison of the rut depth obtained for both the US-281-AR and I-35-PG mixtures shows higher rut resistance in the HWTT for the PG mixture compared to the AR mixture. This comparison is reasonable in terms of similar materials and comparable AV contents, but the result is limited by the fact that the aggregate gradations are different as required by the specifications. The OT results showed greater maximum number of cycles to failure for the AR mixture system, which may indicate longer cracking life for this system. However, this conclusion is affected by the large variability in the number of cycles to failure quantified using the OT.

In summary, the PG mixture system showed better response in the Cantabro test, the HWTT, and the OT, and general trends are as expected with increases in binder content compared to those obtained with the AR mixture system. The high variability and the lack of defined trends in the results obtained for the AR mixture system might be an indication of the limitations of these tests to capture the response of this particular material. However, the lack of defined trends in the mixture response as the AR binder content increases can be associated with limited development of the potential modification that the crumb rubber might induce in the binder due to the large particle size of the specified crumb rubber. As suggested in previous research, smaller crumb rubber particles (0.007 in. [0.18 mm] in diameter) can more easily promote the formation of a tridimensional network of rubber within the AR binder that can substantially change its rheological properties (*34*).

5.9. SUMMARY AND RECOMMENDATIONS

Researchers evaluated different tools that could be applied for mix design and laboratory performance determinations in terms of moisture susceptibility, aging potential, and permanent deformation. They limited this assessment to laboratory determinations because field data on long-term performance in terms of durability were not available at this time to define actual service life of PFC mixtures, failure mechanisms, and their relation with laboratory evaluations. The following conclusions are stated based on the results and previous discussion:

- Draindown evaluations conducted in this study and the information collected based on interviews conducted with selected TxDOT district personnel and mix design results of the plant mixtures evaluated did not reveal the existence of draindown problems in PFC mixtures.

- Considering the variability in the testing results gathered in this study, time involved for actual testing, and ease of specimen fabrication to meet specific AV content ranges, the Cantabro test is recommended over the TSR, HWTT, and the OT.
- The Cantabro test was sensitive to changes in chemical and viscoelastic properties of the asphalt induced by the conditioning processes applied in this study (dry, wet, low temperature, and aging), providing an indirect indication of the potential impact of these changes on mixture resistance to disintegration.
- The Cantabro loss values of the mixtures evaluated in this study suggest that aggregate properties impact mixture performance more than those of the asphalt. These results also indicate that the Cantabro test can be used as a screening tool for PFC mix design.
- The Cantabro loss values showed a direct relationship with water accessible AV content, providing evidence of the importance of the volumetric properties on PFC mixture durability. Similarly, HWTT laboratory results provided rationale of the importance of controlling the AV content to guarantee adequate permanent deformation resistance in PFC mixtures. These laboratory findings support the necessity of establishing field compaction controls given the substantial differences in total AV contents for specimens compacted in the laboratory (PMLC) and in the field (road cores) reported in Chapter 3.
- The trends and the variability in Cantabro loss values obtained for the mixtures included in this study suggest that the Cantabro test may not provide enough sensitivity to become a definitive tool for selecting the OAC of PFC mixtures from the point of view of durability. However, the Cantabro test is a simple and quick test that may be useful as an initial screening tool for selecting material combinations to include in more advanced testing toward selection of the OAC.
- A defined tendency was not found for the comparison of work of adhesion (based on surface free energy measurements) and Cantabro loss (used in the comparison after identifying it as the best currently available tool for mixture evaluation), which impedes explaining the mixture resistance to disintegration based only on the asphalt-aggregate interaction computed by the work of adhesion.
- Therefore, additional research to develop an improved mix design system based on an analytical model that combines both physical and chemical properties of the PFC mixture to evaluate its durability supported by material properties and analytical techniques is

recommended. Potential advantages of this type of approach include less variability, better understanding of material response, and an improved relationship with field performance for design and remaining life evaluations. In the absence of this or any other analytical model for PFC mixtures, the Cantabro test can be temporarily used for mix design purposes. Since no field performance data are available at present to define maximum Cantabro losses for PFC mixtures, 20 and 35 percent are suggested as limits for Cantabro loss in dry and wet conditions, respectively, based on previous research. Further research is required to evaluate these tentative limits.

- A preliminary comparison of mixtures fabricated using both the PG (which includes PG-76-22 asphalt, lime, and fibers) and the AR (asphalt with a minimum of 15 percent by weight of asphalt of Grade C or Grade B crumb rubber) mixture systems showed that the PG provided better resistance to disintegration, permanent deformation, and cracking. However, the high variability and the lack of defined trends in the results obtained for the AR mixture system might be an indication of the limitations of the evaluated tests to capture the response of this particular material, which can limit this comparison.

The following recommendations are provided based on the conclusions and analysis developed from data gathered during this study:

- Use the draindown test (Tex-235-F) for mix evaluation and design.
- Utilize the Cantabro test in both dry and wet conditions to evaluate mixture durability in the laboratory and subsequent selection of the OAC. Maximum losses of 20 and 35 percent should be required for the Cantabro loss in dry and wet conditions, respectively, when the test is conducted at room temperature (77°F [25°C]).
- Specify density requirements for field compaction.
- Direct future research efforts toward the development of a more fundamental analytical model that provides a better understanding of PFC mixture performance and a more reliable mix design method.

6. PFC BINDER RHEOLOGY AND AGING DURABILITY

6.1. INTRODUCTION

PFC mixtures present unique requirements for asphalts. Because of the open-grade mixture and thick asphalt films, road engineers must take care that the asphalt not be susceptible to draindown once it is in place. This requires a stiffer asphalt than would normally be used in a dense-graded mixture. Furthermore, because of the increased porosity of the PFC mixtures, the asphalts may be more susceptible to oxidative aging than are dense-graded mixtures, although such a hypothesis has not been proven, as yet. Finally, upon oxidation the asphalt should remain ductile for as long as possible in order to avoid cracking of the asphalt under load and consequent raveling of the layer.

Because of these criteria the asphalts used in PFC mixtures are polymer-modified materials, typically a PG-76-22 modified asphalt, or an AR that contains approximately 18 percent ground tire rubber blended with the base asphalt. As seen from the data presented in this chapter, these materials are two rather two different kinds of binders and it would be expected that their performance in service might be significantly different.

In this chapter the asphalts are evaluated according to their rheological behavior, as determined by dynamic shear rheometer (DSR) measurements and by ductility and force ductility, all measured at different levels of asphalt aging. The rheological characterizations provide information on the relative contributions of elastic and viscous behavior of the asphalt, important because of the way these properties convert deformation under thermal or traffic load to stress and thus perhaps to failure. The ductility and force ductility measurements provide an indication of these stresses and of the manner in which the asphalts might fail under load.

The levels of aging studied span from unaged asphalt to a level that would represent several years in a conventional dense-graded mixture and probably several years as well in a PFC layer, although the rate of asphalt aging in these types of mixtures and at the surface of the pavement is not yet known. Two intermediate levels of aging also were considered, with one level approximately equivalent to the rolling thin-film oven test (RTFOT) aging (which is considered to approximately match the asphalt aging that occurs in the hot-mix fabrication process). The third level of aging is approximately equivalent to standard pressure aging vessel

(PAV) aging, which is roughly equivalent to hot mix plus transportation plus laydown and cooling with perhaps some additional aging as well. Additionally, all of these aging levels were obtained by oven aging at elevated temperatures (either 90°C [194°F] or 163°C [325°F]). For some of the asphalts, oxidative aging was also conducted in an environmental room (ER) at a much more moderate temperature (60°C) but for an extended period of time, ranging from three to eight months. This aging time would be equivalent to eight to 15 years in dense-graded pavements, but again, an equivalent age for PFC layers is unknown.

This chapter presents several comparisons of the PFC asphalts studied in the course of this project. The first comparison (Section 6.3) is between one AR material and one SBS polymer-modified asphalt as a way of introducing the types of tests that are presented throughout the chapter and the manner in which the different asphalts respond to these tests.

Section 6.4 discusses measurement issues that are specific to the AR asphalts. These asphalts are blends of a base asphalt with rubber particles and thus are decidedly inhomogeneous materials compared to conventional base asphalts and typical modified asphalts. The texture of the AR is very grainy and the presence of particles is obvious, and there are differences in the rheology as well. These differences present some specific difficulties with respect to measuring the rheology and with respect to the results that are obtained in terms of asphalt rheology, ductility, and force ductility, and these differences are discussed in this part of the chapter.

Section 6.5 presents data on the PG polymer-modified asphalts that contain SBS or a blend of SBS and well-digested tire rubber. These materials are much more homogeneous in appearance than the AR materials and also possess significantly different rheological characteristics. This section also includes the small amount of data that were obtained on asphalts that were extracted and recovered from PFC road cores.

Section 6.6 presents a brief comparison of the polymer-modified PFC asphalts to polymer-modified asphalts that were previously studied in a prior project and used in dense-graded mixtures. The issue addressed was whether the PFC asphalts behave significantly differently from those that are used in dense-graded mixtures.

6.2. METHODOLOGY

Five polymer modified binders were supplied, aged, and tested: Valero-Houston US-281-AR, Valero-Houston IH-35-PG-76-22 (SBS), Wright/Valero US-288-AR, Alon

IH-20-PG-76-22 SBS, Alon IH-20-PG-76-22TR, Lion IH-30-PG-76-22 SBS, and Fina US-59-PG-76-22. These binders were then subjected to aging by several methods and subsequently to a number of physical tests of rheology and strength.

6.2.1. Aging Methods

Stirred Air-Flow Test (SAFT). This aging method (*35*) simulates changes in the properties of asphalt during conventional hot-mixing processes in lieu of the rolling thin-film oven test (RTFOT). Preheated materials weighing 250 g were placed in an air-flow vessel equipped with an impeller, temperature control sensor, and air-cooled condenser. Air was blown through materials that were heated in a vessel for 35 min at 163°C. The mixing of air and materials was performed by the air flow at a rate of 2000 mL/min and the impeller speed at a rate of 700 rpm.

Pressure Aging Vessel* (PAV*). The purpose of this aging method, modified from the standard PAV procedure, is to simulate long-term asphalt aging after hot-mix aging such as SAFT and RTFOT. Materials with 1 mm film thickness were placed in a PAV pan and aged for 16 hours at 90°C. Pressure and temperature conditions of the test were 2.2 MPa and 90°C, respectively. PAV*16 aging is for 16 hours, while PAV*32 aging is for 32 hours. A total of 85 g of binder and five plates were used for each condition. Each plate contained 17 g of binder, giving a 1 mm thick film.

Environmental Room (ER). Road aging is approximately simulated using an environmental room controlled to 60°C (140°F) and 1 atm air pressure with 25 percent relative humidity. Samples placed in trays measuring 4 cm by 7 cm (0.157 in by 0.276 in) were measured for ductility, resulting in an approximately 1 mm (0.039 in) thick film. The US-281-AR binder was aged in the environmental room at 60°C (140°F) and atmospheric air pressure for 3, 6, and 8 months. Each aging condition used four pans with 20 grams of binder per pan.

6.2.2. Analytical Measurements

Dynamic Shear Rheometer. Complex viscosity (η*) at 60°C and 0.1 rad/s, storage modulus (G'), and dynamic viscosity (η') at 44.7°C and 10 rad/s of asphalt materials were measured using a Carri Med CSL 500 Controlled Stress Rheometer operated in an oscillatory

mode. A 2.5 cm composite parallel plate geometry was used with a 500 μm gap for the SBS and tire rubber (TR) binders, as well as for the AR binders that had been subjected to the extraction and recovery procedure to remove rubber particles. The (unextracted) AR binders were tested with a gap size of 1500 μm to reduce interference with rubber particles. The operating ranges of temperature, angular frequency, and torque were -10 to 99.9°C, 0.1 to 100 rad/s, and 10 to 499,990 dyne-cm, respectively.

Ductility and Force Ductility (FD). Ductility measurements were performed at 15°C and at an extensional speed of 1 cm/min until binder failure. The initial gauge length of the sample was 3 cm. Force ductility (FD) was measured at 4°C on a specimen of initial uniform cross section 1 cm by 0.5 cm (0.039 in by 0.0195 in). Stress as a function of extension ratio was determined from the force measurement and assuming a uniform but decreasing cross section throughout elongation.

Extraction and Recovery. Binder in the road cores was extracted and recovered based on the procedures outlined by Burr et al. (*18*). These procedures provide for a thorough wash and therefore extraction of the binder from the aggregate but with minimal hardening or softening of the binder in the solvent and with care taken to assure complete solvent removal during the recovery process (*18, 36*). The extraction and recovery process uses washes in a 15 percent ethanol/toluene mixture and size exclusion chromatography to assure removal of the solvent from the recovered binder. It should be noted that the more aged binder requires a more extended recovery time in order to remove the solvent from the stiffer, more heavily aged binder.

6.3. A COMPARISON OF ASPHALT RUBBER AND SBS POLYMER-MODIFIED BINDERS

The DSR map data for both the IH-35-PG-76-22 and US-281-AR binders (Figure 44) track a binder as it hardens with oxidative aging and indicate DSR measurements that relate to a typical unmodified binder's 15°C ductility. As a binder ages, it moves across the map, from the bottom right corner towards the top left corner. Accompanying these changes in DSR properties is a decrease in binder ductility. For an unmodified binder a rather good correlation exists between ductility and the DSR function $G'/(\eta'/G')$ (at a reference temperature of 15°C and frequency of 0.005 rad/s), and this correlation is indicated by the lines of constant ductility

(dotted lines) on the DSR map and represented by the equation: Ductility at 15°C, 1 cm/min = $0.23[G'/(\eta'/G')]^{(-0.44)}$ (*37*).

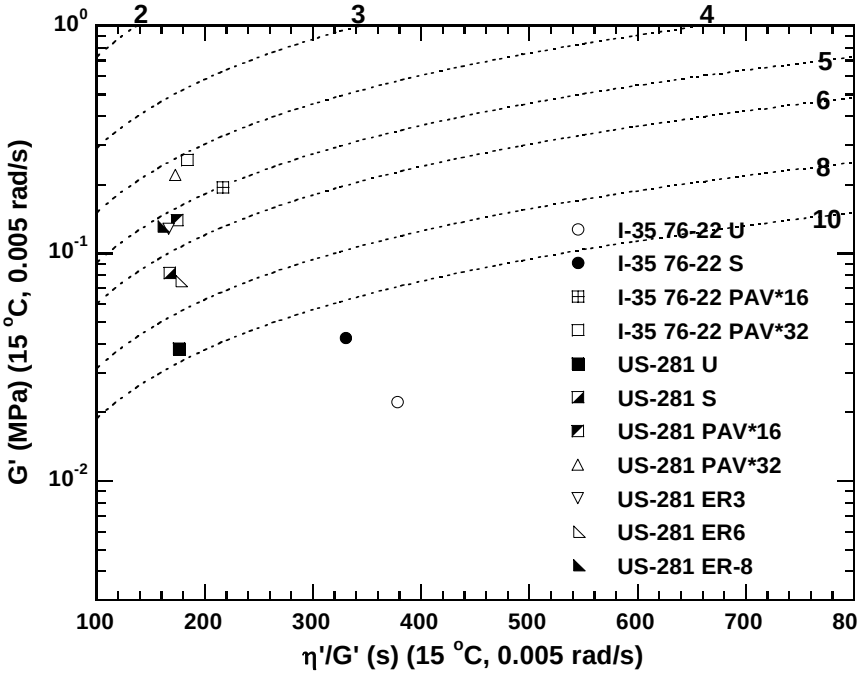

Figure 44. **DSR Map for IH-35-PG-76-22 and US-281-AR Asphalts.**

The SBS modified binder (IH -35-PG-76-22) follows the general trends described above. Each level of aging moves the binder diagonally towards the top left corner. The unaged binder starts towards the bottom of the map and by the PAV*32 aging level the binder has moved to the four cm ductility line. It should be noted again that these ductility values are for unmodified binders and do not necessarily hold for SBS modified binders.

The AR binder (US-281-AR) exhibits distinctly different behavior from the that described above. Even the unaged AR binder shows a low ratio of η'/G', accompanied by a moderately higher value of G', than most unaged binders. Probably, this characteristic is the result of the stiffening ability of the crumb rubber in the presence of a soft (low η') base binder. Then upon oxidative aging, the binder moves vertically as both G' and η' increase.

As with the DSR map, there are clear differences in the dynamic viscosity rheological behavior of the two binders, Figure 45 and Figure 46. The US-281-AR unaged and SAFT aged binder has a higher complex viscosity than the equivalently aged IH-35-PG-76-22 SBS-modified

binder. At 0.1 rad/s, the US-281-AR unaged binder has a a dynamic complex viscosity of nearly 50 kP and the SAFT aged binder viscosity is over 200 kP. By comparison, the IH-35-PG-76-22 binder viscosities are 20 kP (unaged) and 33 kP (SAFT aged). Not as much difference is seen between the two binders at the PAV*16 and PAV*32 aging levels, however, as both materials viscosities at these levels of aging are in the range of 200 to 300 kP. Additionally, the two PAV* aged AR binders show very little, if any, leveling off to a low shear rate viscosity. Figure 45 shows that while the I-35 binder does not have a η* limiting viscosity for the PAV* aged materials, it does show a decrease in slope at lower frequency and there is a clear η* low shear rate limiting viscosity for the unaged and SAFT aged binders. By contrast, for the US-281 binder, only the unaged binder has a η* low shear rate limiting viscosity as shown in Figure 46.

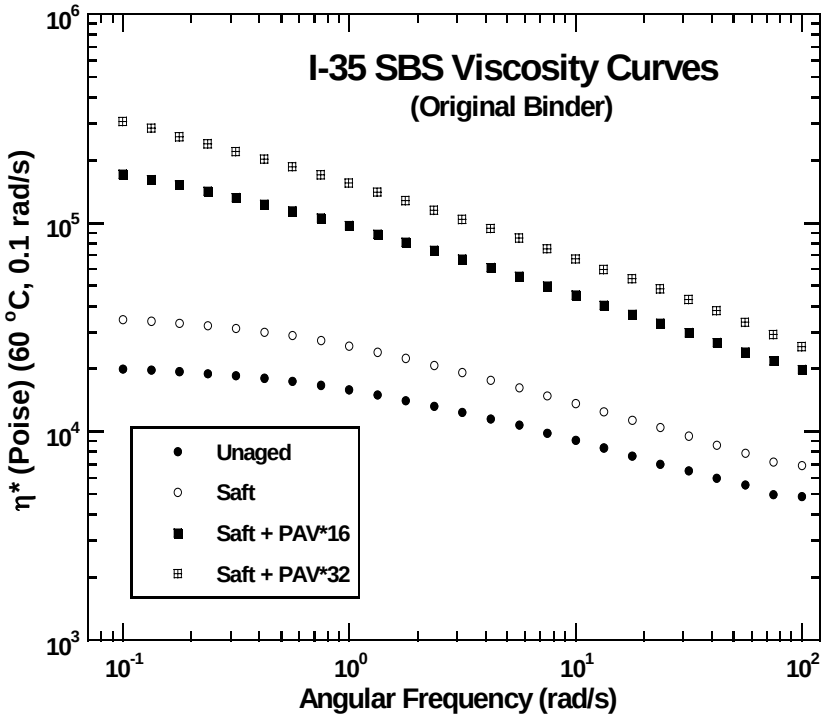

Figure 45. Viscosity Curves for IH-35-PG-76-22 (SBS).

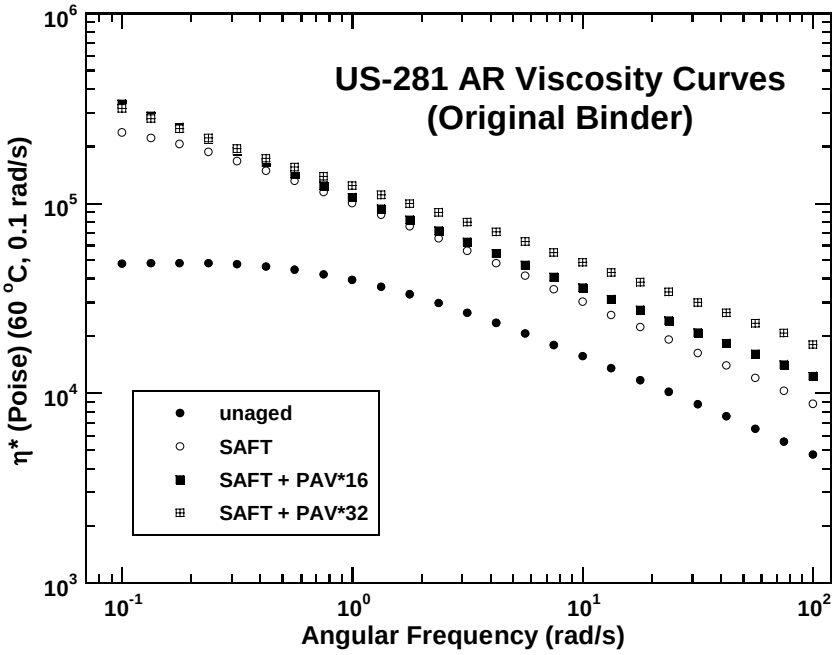

Figure 46. **Viscosity Curve for US-281-AR.**

The phase angle (phase shift between maximum stress and strain in the test specimen), δ, is a measure of the extent to which a viscoelastic fluid is elastic or viscous. At a phase shift of 90°, the material is purely viscous, whereas a phase shift δ of 0° indicates a purely elastic material. Unmodified, unaged asphalt materials are mostly viscous at molten temperatures and moderate shear rates and become more elastic with hardening due to either oxidation or low temperature, or due to testing at high frequency (which corresponds to low temperature by the principle of time-temperature superposition).

Figure 47 and Figure 48 show the phase shift behavior for the IH-35-PG-76-22 and US-281-AR materials. Both materials show more viscous behavior (δ closer to 90°) at low frequency (high temperature) than at higher frequency (lower temperature). Also, both materials show more elastic behavior at higher levels of aging. Then, comparing the two to each other, the AR material is more elastic than the SBS across the frequency range. This higher degree of elasticity is most likely due to the effect of the undigested rubber particles, which are essentially purely elastic. This added elasticity from the rubber particles also is likely the cause of the unusual vertical path taken by the AR material in the DSR map (Figure 44), compared to the SBS modified material or to unmodified materials. The higher degree of elasticity of the AR

material is reflected in this map by lower values of η'/G' for the AR binder that is not heavily aged.

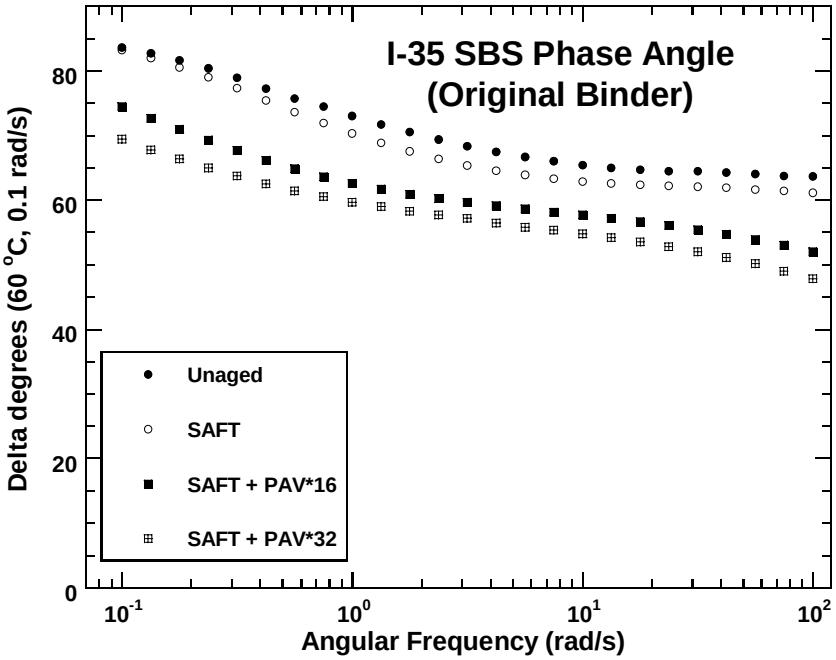

Figure 47. Phase Angle Curves for IH-35-PG-76-22 (SBS).

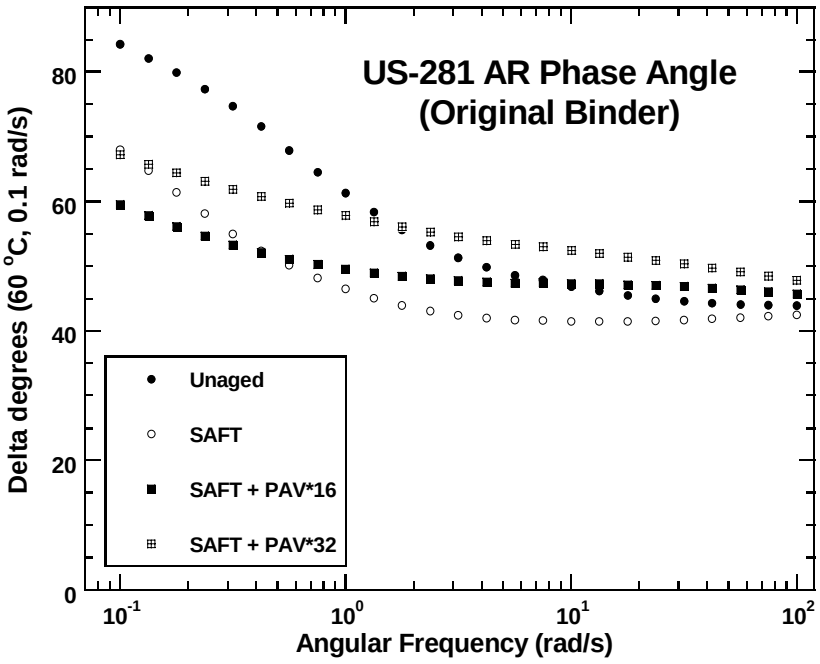

Figure 48. Phase Angle Curves for US-281-AR.

Previous work for TxDOT has shown that for unmodified binders there is a remarkably good relationship between the 15°C log ductility of a binder and its corresponding log DSR function (*37*). The correlation is shown in Figure 49 as the solid line on this log-log plot. The relationship is quite linear below a ductility of 10 cm. It should be noted that a number of literature references indicated that at a ductility of 3 cm pavements begin to exhibit difficulties with cracking. It should also be noted that as binders oxidize this DSR function increases as the binder stiffens and consequently the binder ductility decreases. There is no magic ductility at which a pavement fails in cracking; instead as the ductility decreases, the likelihood of failure increases. Other factors besides binder stiffness affect the actual pavement performance, including pavement loading (frequency and size of the load), overall pavement stiffness due to other elements of the pavement structure, and low temperature extremes. Nevertheless, binder stiffening results in a loss of ductility that is critically important to pavement durability.

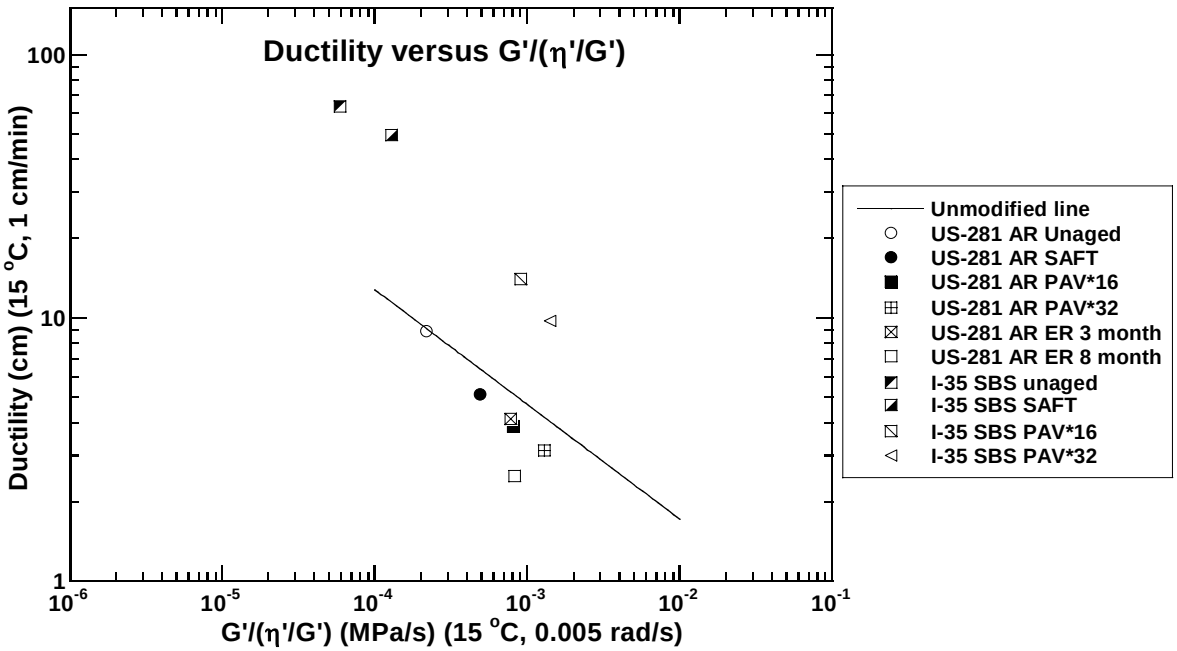

Figure 49. Ductility versus DSR for IH-35-PG-76-22 (SBS) and US-281-AR.

Shown in Figure 49 are data for the IH-35-PG-76-22 binder (SBS modified) and the US-281-AR binder. Differences in ductility relative to the binder rheology (as reflected in the DSR function) are very evident. For each data point of the SBS modified material, the binder

ductility lies well above the unmodified binder reference line, indicating that for each value of the DSR function, the ductility exceeds that of the typical unmodified binder significantly. Even for the binder that is aged to the PAV*32 level, the ductility has a value of about 10 cm versus the typical unmodified binder ductility of about 3 cm. For the US-281-AR binder, however, the values of ductility at each aging level exhibit a ductility that is less than the typical unmodified binder. Also note that this AR binder has a higher binder stiffness, as indicated by the magnitude of the DSR function, than the SBS modified material. For example, the two unaged binders have DSR function values for the SBS modified material of about 6×10^{-5} MPa/s, whereas that for the AR material is about 2×10^{-4} MPa/s, a four fold increase in the DSR function for the AR material over that of the SBS modified unaged material. However, it should also be noted that by the time both binders are aged to the PAV*32 level, they have identical DSR function values; nevertheless, the ductility of the SBS modified material remains significantly higher than the AR material.

These results are further indicated in Table 27 and Table 28. Table 27 shows the actual ductility values for both the IH-35-PG-76-22 and US-281-AR materials at the four levels of aging. The IH-35-PG-76-22 material decreases from a value of about 64 for the unaged binder to a value of just under 10 for the PAV*32 material. By contrast the AR material starts at a value of less than 9 cm and decreases to 3 cm at the PAV*32 aging level. These are dramatic differences in the two materials. Table 28 compares these ductility values to the unmodified binder correlation by dividing the ductility values as measured in the laboratory by the ductility calculated using the unmodified binder correlation of Ruan et al. (*38*) at a corresponding DSR function value. For this comparison, a value of unity indicates equivalence to the unmodified binder correlation. In Table 28, we see that the IH-35-PG-76-22 material starts at a ratio of four and decreases to 2.4, indicating that even at the PAV*32 level, the IH-35-PG-76-22 binder ductility is still over twice that given by the unmodified binder correlation. For the US-281-AR material however, all numbers are less than unity; the ductilities are less than that calculated by the correlation.

Table 27. Ductility Values for US-281-AR and IH-35-PG-76-22 (SBS).

Aging Levels	Ductility (cm)	
	US-281-AR	IH-35-PG-76-22 (SBS)
Unaged	8.91	63.61
SAFT	5.13	49.50
PAV*16	3.86	14.03
PAV*32	3.13	9.77

Table 28. Ductility Ratio Values and PAV*16 DSR Values Divided by 0.0001 for US-281-AR Asphalt Rubber and IH-35-PG-76-22 (SBS).

Aging Levels	Ductility Ratio[a]		PAV*16 DSR Value/0.0001[a]	
	US-281 AR	IH-35-PG-76-22 (SBS)	US-281-AR	IH-35-PG-76-22 (SBS)
Unaged	0.95	3.80		
SAFT	0.78	4.18		
PAV*16	0.73	2.78	8.05	8.96
PAV*32	0.73	2.36		

[a]Both the ductility ratio and DSR value/0.0001 are dimensionless.

Also shown in Table 28 is a comparison of the binder stiffness at the PAV*16 level made by dividing the DSR function value by 10^{-4} MPa/s. This is an arbitrary comparison recommended by Project 0-4688 (*39*). A ratio value of unity is recommended, although admittedly, it may well not be achieved by most modified binders. For both the US-281-AR and the IH-35-PG-76-22 materials values of this ratio were eight and nine, respectively, at the PAV*16 aging level. These ratios suggest that both of these binders are stiffer than would be desired at the PAV*16 level. In the case of the SBS modified material, the enhanced ductility may be an important benefit that outweighs the apparent high stiffness of this material. It should also be noted that these binders use polymer modification and the rubber for the explicit purpose of producing stiffer binders that are necessary for the PFC mixtures in order to avoid draindown or rutting in these open mixtures.

Figure 50 provides additional insight to the ductility enhancement provided by the SBS modifier. This figure is a force ductility curve, which is a graph of the stress in the binder as it undergoes elongation. The force ductility is measured at 4°C at an elongation rate of 1 cm/min. For the SBS modified binder in Figure 50, for both the unaged and SAFT aged materials, we see

that at the beginning of the test the stress increases to a maximum of about 1 MPa and then decreases upon further elongation as binder flow relieves the elongational stress. Then after an elongation to a ratio of about four, the stress increases further and continues to increase up to a level of about 5 MPa as the elongation ratio increases to 16. This second wave of increasing stress is the result of the polymer modifier absorbing the stress in the material and preventing the viscous flow as the intertwined polymer molecules elongate. In this portion of the curve, the material again looks elastic as it did in the very early portion of elongation. It is in this second wave of increasing stress (elastic deformation) that the enhanced ductility of the material occurs and even allows the material to sustain a fairly high level of stress beyond that for a normal unmodified binder. At the PAV*16 and 32 hour levels we see an even more rapid rise in stress with elongation which is the result of the typical, very significant stiffening of the binder with oxidation. Furthermore for these more heavily aged materials, the stress builds to a failure level before the flow can occur and also before the polymer modifier can absorb the stress, and thus the material breaks in this case at a little over 2 MPa. It should be noted again that this force ductility test is done at 4°C compared to the 15°C ductility test and thus the elongation ratio that is seen is much less than the ductility of 10 cm for the PAV*32 IH-35-PG-76-22 material.

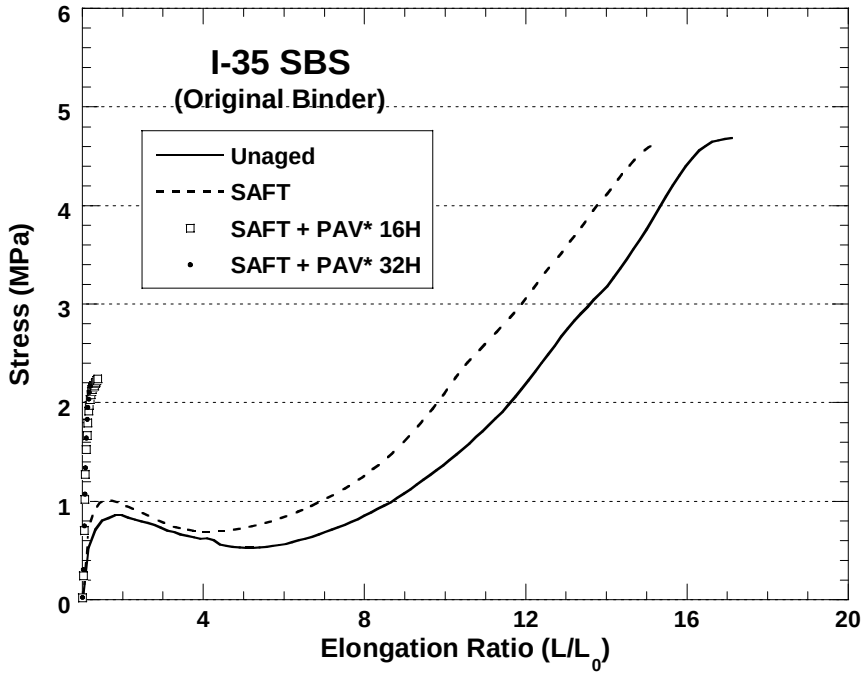

Figure 50. Force Ductility for IH-35-PG-76-22 (SBS).

Figure 51 shows corresponding experiments for the US-281-AR material, and the contrast to the SBS modified material is striking. For the AR material there is no second rise due to a polymer elongation that can absorb the stress. Note the difference in scale for the AR material and the SBS. It is still seen that at each additional level of aging the asphalt binder stiffens (the slope of the stress verses elongation curve is steeper at the origin) and the binder curve still goes through a stress maximum. However, in no case is there the characteristic second modulus that would indicate an active polymer modifier. Furthermore, the level of this maximum stress is quite low, on the order of 0.5 MPa. On the other hand, it should be noted that even for the most heavily aged asphalt rubber material, the binder is able to flow to relieve stress as there is no indication of a sharp break in the material at the maximum stress. The AR material's ability to avoid sharp fracture, even after significant aging, may significantly affect its performance in the field. On the other hand, its lack of high ductility is notable. But then again, if the material can maintain a low stress by undergoing flow, even after significant aging, that behavior could be significant in preventing cracking in service.

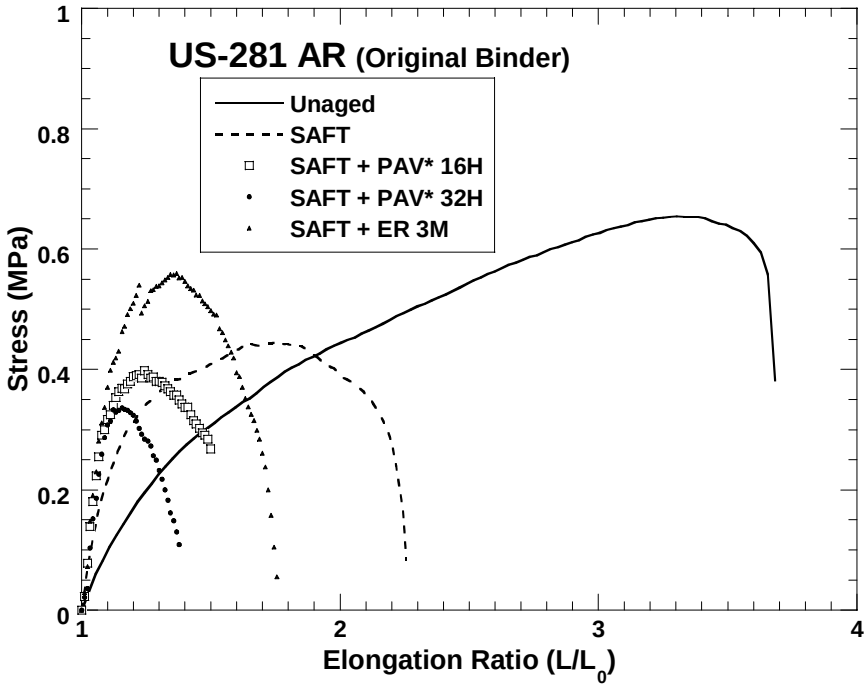

Figure 51. Force Ductility for US-281-AR Asphalt Rubber.

6.4. SPECIAL CONSIDERATIONS FOR ASPHALT RUBBER MATERIALS

6.4.1. Introduction

Asphalt rubber is an asphalt binder with 15-21 percent crumb rubber produced by the MacDonald process, also known as the wet process (*40*). In addition to the wet process, a dry process also exists. The dry process adds the rubber directly to the aggregate rather than to the binder. Arizona began using asphalt rubber in 1964. Today, Arizona still uses AR. Arizona has used AR for seal coats, stress absorbing membranes (SAM), stress absorbing membrane interlayers (SAMI), open-graded mixes, and gap-graded mixes. Reported benefits of the AR wet process are improved reflection cracking, improved durability, decreased noise, and improved environmental impact, having reused 4 million tires since 1988 (*40*).

The laboratory observations of the AR binder also have experimental difficulties which makes accurate testing of the binder difficult. Many of these testing difficulties come from the large size rubber particles in the AR binder. Because of the large size rubber particles, one of the tests needed to be modified. This section discusses the testing difficulties, the size of the asphalt rubber, and the modification to one of the tests. This section also presents additional AR DSR data.

6.4.2. Results and Discussion

The data presented above indicate that AR materials have unique characteristics compared to conventional unmodified binders and even compared to polymer-modified binders. It was noted in the DSR map that the path AR binders take with increased oxidation deviates significantly from that of conventional binders and polymer-modified binders. The AR materials, based upon the DSR map shown above, move much more nearly vertically with binder oxidation, whereas the more conventional materials start at the lower right of the DSR map and track diagonally towards the upper left corner.

This section further evaluates the DSR map and other rheological characteristics. It should be noted that some of the tests discussed below were conducted on complete asphalt rubber binder, in contrast to other tests that were conducted on binders that had been subjected to the extraction and recovery process that is used to recover binders from pavements. This

recovery process separates binders in pavements from aggregate material by filtration. Because the AR material contains rubber particles of varying size, up to approximately 1 mm in diameter, this filtration process necessarily removes the rubber particles from the binder, thereby changing its rheological characteristics. Nevertheless the process is required as part of the testing procedure for characterizing aged binders in pavements. As is seen in the discussion of this section, removing these particles alters the rheological character of the binders significantly.

DSR map data for the two AR materials (US-281-AR and US-288-AR) are shown in Figure 52 for various levels of aging and together with the US-281 AR material after it has been subjected to the extraction and recovery procedure. In the figure, the two AR materials that have not had the rubber particles removed appear at the left of the map and move essentially vertically as binder oxidation occurs. The US-281-AR material is shown after aging by both the PAV*16 and 32 methods and by environmental room aging at 60°C for 3, 6, and 8 months. The PAV* method uses the standard PAV apparatus at 20 atm of air pressure, but for either 16 or 32 hours of aging and in films that are 1 mm thick compared to the standard PAV procedure which calls for 3 mm thick films. The thinner film allows for better access of oxygen and therefore faster oxidation rates, and the level of aging achieved in the 16 hour aging is approximately equivalent to that achieved of the standard 20 hour test. ER aging is also conducted in 1 mm films but at 1 atm air pressure and at 60°C; therefore, it requires much more time to achieve a comparable level of aging.

It should also be noted that whereas additional oxidation stiffens the binder and should move it more towards the top left corner of this DSR map, AR materials did not universally exhibit this trend. For example, the US-281-AR material aged at 3 months is more towards the top left corner than is the material that was aged for a longer period of time, i.e., for 6 months. This kind of inconsistent rheological behavior is almost certainly an artifact of testing these binders that contain a significant amount of fairly large particles. Such effects could be the result of settling of the rubber particles in the rheometer or even the result of nonrepresentative sampling of the binder for testing. If more or fewer particles are obtained from one sample versus another, then this will impact the measurements that are obtained. Unfortunately these kinds of inconsistencies are unavoidable when dealing with the AR materials. Probably more accurate data could be obtained by testing multiple samples and these kinds of inconsistencies

could then be evened out by averaging the results. The additional testing however, would require more time and expense in dealing with these materials.

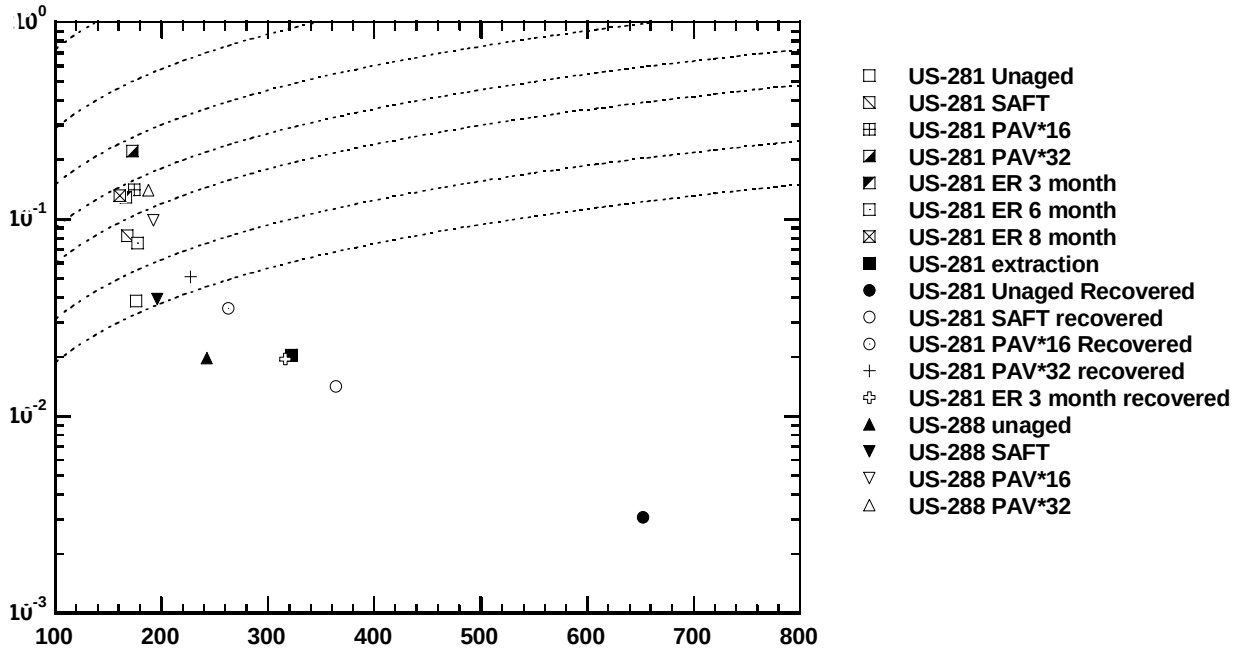

Figure 52. DSR Map for US-281-AR and US-288-AR Asphalt Rubber.

The US-281-AR material that was subjected to the extraction and recovery procedure is also shown on this DSR map in Figure 52 and is indicated as "recovered" material. The unaged recovered binder appears quite low on the DSR map ($\eta'/G' = 650$, $G' = 0.003$) at a fairly high value of η'/G'. This location on the map is an indication that the recovered binder was quite soft even compared to normal unmodified binders. Then the SAFT aged binder has moved significantly away from this unaged binder and the PAV*16 and PAV*32 recovered binders straddle the 10 cm ductility line that represents unmodified binders. The path established by this recovered AR material is much more like that which would be observed for unmodified materials or even for SBS modified materials; the path moves much more diagonally across the DSR map having started at a position in the lower right.

Note also that there is a point that lies beyond the SAFT aged level that indicates a binder that was actually recovered from the US-281-AR PFC layer. This binder falls exactly on the path established by the tested binder that was never in a pavement but aged to different levels and

then also subjected to the extraction and recovery process. Note that the core that provided this binder was collected at the time of the PFC placement, and the aging level is in approximate agreement with the SAFT level of aging plus an additional amount that would have occurred beyond the hot-mix plant in transportation, placement, and cool down prior to coring the pavement. Further note that the US-281-AR material subjected to 3 months ER aging and then extracted and recovered shown on this DSR map indicates a level of aging that exactly matches that of the binder extracted from the PFC core obtained from the US-281-AR pavement. It should be noted that the ER aging is conducted on the material that has first been SAFT aged so that the three months in the environmental room at 60°C moved the binder from the SAFT data point to the ER 3 month data point.

There is one further comparison that should be made using these DSR data, and this is the effect of removing the asphalt rubber particles from a material. The US-281-AR material aged at PAV*16, and PAV*32, and ER-3 levels, but without being subjected to the extraction and recovery procedure, appear near the 5 cm ductility line that represents unmodified binders. When these materials are subjected to the extraction and recovery procedure which removes the rubber particles they move back to their points shown on the recovered line, which places the PAV*16 and PAV*32 data points straddling the 10 cm line and the ER-3 recovered data point appears even further towards the lower right. From this comparison, the significant effect of the asphalt rubber particles on the rheological stiffening of the binder is clear.

Figure 53 to Figure 58 provide additional rheological data for both AR materials.

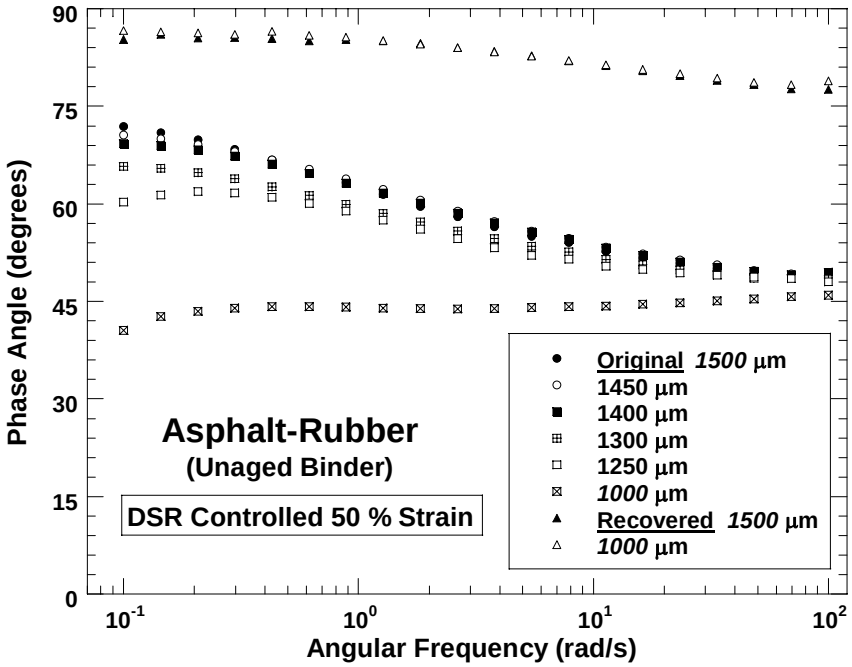

Figure 53. Asphalt Rubber Phase Angle for Original and Recovered US-281-AR.

Figure 53 presents phase angle measurements for the US-281-AR binder in the unaged state. The measurements shown are at six different gap settings, ranging from 1500 µm to 1000 µm. For comparison the figure shows the same binder after being subjected to the extraction and recovery procedure at both 1500 and 1000 µm. The phase angle measurement is an indication of the extent to which the binder exhibits viscous versus elastic behavior, with a 90° phase shift indicating purely viscous behavior and a 0° phase shift indicating purely elastic behavior. The rubber particles add elastic behavior to the binder so that such a binder exhibits more elastic behavior than the binder from which the particles have been removed. Also, it should be noted that, as the gap decreases starting at 1500 µm, the phase angle decreases also, especially at the lower frequencies. This is the result of the narrower gap impinging upon the rubber particles so that, as the gap decreases, the behavior is more influenced by the rubber particles at the expense of the fluid behavior of the base binder. The change is particularly evident once the gap setting decreases to about 1300 µm and clearly there is a very significant effect in the 1000 µm range.

This effect of gap setting is an indication of the approximate size of the particles in that if the particles are significantly smaller than the gap setting, then decreasing the gap does not

drastically change the results. The recovered binder has the rubber particles effectively removed and there is very little difference seen between the 1500 µm and 1000 µm gap settings.

Also it should be noted that at higher frequencies, materials tend to behave more elastically and this is certainly true of the asphalt rubber material. At 100 rad/s, there is little difference between the 1500 and 1200 µm gap setting.

Figure 54 shows the dynamic viscosity for the same unaged binder at the different gap settings and also the binder that has been subjected to the extraction and recovery procedure. Again, for the original material and below a gap setting of 1300 or 1400 µm there are significant differences in the viscosity measurements as the gap setting impinges upon the rubber particles. Also the viscosity of the recovered material is significantly reduced (by more than an order of magnitude) compared to the unrecovered material, showing the large effect of the rubber particles on the binder viscosity. As the test frequency increases, the dynamic viscosity decreases, a further indication of a shift to a more elastic material at the expense of dynamic viscosity. In order to avoid the artifacts caused by rubber particles being sandwiched between the plates of the rheometer, a gap of at least 1500 µm should be used for rheological measurements of AR material.

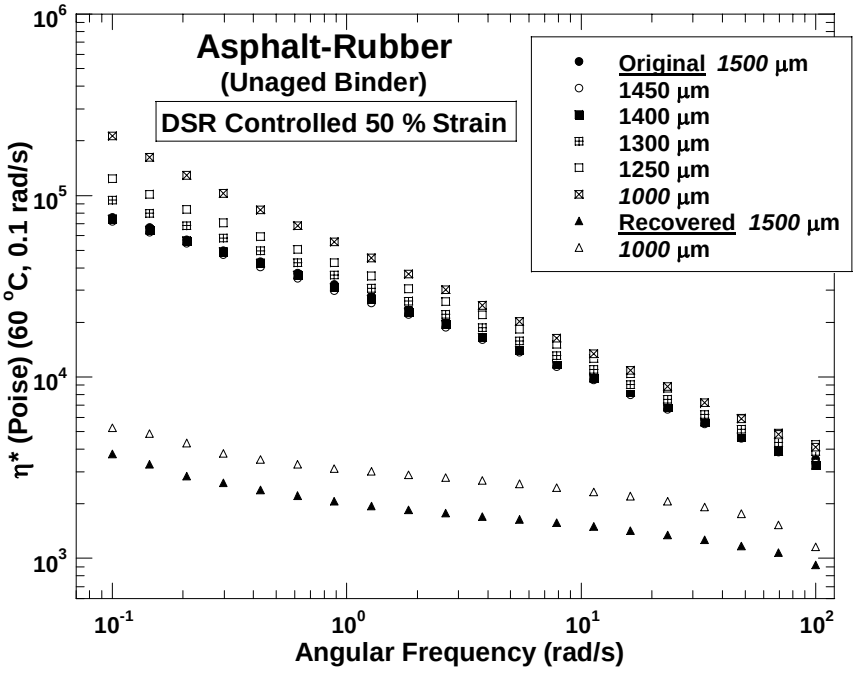

Figure 54. Asphalt Rubber Viscosity for Original and Recovered US-281-AR.

Figure 55 and Figure 56 show the phase angle measurements for US-281-AR binder (Figure 55) and US-288-AR (Figure 56) at different levels of binder aging. The measurements were made at a gap setting of 1500 µm. For both binders, increasing binder oxidation generally results in the material being more elastic (a decrease in phase angle). This decrease is most obvious at the lower frequencies. Furthermore, even though this is a general trend, it is not a universal result, probably because of the difficulty of obtaining consistent results with the AR either because of uniform sampling problems or settling problems with the rubber particles, as discussed above.

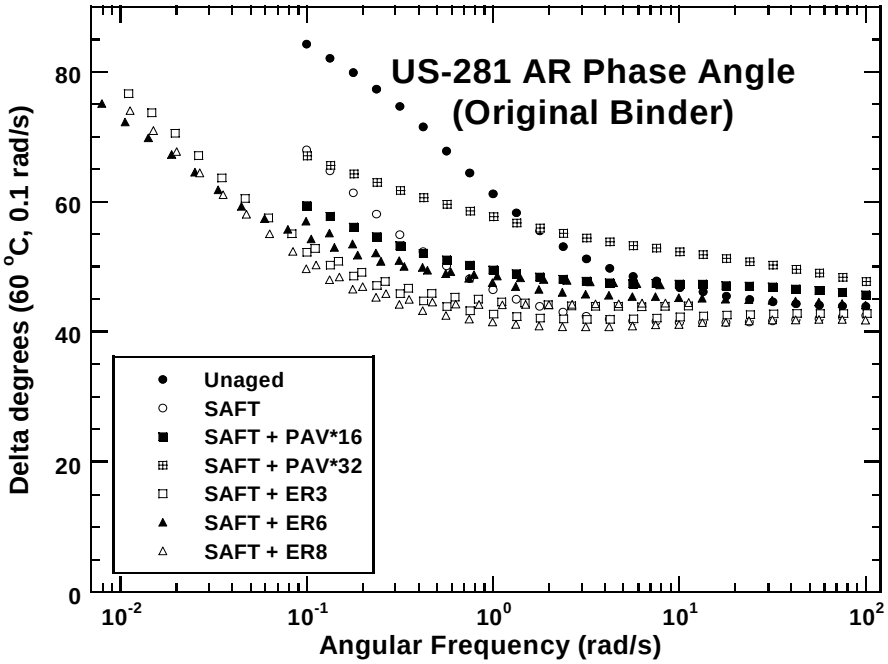

Figure 55. US-281-AR Phase Angle.

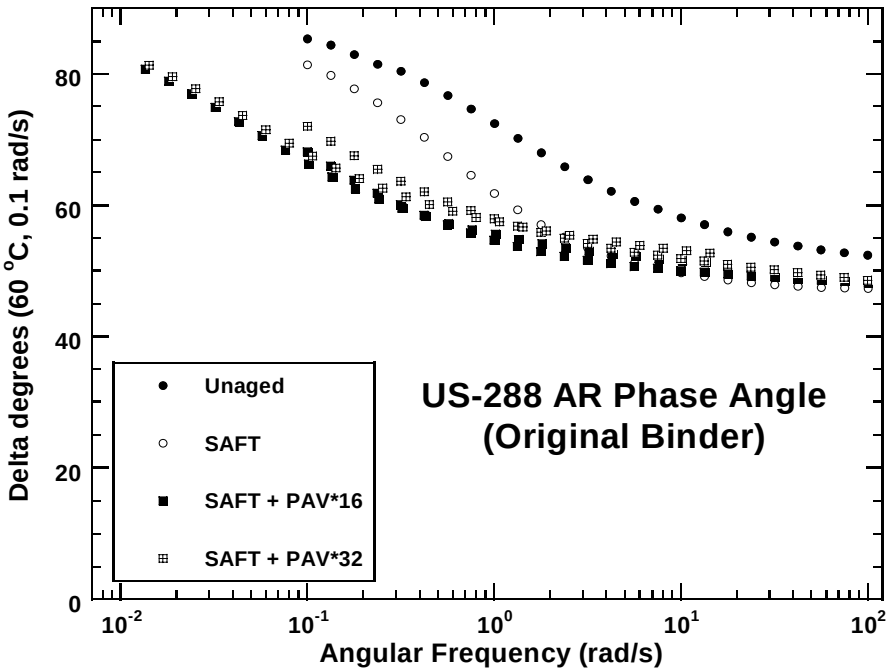

Figure 56. US-288-AR Phase Angle.

Figure 57 and Figure 58 show the dynamic viscosity data for these two AR binders, again at the four levels of aging. As with other binders, the general trends are that the viscosity increases with oxidation and again this is most apparent at the lower frequencies. Also, again there is some misordering of the stiffening that is certainly the result of the above mentioned measurement artifacts with the AR materials. Comparing the actual rheology of the US-288-AR and the US-281-AR binders we see that the US-281 viscosity at the low frequencies is significantly higher than that of the US-288-AR binder with the unaged low shear rate limiting viscosity of the US-281-AR materials being approximately 40,000 to 50,000 poise, whereas the US-288-AR material is less than 20,000 poise. Also, the PAV*16 and PAV*32 viscosities for the US-281-AR material are approximately 400,000 poise, whereas for the US-288-AR material they are about 200,000 poise.

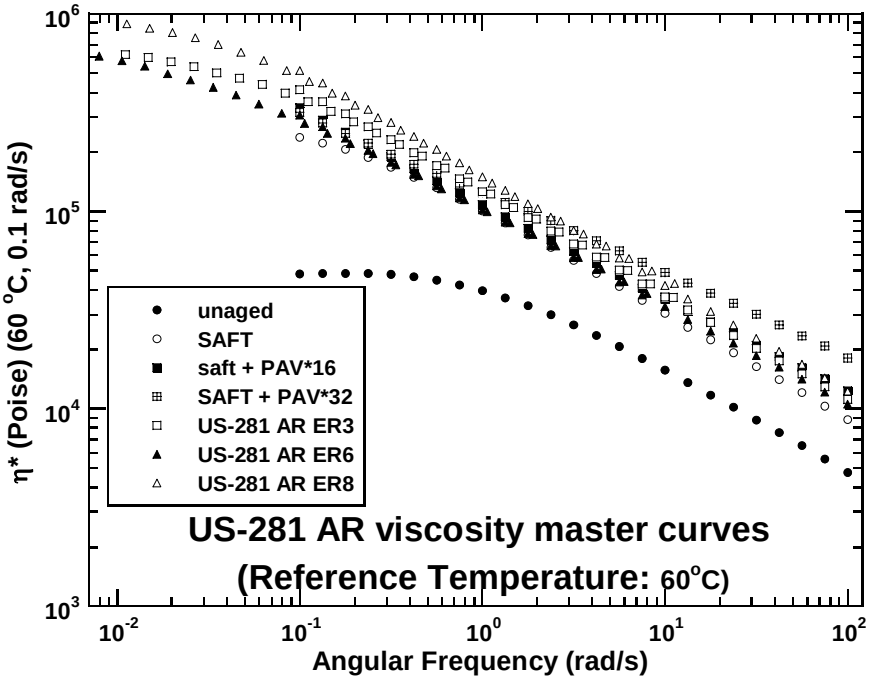

Figure 57. US-281-AR Viscosity Master Curves.

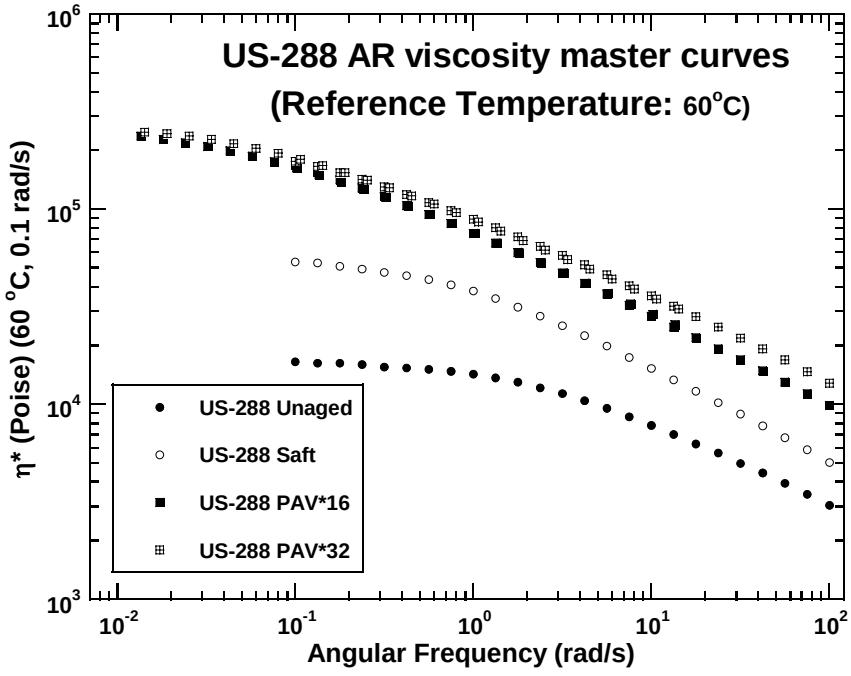

Figure 58. US-288-AR Viscosity Master Curves.

Finally, Figure 59 compares both the US-281-AR and US-288-AR binder ductility values to the typical unmodified binder correlation values, indicated by the straight line. The AR data

fall below the correlation line, indicating that at a given DSR function value of binder stiffness, the AR ductility is less than would be expected for an unmodified base binder.

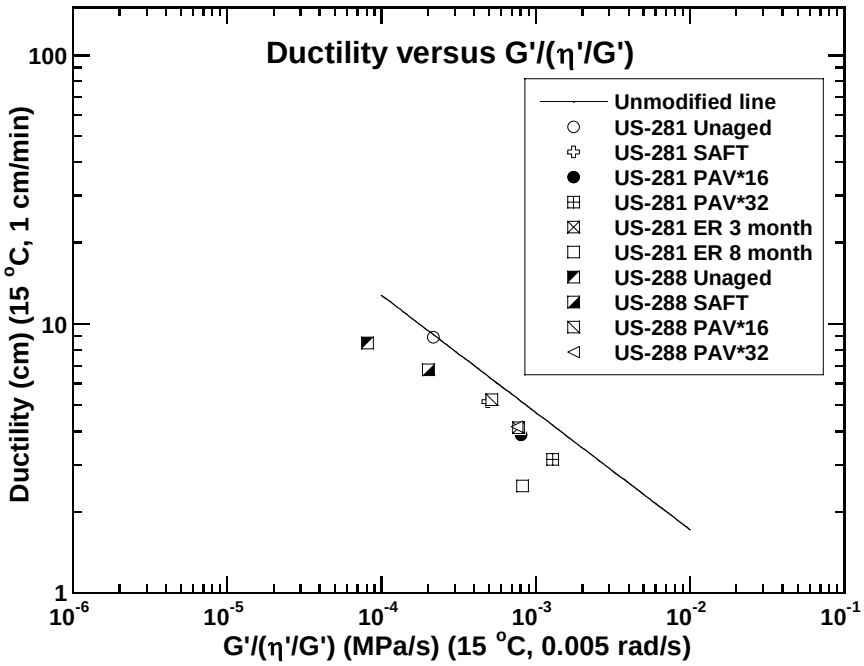

Figure 59. Ductility versus DSR for AR Asphalts.

6.5. COMPARISON OF SBS, TIRE RUBBER, AND AR BINDERS

6.5.1. Introduction

This section compares tire rubber (TR) asphalt to SBS binders that were used in this project as well as the AR binders discussed in previous sections. The comparisons are made using a DSR map, force ductility data, ductility data, and a ductility versus DSR graph.

6.5.2. Results and Discussion

Whereas the previous sections have presented comparisons between AR binders and SBS polymer-modified binders, this section compares a wider set of polymer-modified binders to each other. This set includes one PG 76-22 binder that is modified with both SBS and a well-digested tire rubber material. The tire rubber in this binder is well enough digested that the

presence of particles is not evident and the binder has the smooth consistency of a typical polymer-modified binder.

Five polymer-modified binders were evaluated and they are shown in Figure 60 as they progress across the DSR map with increased levels of aging. Each binder was subjected to four levels of aging: unaged binder, SAFT aging (approximately equivalent to RTFOT aging), PAV*16, and PAV*32 aging. As is typically observed with increased aging, the binders move from the lower right portion of the graph diagonally towards the top left corner. The exact path followed, however, is characteristic of each binder and the position of the path on the DSR map, as well as the slope of the path, are characteristics that may vary from binder to binder. As was noted before, this graph includes lines of constant ductility that were obtained for unmodified binders and, in the case of polymer-modified binders, serve only as reference points along the aging path and not as true indications of the binder's ductility.

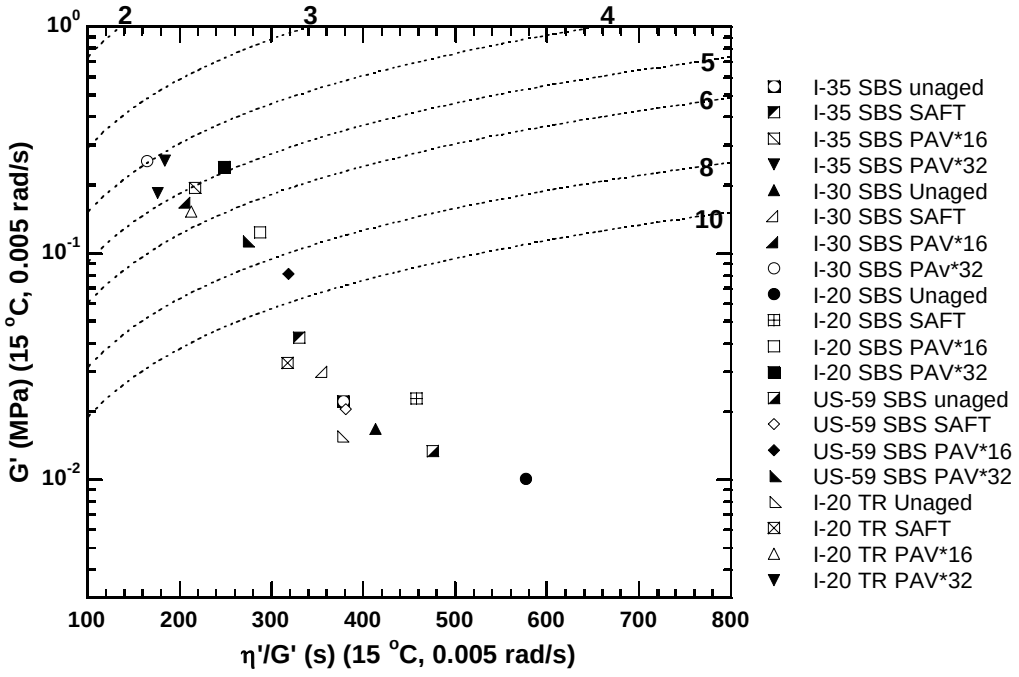

Figure 60. DSR Map of SBS and TR 76-22 Asphalts.

Figure 61 shows the actual measured ductilities for each of these binders compared to the binder stiffness, as characterized by the DSR function. As was done with this type of graph before, the solid line shows the correlation between ductility and DSR function that was obtained

for unmodified binders below a ductility of about 10 cm. Note that for each of these polymer-modified binders their actual measured ductilites are significantly greater than would be expected, based on the correlation for the typical unmodified binders at the same DSR function value. Furthermore, note that the IH-20-PG-76-22TR material looks much like the other materials that are SBS modified binders, in that its ductility values fall about the same amount above the unmodified line as the others. This enhanced ductility performance almost certainly is beneficial to mixture durability even though in the long run with binder oxidation it has been noted that this enhancement decreases and eventually the binder shows the same response as the unmodified binder. However, a key issue is how long it takes the binder to revert to the unmodified binder behavior and ultimately by how much pavement service is increased.

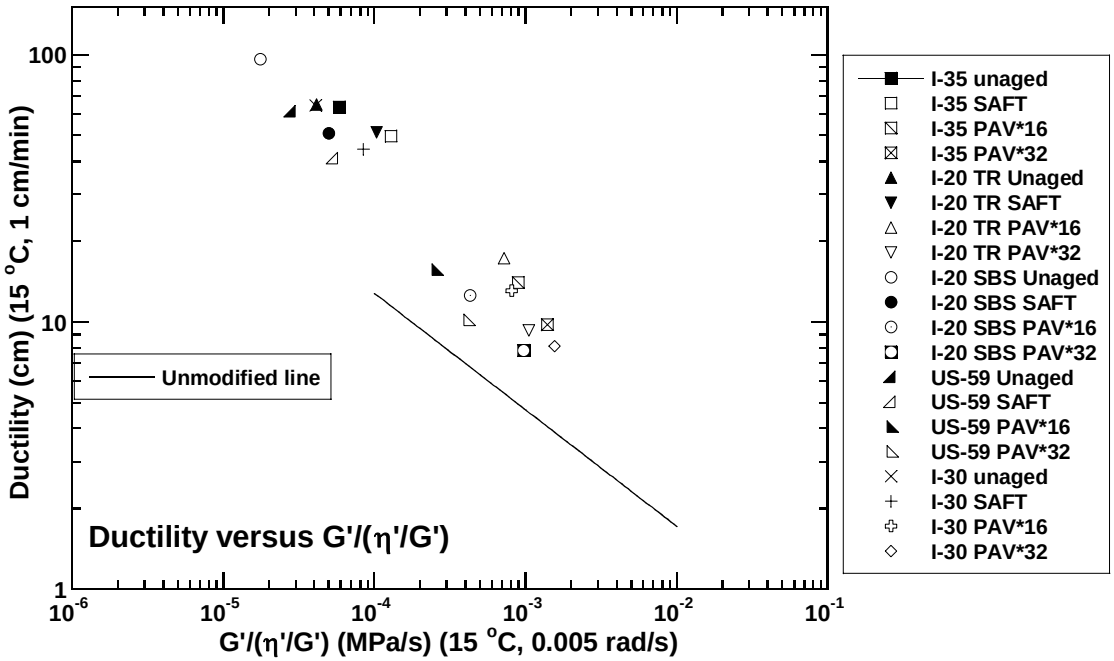

Figure 61. Ductility versus DSR Function for SBS and TR PFC Asphalts.

As a further comparison of this ductility improvement of the polymer-modified binders, Figure 62 shows the ratio of the measured ductility to the calculated ductility (obtained from the unmodified binder correlation) for the typical unmodified binder at the PAV*16 aging level, as indicated by the value of the DSR function. This comparison was suggested as a criterion for comparing modified binders (*39*). This comparison shows that the IH-20-PG-76-22TR provides

the highest level of ductility improvement at a ratio of three, although, as mentioned above, the extent to which this ratio indicates superior durability in pavements and especially in PFC overlays is unknown, pending additional long-term field performance data. The actual measured ductility values for the five polymer-modified binders at each of the four aging levels are summarized in Table 29.

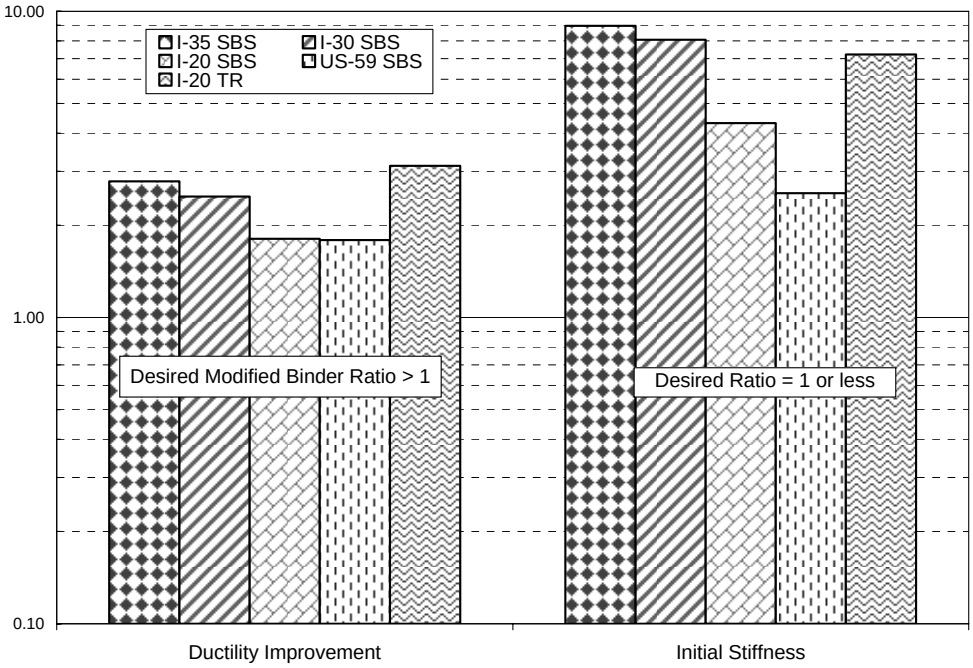

Figure 62. Ductility Improvement and Initial Stiffness for the PFC Asphalts.

Table 29. Ductility Values for SBS, AR, and TR Asphalts.

Aging Levels	Ductility (cm)						
	US-281-AR	US-288-AR	IH-35 PG-76-22 (SBS)	IH-30 SBS	IH-20 SBS	US-59 SBS	IH-20 TR
Unaged	8.91	8.50	63.61	64.40	96.47	61.28	65.00
SAFT	5.13	6.74	49.50	44.41	50.88	40.98	51.28
PAV*16	3.86	5.23	14.03	13.10	12.57	15.70	17.34
PAV*32	3.13	4.15	9.77	8.11	7.83	10.17	9.32

Also shown in Figure 62 is measure of polymer-modified binder stiffness, the ratio of the DSR function at PAV*16 aging multiplied by 10^4. This is an arbitrary comparison that is designed to indicate how far a binder has progressed along the path to excessive stiffening *(39)*.

Its relevance, especially for PFC pavements, is unknown pending pavement durability results. While these stiffness levels are fairly high, undoubtedly, they are necessary to prevent draindown of binder in the PFC mixtures.

Figure 63 through Figure 65 compare force ductility data for the seven binders that were studied in this project. Figure 63 presents the data for the PG-76-22 SBS modified binders with each one identified by the highway in which it was used. As discussed previously in this chapter, force ductility data show the stress that develops in a binder as it is elongated at 1 cm/min at 4°C. For each of the four SBS modified binders in the unaged state the initial response is to the underlying stiffness of the base binder and in this region of the force ductility the stress builds to approximately 1 MPa. Upon further elongation, the stress reaches a plateau or even declines, and then, as the polymer network tightens upon further elongation, increases to approximately 6 MPa before binder failure occurs at an elongation ratio of approximately 16. The force ductility performance of each of these four binders is remarkably similar. Upon aging to the SAFT (RTFOT) level, similar behavior is observed although the stress levels at a given elongation are higher than for the unaged state, due to the stiffening of the base binder upon oxidation. In this case three of the four SBS modified binders behave similarly (IH-35-PG-76-22, US-59-PG-76-22, IH-30-PG-76-22) while the fourth binder (IH-20-PG-76-22) is noticeably stiffer than the others, indicated by the significantly higher stress levels at equal elongation ratios. At PAV*16 and PAV*32 aging levels, binders further stiffened as the initial rise in stress due to the underlying binder stiffness is now in the range of 2 to 3 MPa and furthermore, the elongation ratio is significantly reduced compared to the unaged and SAFT aged levels. In fact, for the IH-35-PG-76-22 and IH-20-PG-76-22 binders, at both of these aging levels, the binder fails before the polymer elongation region is reached. For the US-59-PG-76-22 and IH-30-PG-76-22 binders, however, at the PAV*16 level the US-59-PG-76-22 and IH-30-PG-76-22 binders still show significant elongation due to the effect of the polymer modifier. It should be noted, however, that the reduced ductilities at these higher levels of aging were not observed in the ductility test (Figure 61) that was conducted at 15°C instead of 4°C. The lower temperature further increases the stiffness of the binder beyond that due to oxidative aging and the increased stiffness results in a higher stress and thus failure at the reduced level of elongation.

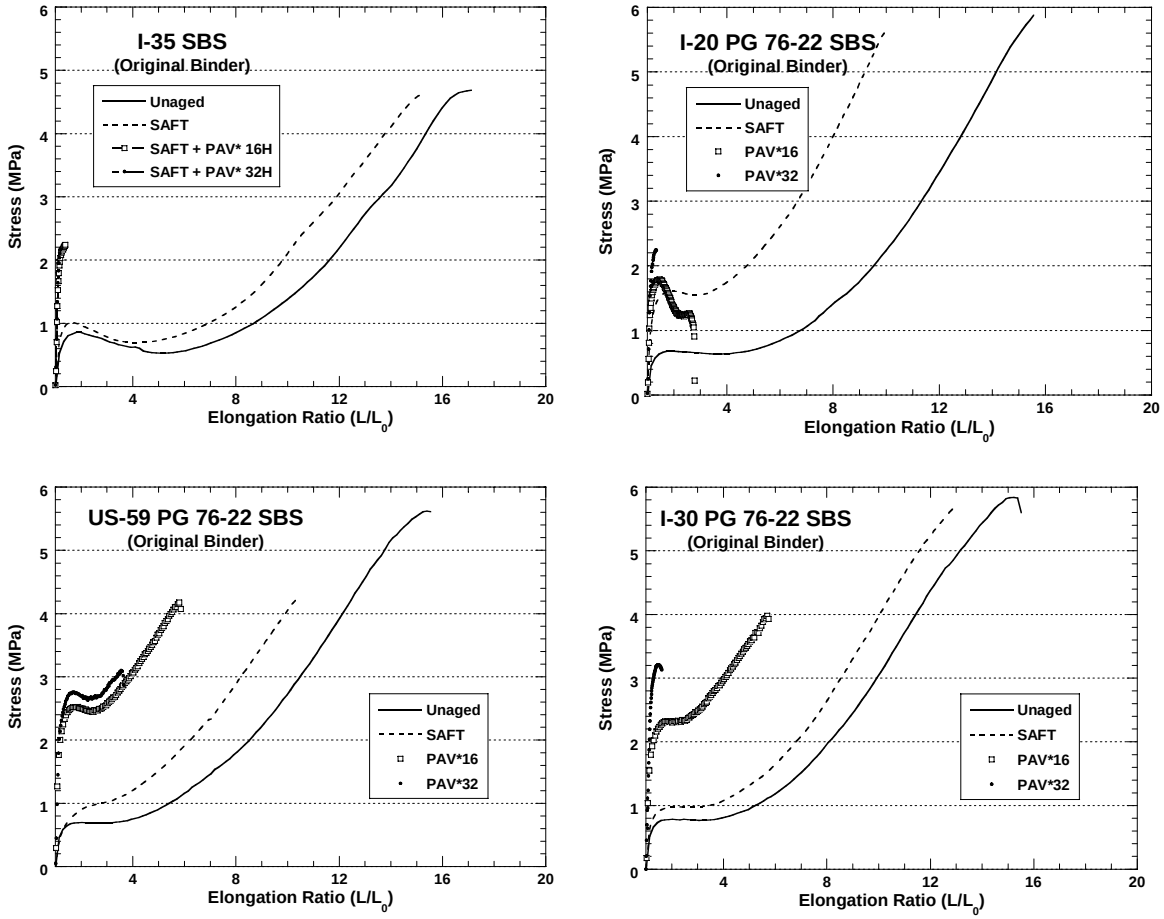

Figure 63. Force Ductility Data for SBS PFC Asphalts.

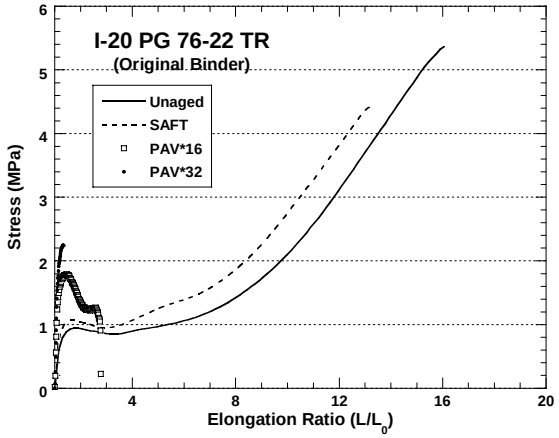

Figure 64. Force Ductility Data for TR Asphalt.

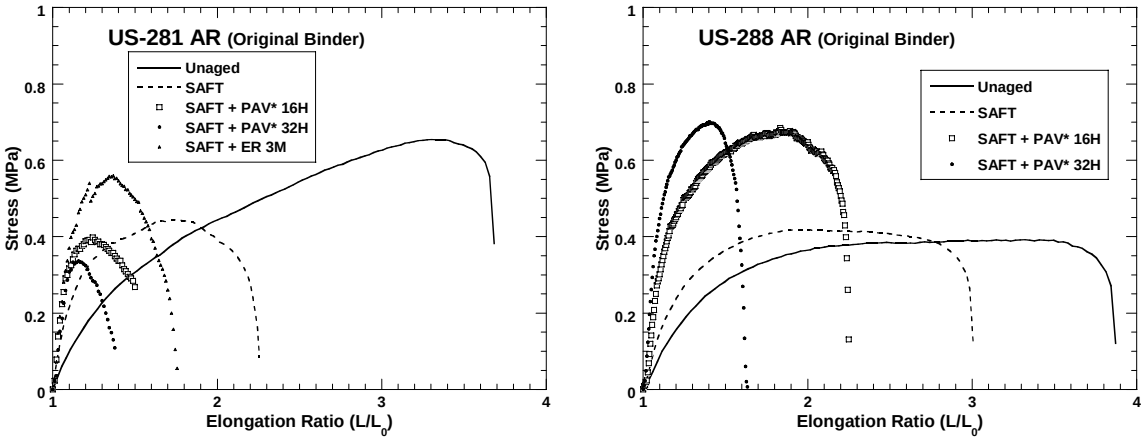

Figure 65. Force Ductility Data for AR Asphalts.

Figure 64 presents the force ductility data for the IH-20-PG-76-22TR binder. This binder is modified with a blend of SBS and well-digested tire rubber and, in fact, the force ductility data look very much like the SBS modified binder data shown in Figure 63. Again, the unaged binder at low elongation ratios increases to a stress level of about 1 MPa before reaching a plateau region and then, under the influence of the polymer modification, the stress level further increases to nearly 6 MPa as the elongation ratio reaches 16. The SAFT-aged force ductility follows a similar behavior, although again the stress level is somewhat higher than for the unaged binder due to the stiffening of the base binder with oxidation and the failure occurs at a reduced elongation ratio of about 13. Likewise, the PAV*16 and PAV*32 aging levels produce force ductility curves much like the SBS modified binders, although the increase in the stress for the PAV*16 binder beyond the initial asphalt stiffness response does not occur, and in fact the stress level decreases before final failure of the binder at an elongation ratio of nearly 3. Nevertheless, the TR material by this evaluation looks very much like the other SBS modified binders.

The force ductility data for both of the asphalt rubber binders are shown in Figure 65. Careful note should be made of both the ordinate and abscissa axis scales, however, and that the maximum stress level and the maximum elongation ratio for these binders both are significantly less than for the SBS modified binders. The US-281-AR was shown previously in Figure 51 and here it is seen that the US-288-AR material behaves similarly to the US-281-AR binder and not at all like the SBS or SBS/TR modified binders. Note that both of these binders, whether unaged or aged, follow the same qualitative behavior in that there is an increase in stress with elongation,

with no accompanying second wave of stress increase due to the polymer modification. The AR materials exhibit distinctly different elongational behavior, compared to SBS modified binders.

A further comparison of the TR and SBS binders is shown in Figure 66, a DSR map of the binders that includes binder recovered from pavements. For each of the three binders shown, aging the binder moves it progressively from the lower right of the figure, as an unaged binder, towards the upper left after PAV*32 aging. Furthermore, the binder that is recovered from the pavement generally lies on the path established by the laboratory-aged binder, although the US-59-PG-76-22 recovered binder is an exception, lying above the laboratory path. Both the US-59-PG-76-22 and the IH-30-PG-76-22 recovered binders are relatively unaged; and in fact, they lie quite close to the unaged binder on the DSR map, in spite of the hot-mix process. Both of these pavement samples were obtained at the time of placement and minimal aging would be expected. The IH-20-PG-76-22TR binder is significantly more aged, in that it lies closer to the PAV*16 aged binder than to the SAFT aged binder. The core from this pavement was obtained five months after placement in October 2005.

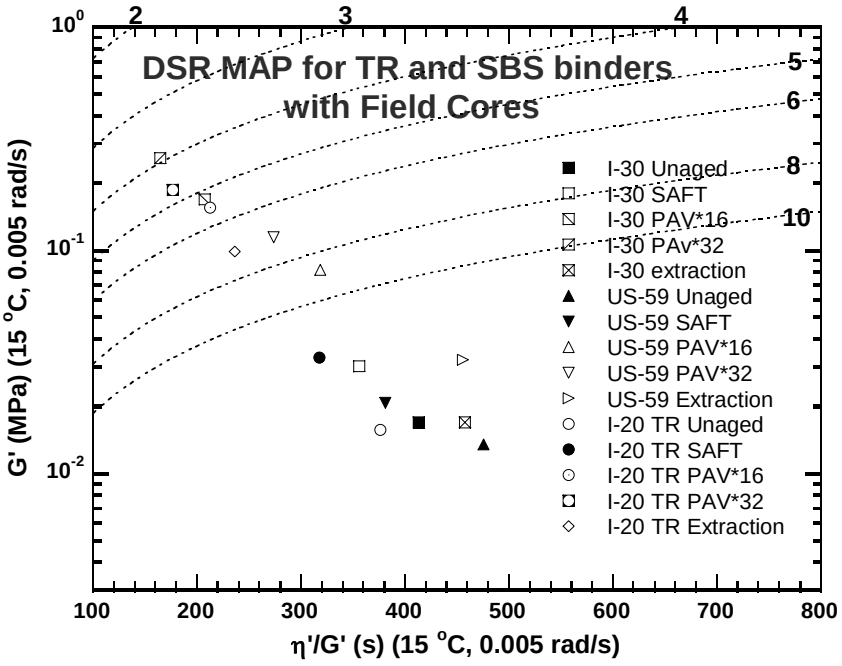

Figure 66. DSR Map of TR and SBS Asphalts Plus Their Extracted Field Road Cores.

6.6. COMPARISON BETWEEN PFC ASPHALTS AND DENSE-GRADED ASPHALTS

Figure 67 is a DSR map of both PG-76-22TR and PG-76-22 SBS binders that were used in the comparison of rheological properties between PFC and dense-graded mixes. Table 30 lists the binders that were used for the comparison. All binders have four aging levels shown in the DSR map: unaged, SAFT, PAV*16, and PAV*32. As these binders age, they move across the DSR map from bottom-right to top-left. The track of the PG-76-22TR and PG-76-22 SBS binders are similar. Because the paths of these binders are similar, the rheological properties of these binders as they age are similar.

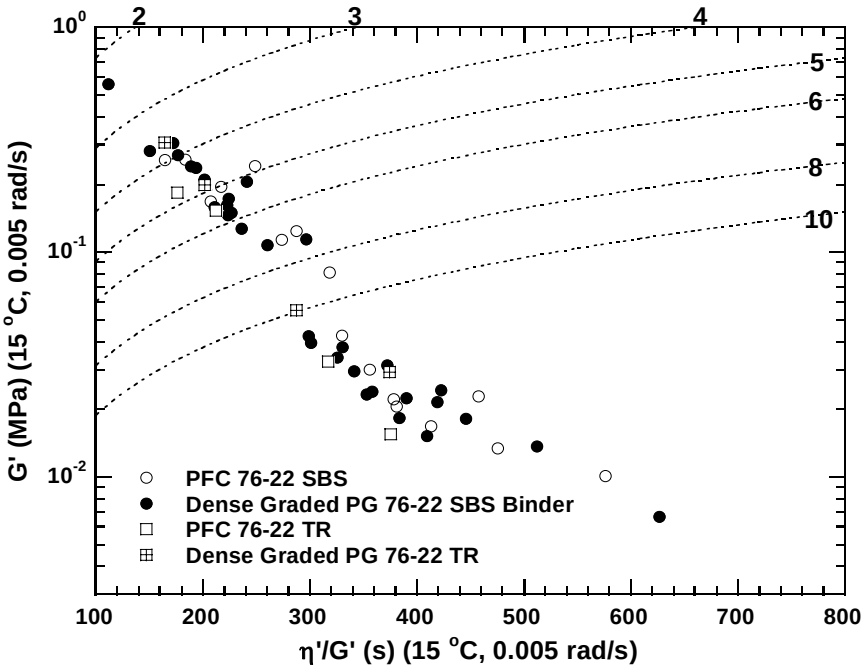

Figure 67. Examination of PFC versus Dense-Graded PG-76-22 Asphalt.

Table 30. Binders Used for the Examination of PFC vs. Dense-Graded PG-76-22 Asphalt.

PFC PG-76-22 SBS	Dense-Graded PG-76-22 SBS	PFC PG-76-22TR	Dense-Graded PG-76-22TR
Alon IH-20	Koch	Alon IH-20	Wright (T)
Lion IH-30	Lion		
Fina US-59	Valero-C		
Valero-Houston I-35	Valero-H		
	Valero-O US		
	Valero-O		
	Wright (S-B)		
	Wright (S-A)		

6.7. BINDER AGING IN CANTABRO SPECIMENS

Of particular interest to this project was the extent to which binder aging would affect the durability of PFC mixtures. Specifically, would the aging and consequent stiffening of the binder be sufficient to result in enough embrittlement of the binder that PFC layers would be susceptible to raveling or fatigue, perhaps aggravated by the lesser degree to which the aggregate interlocks, thereby holding itself in place. To assess these possible effects, the Cantabro test was conducted as described previously in Section 5.1. These tests are further discussed in this section from the perspective of binder aging.

The binder was extracted and recovered from the aged Cantabro IH-35-PG mixture specimens. The recovered binder was tested for its DSR properties and compared to the properties of the same binder aged neat in the laboratory by the previously discussed SAFT, PAV*16, and PAV*32 procedures. Additionally, the same binder from a field core was extracted, recovered, and tested.

Figure 68 shows the DSR map data for these binder specimens. The laboratory neat-aged binder forms a very well defined path across the map that follows the usual direction from the lower middle of the map and progressing towards the top left corner with increased levels of aging. The PAV*32 binder has aged nearly to the 4 cm reference line (as discussed above, these ductility reference lines are calculated from the correlation for unmodified binders and do not actually represent the ductility of polymer-modified binders). The binders recovered from the zero, three, and six month Cantabro specimens range from the 6 cm ductility reference line

nearly to the 4 cm reference line. The binder recovered from the field core lies somewhat off the path of the laboratory-aged binder and nearly to the 4 cm reference line (and thus is as aged as the Cantabro 6 month sample).

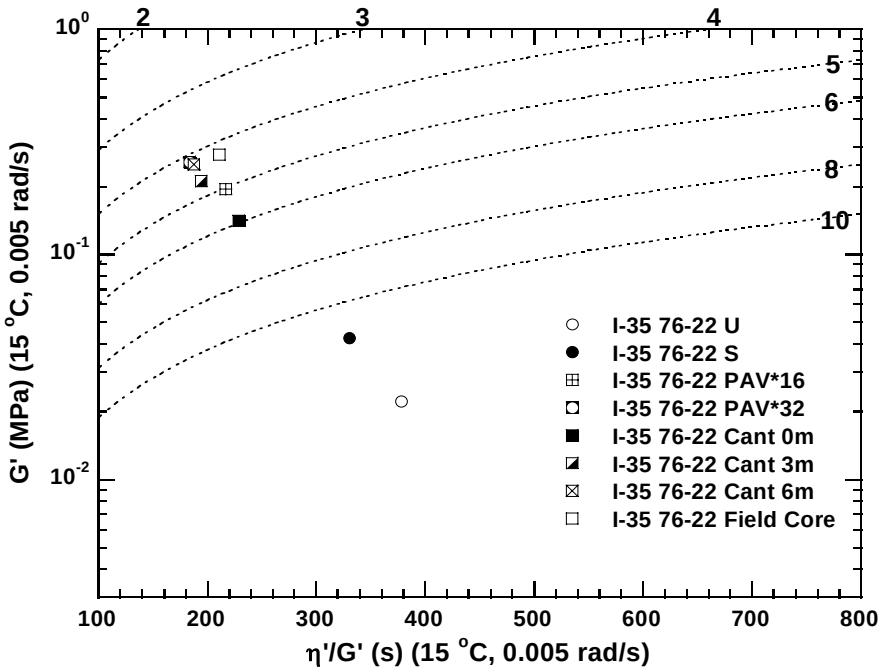

Figure 68. DSR Map of IH-35-PG-76-22 Binders Aged by Several Methods.

Figure 69 is a plot of log ductility versus DSR function for these same materials (except that there was not enough binder recovered from the field core to be able to measure ductility). As discussed for these polymer-modified materials in Section 6.5, there is a clear ductility improvement to these binders compared to the unmodified binder reference line at a comparable level of the DSR function. Again, it is noted that the binders that are recovered from the laboratory Cantabro mixtures follow the same path as the laboratory neat-aged binders. Furthermore, the fairly regular progression from zero to three to six months aging is observed in this plot as well, although it is clear that there is more movement in both ductility and DSR function between zero and three months than there is between three and six months. It is clear that binders age readily within the mixtures.

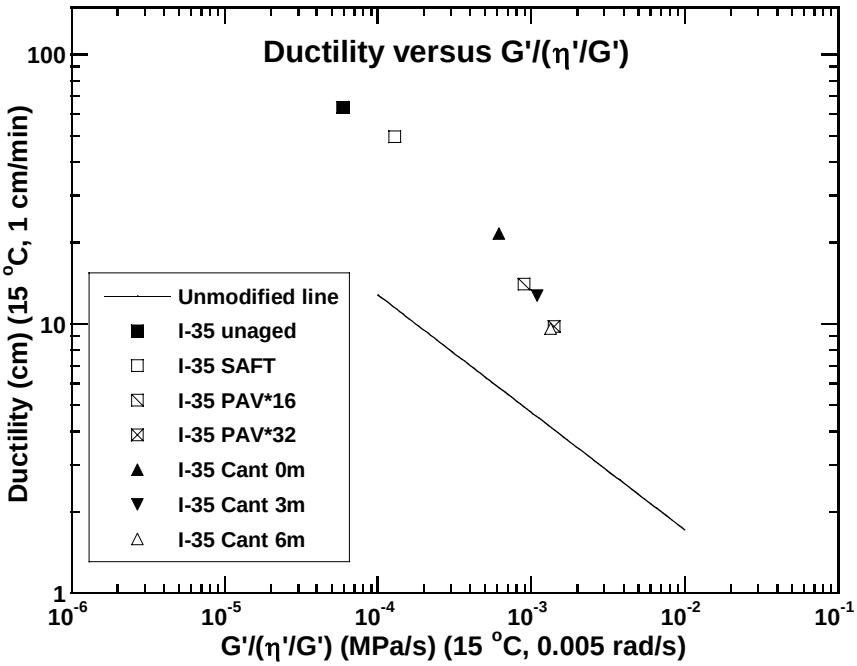

Figure 69. Ductility versus DSR Function for IH-35-PG-76-22 Binder, Aged by Several Methods.

It should also be noted that as the binder becomes more aged, there is a reduction in the ductility improvement in this SBS modified binder, i.e., the distance above the unmodified binder reference line decreases as the binder becomes more heavily aged. This is a trend that has been noted previously in the study of polymer-modified binder aging (*39*).

Table 31 compares the Cantabro loss data to the binder stiffening, as represented by both the DSR and ductility data. As the binder stiffens with increased aging, the ductility of the binder decreases, the DSR function increases, and the Cantabro loss increases.

Table 31. Cantabro Loss Compared to Binder Stiffening.

Aging Level	Cantabro Loss (%)	Ductility (cm)	G'/(η'/G') (MPa/s)
Cantabro 0m	12.5	21.63	0.000615
Cantabro 3m	28.3	12.74	0.001092
Cantabro 6m	30.3	9.63	0.001339

Figure 70 directly compares the Cantabro loss data to log DSR function. With only the three data points, a quantitative correlation is not well established, although clearly, the Cantabro

loss increase relates strongly to the binder stiffening. We also see in this figure the significantly larger increase in both DSR function and Cantabro loss between zero and three months compared to that between three and six months. Unfortunately, the data are limited and we are unable to conclusively determine the reason for this effect although a possible (perhaps likely) cause is that the zero month level of aging (2 hour at compaction temperature) (*10*) was not sufficient to move the binder out of the early, rapid rate aging period, in which case from zero to three months the binder would still be aging at a higher rate than would occur during the slower constant-rate period that from three to six months.

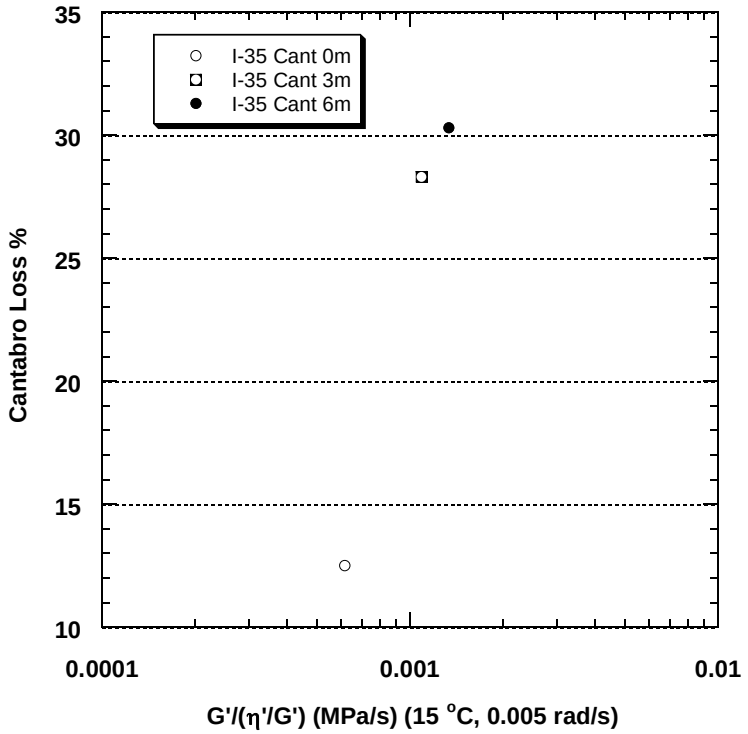

Figure 70. Cantabro Loss Compared to the DSR Function for the IH-35-PG-76-22 Binder.

6.8. SUMMARY, CONCLUSIONS, AND RECOMMENDATIONS

Binders used in PFC layers are designed to be resistant to rutting and draindown in the open PFC mixture application. Two distinct kinds of PFC binders were studied in this research, AR binders and PG-76-22 polymer-modified binders:

- AR binders stiffen the binder by blending rubber particles with the base asphalt.

- PG-76-22 SBS and SBS/TR binders stiffen the binder by dispersing a polymer network into the base binder.
- These different materials provide binders of distinctly different rheological behavior.
- The PG binders have a significantly higher ductility than either typical base binders or AR binders, a benefit that continues, although with decreasing degree, even as the binder ages. Force ductility testing shows that the polymer in the PG binders provides an enhanced strength to the binder as long as the base binder is not too stiffened by oxidative aging.
- The unaged AR binders have a significantly higher low shear rate dynamic viscosity than the PG binders.
- AR binders move nearly vertically across the DSR map of log G' versus η'/G' with increased aging whereas the PG binders move diagonally towards the top left corner of the map, following much the same behavior as unmodified binder.
- Because of the rubber particles, AR binders can pose handling difficulties not evident with PG binders. Among the difficulties are a tendency of the particles to settle, a characteristic that can complicate sampling for binder testing, as well as processing problems in the field.

Evaluating compacted mixtures by the Cantabro test at different levels of binder oxidative aging established that:

- Binders oxidize in compacted PFC mixtures.
- Binder oxidation, beyond AASHTO R30, two hour conditioning, embrittles the binder and results in significantly increased mixture disintegration (Cantabro loss) in the Cantabro loss test.

Binders recovered from most of the field cores showed significant oxidative aging beyond the unaged binder level, even though the cores were taken at the time of placement or within six months of placement. The impact of binder oxidation on pavement performance and in view of the impact of aging on the Cantabro loss test, is expected to be significant, but it is recommended that further long-term field observation be conducted to establish a quantitative relationship.

7. RECOMMENDATIONS, FUTURE WORK, AND MIX DESIGN EVALUATION

This chapter summarizes the recommendations and future research suggested based on the evaluations and conclusions achieved in this study. In addition, the recommendations are integrated in a proposed design methodology.

7.1. RECOMMENDATIONS AND FUTURE WORK

The evaluation of volumetric properties and methodologies used for their determination conducted in this study led to the following recommendations:

- Utilize dimensional analysis for determining both G_{mb} (total AV) and water accessible AV.
- Measure G_{mm} at two low asphalt contents (i.e., 3.5 and 4.5 percent are suggested) to determine the average G_{se} of the aggregate, then calculate G_{mm} at the actual asphalt content at the design range for establishing total AV content.
- Include durability mixture testing in PFC mix design in addition to volumetric criteria.
- Specify density requirements for field compaction.

Additional research should focus on:

- Establish if a vacuum is required to obtain a representative saturated mass for calculating the water accessible AV content using dimensional analysis in PFC mixtures. If vacuum saturation is required, determine the vacuum magnitude that may be needed to obtain saturation without inducing micro-damage in the specimen.
- Further explore the variability of AV content obtained from replicate compacted specimens used for mix design and how to better include this source of variability into the mix design procedure.
- Explore the use of water accessible AV as a parameter to relate to mixture functionality and durability.
- Explore the relationship between field density and laboratory density to better define the compaction requirements in the field and the compaction energy to apply in the laboratory.
- Further evaluate the application of ground-penetrating radar (GPR) or other nondestructive methods for computing PFC density and corresponding AV content to minimize time of

evaluation, traffic interruptions, and assessment of the distribution and variability of these parameters throughout the entire project length, which can then be associated with an analytical performance model to predict overall project performance.

- Define alternative gradation(s) for PFC mixtures to allow the use of finer granular materials while retaining high AV contents. The inclusion of higher proportions of filler and better filler combinations should also constitute an important aspect for future research directed to improve mixture durability.

The following recommendations are stated based on the analysis of field and laboratory drainability data:

- Conduct evaluations of drainability in the field as described in Test Method Tex-246-F to guarantee adequate initial mixture drainability properties in the field.
- Limit the maximum WFV to 20 seconds for both AR and PG mixtures as currently recommended in Test Method Tex-246.
- Specify density requirements for field compaction in addition to the control of WFV in the field.

Additional research should focus on the following aspects related to PFC functionality:

- Define relationships between WFV and laboratory water permeability conducted on road cores for each mixture system (PG and AR) and define relationships for poorly draining mixtures (i.e., WFV longer than 35 seconds).
- Evaluate long-term performance in terms of drainability to establish the actual functional life of PFC mixtures and possible maintenance actions required to extend the functional life (i.e., technical and economical appraisal of cleaning techniques versus the nonintervention alternative, or different gradation combinations, for example). Long-term performance in terms of noise reduction capacity should also be monitored to better define the functional life of these mixtures.
- Define an analytical model for permeability to better estimate this property as a function of mixture characteristics (i.e., anisotropic material properties, particle size, and AV characteristics) in the field and in the laboratory to be able to integrate permeability directly as part of the mix design method.
- Integrate the properties associated with noise reduction capacity in the mix design method.

The durability assessment performed using diverse laboratory tests produced the following recommendations:

- Use the draindown test (Tex-235-F) for mix evaluation and design to verify proper draindown resistance.
- Utilize the Cantabro test in both dry and wet conditions to evaluate mixture durability and subsequent selection of the OAC. Maximum losses of 20 and 35 percent should be required for the Cantabro loss in dry and wet conditions, respectively, when the test is conducted at room temperature (77°F [25°C]).
- Specify density requirements for field compaction.

The following aspects should be the focus of future research to address mixture performance in terms of durability:

- Gather long-term performance data (i.e., mixture resistance to disintegration under field service conditions) and evaluate more aggregate-asphalt combinations to establish if the asphalt and aggregate quality can be related to mixture resistance to disintegration in the laboratory and in the field through the Cantabro loss test. In addition, these data are required to confirm the tentative limits indicated for the Cantabro loss in dry and wet conditions. The baseline information required to conduct this evaluation and that required in terms of drainability was established in this project based on the study of selected field sections.
- Develop a more fundamental analytical model that provides a better understanding of PFC mixture performance and a more reliable mix design method. This approach can lead to a PFC performance model that integrates more fundamental material properties, in addition to surface energy and corresponding work of adhesion of the mixture components, with numerous advantages over the conventional phenomenological approaches studied. These advantages may include reduced variability, better understanding of material response (i.e., moisture damage, aging), and the substantial enhancement of the relationship with field response (i.e., service life estimation and failure mechanisms) for design and remaining life evaluations. The high variability and the lack of defined trends in the results obtained for the AR mixture system might be an indication of the limitations of the tests evaluated to capture the response of this particular material, which also suggest again the necessity of establishing more fundamental characterization techniques for its study.

At present, the surface energy of a large number of aggregates and asphalts have been determined under recent and ongoing research performed at Texas A&M University permitting the use of these known properties in the optimum selection of future materials combinations for fabricating PFC mixtures, which can constitute the first component of the recommended PFC performance model.

- Further investigate surface energy characterization for AR to determine the most reliable methodology for measuring this material property.

Additional research should focus on the following topics related to aging in PFC mixtures:

- Investigate the oxidation rate of asphalt rubber binder to assess whether the rubber particles affect the diffusion rate.
- Track the performance of the PFC and correlate binder properties to performance.

7.2. MIX DESIGN EVALUATION

The design of a PFC mixture should lead to a durable compacted mixture with a total (or water accessible) AV content higher than the minimum AV content that guarantees the expected functional properties (i.e., drainability and noise reduction capacity) and smaller than the maximum AV content that can generate durability problems due to limited mixture resistance to disintegration. Durability is also related to the mixture response in terms of moisture damage and aging, and mixture resistance to these two phenomena also requires proper assessment.

Current PFC mix design as defined by TxDOT (*10*) focuses on guaranteeing mixture functionality through a minimum total AV content, which only accounts for durability indirectly in terms of accessibility to air and water that may cause excessive aging or moisture damage, respectively. The "boiling test" assesses potential moisture damage problems, and a draindown test complements the mixture evaluation. Having as a starting point the current mix design method, an evaluation of volumetric, functionality, and durability (laboratory) aspects for PFC mixtures was conducted as previously discussed. The conclusions of this evaluation served to propose the mix design improvements (over the current design methodology) summarized in Figure 71 (dashed lined boxes indicate modified procedures).

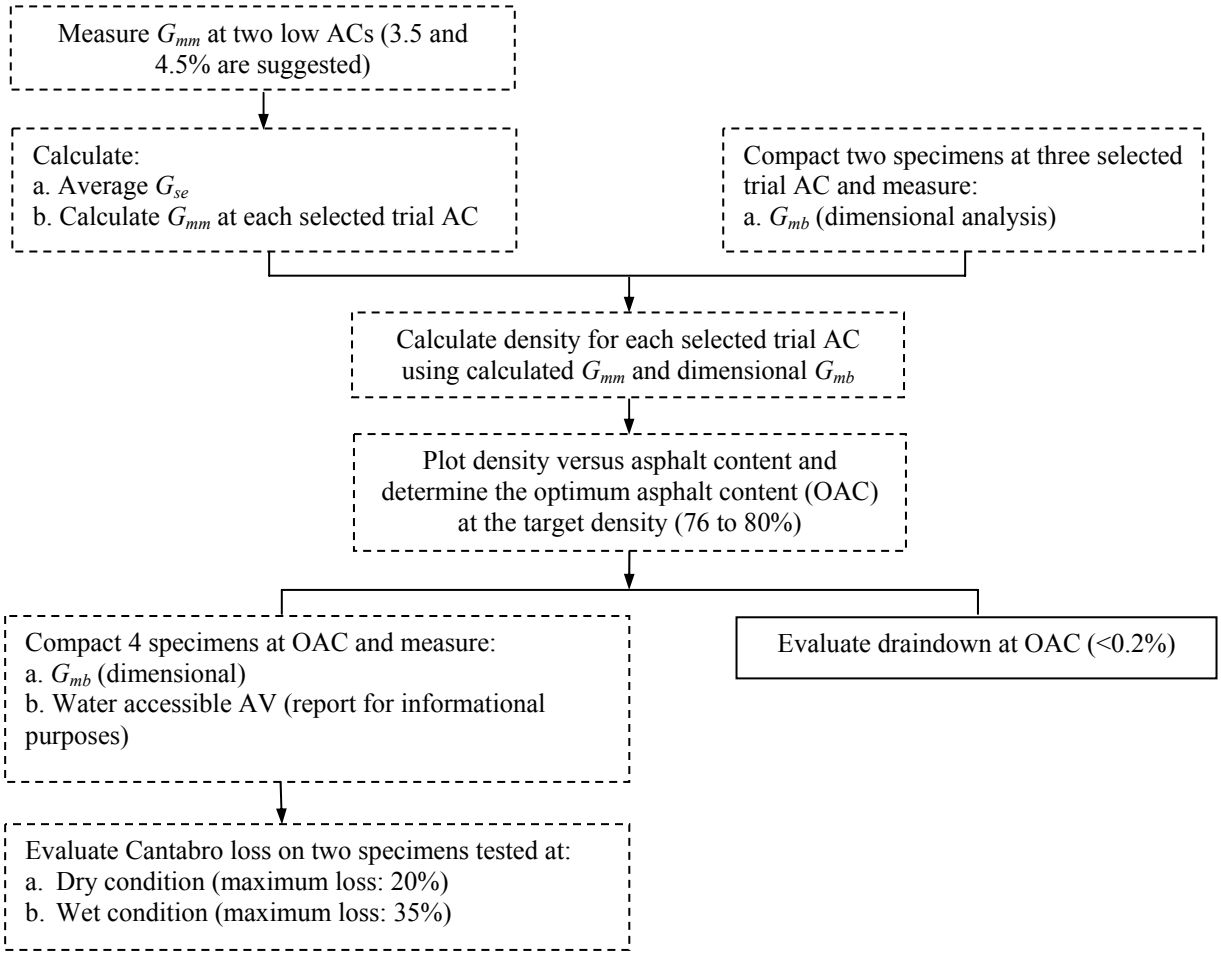

AC=asphalt content

Figure 71. Summary of the Improved Mix Design Method for Volumetric and Durability Evaluation.

Technical details of the proposed changes for the test methods included in this improved mix design are presented in the Appendix. The modifications introduced in the improved mix design method are described as follows:

- The calculation of density (used to select the OAC) and corresponding total AV content on specimens compacted at a particular trial asphalt content (AC) was improved by computing density based on calculated G_{mm} (over measured G_{mm}) and dimensional analysis for G_{mb} determinations (using direct measurements of two heights and diameter at the top, bottom, and center of the specimens to further improve the accuracy of the total volume). The same parameters are suggested for field compaction control. At present, this field control is not

conducted, leading to substantial differences between the design AV content and the actual AV in road cores.

- The density specification was modified (from 78-82 percent to 76-80 percent) to ensure adequate drainability.
- Since laboratory evaluations showed that water accessible AV better correlate with drainability and durability parameters compared to total AV content, the design methodology includes the determination of water accessible AV by applying a proposed methodology for this computation using dimensional analysis. The water accessible AV are quantified for future application in design and performance assessments.
- A durability evaluation of the design mixture conducted by applying the Cantabro loss test in both dry and wet conditions was included. The Cantabro loss test performed in a dry condition constitutes an indirect measurement of the mixture resistance to disintegration, and the test conducted after wet conditioning determines the moisture sensitivity of the design mixture.

APPENDIX

This Appendix presents modifications proposed for the mix design procedure of PFC mixtures and laboratory testing procedures integrated in the mix design. Suggested modifications are underlined to facilitate comparison with current TxDOT procedures.

TxDOT Designation: Tex-204-F

Part V—Mix Design for Permeable Friction Course (PFC) Mixtures Using the Superpave Gyratory Compactor (SGC)

13. SCOPE

13.1 Use this method to determine the proper proportions by weight of approved materials to produce a PFC mixture that will satisfy the specification requirements. This mix design procedure incorporates the use of the SGC.

14. PROCEDURE

14.1 *Selecting Materials:*

14.1.1 Select the necessary type and source for each aggregate. Obtain representative samples consisting of a minimum of 23 kg (50 lb.) of each aggregate. Take samples in accordance with Tex-221-F.

14.1.2 Obtain an adequate quantity of the asphalt and additives. Take samples in accordance with Tex-500-C. Polymer-modified asphalt binder with a PG of 76-XX or higher is required or Asphalt Rubber (A-R), Type I or II. Use of fibers is required for mixes with PG 76-XX. Use loose fibers for mixtures prepared in the laboratory.

14.1.3 Dry the aggregate to constant weight at a minimum temperature of 38°C (100°F).

14.1.4 If the stockpile gradation is unknown, obtain the average washed gradation of each proposed aggregate stockpile in accordance with Tex-200-F, Part II. Enter the stockpile gradations on the "Combined Gradation" worksheet. Use the construction stockpile gradation when it is available.

14.1.5 Check the aggregate gradation for compliance with the applicable specifications. Check the individual aggregate stockpiles for compliance with the applicable specifications.

14.1.6 Check the asphalt and additives for compliance with the applicable specifications.

14.1.7 If the specific gravity values for the aggregate sources are unknown, determine the 24-hr. water absorption, the bulk specific gravity, and the apparent specific gravity of individual sizes of each aggregate in accordance with Tex-201-F and Tex-202-F. Enter these results or the known values from previous history on the "Bulk Gravity" worksheet. Test lightweight aggregate, when applicable, in accordance with Tex-433-A.

14.1.7.1 Normally, specific gravities are not determined for aggregate size fractions consisting of less than 15% of the individual aggregate. Assign the water absorption and specific gravity of smaller aggregate size fractions close to the next adjacent size fraction for which values were determined.

14.1.8 Use the "Combined Gradation" worksheet to calculate the bin percentages with the proposed aggregate such that the blended combination will fall within the specified gradation ranges for the specified mixture type.
Note 11—Consider material availability, mixture strength, handling, compaction, pavement texture, and durability as the primary factors of the combination to be tested.

14.1.9 Add 1% hydrated lime as a mineral filler for mixes with PG 76-XX. Use hydrated lime as an aggregate type when determining the bin percentages for the combined aggregate blend. The combined gradation will include the hydrated lime.

14.1.10 Check the aggregate classification of the combined aggregate blend using the "Aggregate Classification" worksheet when blending Class A with Class B aggregate. Determine whether the percentage of the Class A aggregate in the combined aggregate blend meets the specification requirement in accordance with Section 19.1.

14.1.11 Plot the combined gradation and specification limits on the Power 0.45 Curve using the "Power 45 Curve" worksheet.

14.2 *Preparing Laboratory-Mixed Samples:*

14.2.1 Separate the material larger than the 2.36 mm (No. 8) sieve into individual sizes for each stockpile for preparation of laboratory mixtures. Separate the material passing the 2.36 mm (No. 8) sieve into individual sizes if it is prone to segregation.

14.2.2 Start the mixture design with the minimum allowable percentage of loose fibers for mixes with PG 76-XX. Increase this percentage when necessary to achieve the required mixture properties.

14.2.3 Select a minimum of three asphalt binder contents in increments of 0.5% for the laboratory-molded specimens. Start at an asphalt content of 6.0% or greater for

PFC mixtures with PG 76-XX. Start at an asphalt content of 8.0% or greater for PFC mixtures with Asphalt-Rubber (A-R) binder. Lower asphalt contents are allowed when using an aggregate with a bulk specific gravity greater than 2.750.

14.2.4 Select three asphalt binder contents in increments of 0.5% for the G_r samples. Start at an asphalt content of 3.5%. Ensure all samples are thoroughly coated with asphalt binder.

Note 12 —Perform this step to determine accurate G_r values at the higher asphalt contents selected in Section 14.2.3 for the laboratory-molded specimens. The G_r values for the mixtures with the higher asphalt contents are back-calculated (obtaining G_t values) using the equations in Sections 19.2 and 19.3.

14.2.5 Calculate the weights of individual aggregates required to produce the specimens and samples specified in Sections 14.2.3 and 14.2.4. Generally, 3500-3700 g of aggregate are required to achieve the specified molded specimen height of 115 ± 5 mm (4.5 ± 0.2 in.); however, this may vary. It may be necessary to produce a trial specimen to achieve this height requirement.

14.2.6 Prepare the asphalt mixtures in accordance with Tex-205-F. Determine the mixing and compaction temperatures from Table 1 in Tex-241-F. Oven-cure all the mixtures for 2 hr. at the selected compaction temperature.

14.2.7 Mold two specimens at each asphalt content selected in Section 14.2.3 in accordance with Tex-241-F. Mold specimens to 50 gyrations or as shown on the plans.

14.2.8 Determine the G_r at the asphalt contents selected in Section 14.2.4 in accordance with Tex-227-F. Enter the G_r in the "Summary" worksheet.

14.2.9 Determine the G_a of the specimens using dimensional analysis in accordance with Tex-207-F, Part VIII. Enter the G_a in the "Summary" worksheet.

14.2.10 Use the "Mix Design" program to calculate the average G_e of the blend in accordance with Section 19.2. Use the "Mix Design" program to back-calculate the G_r value (G_t). Use the equation in Section 19.3 and the average G_e for the combined blend to calculate G_t for the mixtures with the higher asphalt contents used for the laboratory molded specimens.

14.2.11 Use the "Mix Design" program to calculate the percent density of the molded specimens in accordance with Section 19.4.

14.3 *Determining the OAC:*

14.3.1. Use the "Mix Design" program to plot densities versus asphalt content for the molded specimens. Determine the OAC by interpolating mathematically between

the asphalt contents above and below the target laboratory-molded density on the "Summary" worksheet.

14.3.2. Adjust the percentage of coarse aggregate or fibers to achieve an OAC of 6.0% or greater, when necessary.
Note 13—OAC below 6.0% for PG 76-XX and 8.0% for A-R PFC mixtures may not provide the necessary asphalt film thickness for optimum field performance.

14.4 *Evaluating the Mixture at the OAC:*

14.4.1 Evaluate draindown of the optimum mixture in accordance with Tex-235-F.

14.4.2 Evaluate the G_a and water accessible air voids of compacted specimens using dimensional analysis in accordance with Tex-207-F, Part VIII. Report test results of water accessible air voids for informational purposes only.

14.4.3 Evaluate the durability of the optimum mixture in accordance with Tex-245-F.

14.4.4 Report all data in the automated "Mix Design Report" program.

19. CALCULATIONS

19.1 Calculate %Total CL_A:

$$\% \text{ Total } CL_A = \frac{\% \ CL_A}{(\% \ CL_A + \% \ CL_B)}$$

Where:
% Total CL_A = total percentage retained of Class A aggregate on the 4.75 mm (No. 4) sieve
$\% \ CL_A$ = percentage retained of Class A aggregate on the 4.75 mm (No. 4) sieve
$\% \ CL_B$ = percentage retained of Class B aggregate on the 4.75 mm (No. 4) sieve.

19.2 Calculate G_e:

$$G_e = \frac{(100 - A_s)}{\left[\left(\frac{100}{G_r}\right) - \left(\frac{A_s}{G_s}\right)\right]}$$

Where:
G_e = effective specific gravity
A_s = asphalt content, %
G_r = theoretical maximum specific gravity
G_s = specific gravity of the asphalt binder.

19.3 Calculate the G_t:

$$G_t = \frac{100}{\left[\left(\frac{A_g}{G_e}\right)+\left(\frac{A_s}{G_s}\right)\right]}$$

Where:
G_t = calculated theoretical maximum specific gravity
A_g = percentage of aggregate in the mixture.

19.4 Calculate the percent density of the molded samples:

$$\%\ \text{Density} = \left(\frac{G_a}{G_t}\right)\times 100$$

Where:
% Density = percentage of the ratio of G_a to G_t
G_a = bulk specific gravity.

19.5 Calculate the *VMA*:

$$VMA = \left\{100 - \left[\left(\frac{G_a}{G_t}\right)\times 100\right]\right\} + \left[\frac{G_a \times A_s}{G_s}\right]$$

Where:
VMA = voids in mineral aggregates.

19.6 Calculate the *VFA*:

$$VFA = \left[\frac{(VMA - \%AirVoids)}{VMA}\right]\times 100$$

Where:
VFA = voids filled with asphalt
% Air Voids = percentage of air voids in the compacted mix.

19.7 Calculate the VCA_{CA}:

$$VCA_{CA} = \left\{\frac{[(G_{CA}\times\gamma_w)-\gamma_s]}{(G_{CA}\times\gamma_w)}\right\}\times 100$$

Where:

VCA_{CA} = voids in the coarse aggregate in the dry-rodded condition
G_{CA} = bulk specific gravity of the coarse aggregate blend (retained on the 2.36 mm (No.8) sieve)
γ_w = unit weight of water
γ_s = unit weight of the coarse aggregate blend fraction in the dry-rodded condition.

19.8 Calculate the VCA_{Mix}:

$$VCA_{Mix} = 100 - \left[\left(\frac{G_a}{G_{CA}} \right) \times P_{CA} \right]$$

Where:
VCA_{Mix} = voids in coarse aggregate for the compacted mixture
P_{CA} = percentage coarse aggregate in the total mix.

TxDOT Designation: Tex–207–F

PART VIII, DETERMINING DENSITY OF PERMEABLE FRICTION COURSE (PFC) MIXTURES

37. SCOPE

37.1 Use this procedure to back-calculate the G_r (G_t) of loose PFC mixtures, to calculate the G_a and the water accessible air voids of laboratory-molded specimens for PFC mixtures using dimensional analysis, and to calculate density of compacted PFC mixtures.

38. APPARATUS

38.1 Use a measuring device, such as a caliper.

39. PROCEDURE

39.1 To determine the density of a compacted PFC specimen, first back calculate G_r (G_t).

39.1.1 Obtain the average G_e of the combined aggregate blend.
Note 33—Obtain the average G_e from the Summary worksheet of the Mix Design template.

39.1.2 Record and designate this as 'G_e' in Section 40.1.

39.1.3 Determine the AC of the PFC mixture.
Note 34—Determine the AC of PFC-Asphalt Rubber (AR) mixtures by using the asphalt flow meter. Determine the AC of PFC PG 76 Mixtures using an ignition oven according to Tex-236-F or by using the asphalt flow meter.

39.1.4 Record and designate this as 'A_s' in Section 40.1.

39.1.5 Determine the specific gravity of the asphalt binder. Round to three decimal places (0.001).

39.1.6 Record and designate this as 'G_s' in Section 40.1.

39.1.7 Calculate G_t as noted in Section 40.1.

39.2 Calculate G_a and water accessible air voids using dimensional analysis.

39.2.1 Measure the weight of the laboratory molded specimen in air, to the nearest 0.1 g.

39.2.2 Record and designate this weight as 'W' in Sections 40.2 and 40.3.

39.2.3 Measure the height of the laboratory-molded specimen at three uniformly distributed positions around the specimen circumference to the nearest 0.1 mm.

39.2.4 Record the average height and designate this height as '*h*' in Sections 40.2 and 40.3.

39.2.5 Measure the diameter of the laboratory-molded specimen at the top, bottom and center of the specimen, to the nearest 0.1 mm, and calculate the average diameter.

39.2.6 Calculate the average radius of the laboratory molded specimen by dividing the average diameter by two as determined in Section 39.2.5.

39.2.7 Record and designate this average radius as '*r*' in Sections 40.2 and 40.3.

39.2.8 Calculate G_a as noted in Section 40.2.
Note 35—Numerical value for π is 3.14.

39.2.9 Measure the saturated weight in water of the laboratory molded specimen, to the nearest 0.1 g.
Note 36— The saturated specimen weight in water is obtained after direct immersion of the specimen without any vacuum application.
Note 37—The minimum saturation time (time required to obtain constant saturated weight) should be four minutes, but this time is variable for each mixture.

39.2.10 Record and designate this weight as 'W_s' in Section 40.3.

39.2.11 Calculate the *Accessible AV* as noted in Section 40.3.

39.3 Calculate density of compacted PFC mixture.

39.3.1 Divide the G_a determined in Section 39.2.8 by the G_t determined in Section 39.1.7.

39.3.1.1 Multiply the results from Section 39.3.1 by 100.
Note 36—Round this calculated value to the tenth decimal place (0.1).

40. CALCULATIONS

40.1 Calculate the G_t of the loose PFC mixture using the following formula.

$$G_t = \frac{100}{\left[\left(\frac{100 - A_s}{G_e}\right) + \left(\frac{A_s}{G_s}\right)\right]}$$

where:
G_t=back-calculated theoretical maximum specific gravity
G_e=effective specific gravity of the combined aggregate, %
A_s=AC, %
G_s=asphalt binder specific gravity, 0.001.

40.2 Calculate the G_a of the compacted specimen using the following formula.

$$G_a = \frac{\left[\frac{W}{\pi r^2 h}\right]}{\gamma}$$

where:
G_a =bulk specific gravity
W =weight of specimen, 0.1 g
π =pi, 3.14
r =radius of specimen, 0.1 mm
h =height of specimen, 0.1 mm
γ =density of water, 0.001 g/mm^3.

40.3 Calculate water accessible air voids of the compacted specimen using the following formula.

$$Accesible\ AV = \frac{\pi r^2 h - \frac{(W - W_s)}{\gamma}}{\pi r^2 h} * 100 \quad (\%)$$

where:
Accessible AV = water accessible air voids (%)
W =weight of specimen, 0.1 g
W_s= saturated sample mass in water
π =pi, 3.14
r =radius of specimen, 0.1 mm
h =height of specimen, 0.1 mm
γ =density of water, 0.001 g/mm^3

41. REPORT FORMAT

41.1 Use the following Excel programs to calculate and report density test results.

41.1.1 Quality Control/Quality Assurance (QC/QA), used in conjunction with hot mix specification, test data worksheets for 1993/1995 Specifications or for 2004

Specifications. Refer to the 'Help' tab for detailed instructions on how to use the program.

41.1.2 'Segregation Density Profile Form'

41.1.3 'Longitudinal Joint Density Profile Form'.

---

42. ARCHIVED VERSIONS

42.1 Archived versions are available

TxDOT Designation: Tex–245–F

Tex-245-F, Cantabro Loss

Contents:

Section 1 — Overview….....2
Section 2 — Apparatus….....3
Section 3 — Test Specimens….....4
Section 4 — Procedure….....5
Section 5 — Calculations….....6
Section 6 — Report Forms….....7
Section 7 — Archived Versions.....8

Section 1
Overview

Effective Date: DRAFT

Use this test procedure to determine the abrasion loss of compacted hot-mix asphalt specimens.

This test procedure measures the breakdown of compacted specimens utilizing the Los Angeles Abrasion machine. The percent of weight loss (Cantabro loss) is an indication of PFC durability and is related to the quantity and quality of the asphalt binder and the aggregate properties composing the mixture. The percentage of weight loss is measured and reported.

Units of Measurement

The values given in parentheses (if provided) are not standard and may not be exact mathematical conversions. Use each system of units separately. Combining values from the two systems may result in non-conformance with the standard.

Section 2

Apparatus

Use:

♦ the apparatus used in "Tex-410-A, Abrasion of Coarse Aggregate Using the Los Angeles Machine" and

♦ a balance, readable to 0.1 g and accurate to 0.5 g.

Section 3

Test Specimens

Compact test specimens:

♦ at the design asphalt content, gradation, and air void percent

♦ with a Superpave Gyratory Compactor at the design number of gyrations and

♦ with the diameter and height specified in the mixture design procedure.

Section 4

Procedure

Follow these steps to determine the abrasion loss of compacted specimens using laboratory-produced mixtures or plant-produced mixtures.

♦ Laboratory-Produced Mixtures

Determining Cantabro Loss for Laboratory-Produced Mixtures

Step	Action
1	Prepare a laboratory mixture according to "Tex-205-F, Laboratory Method of Mixing Bituminous Mixtures."
2	♦ Compact 4 test specimens according to "Tex-241-F, Superpave Gyratory Compacting of Test Specimens of Bituminous Mixtures." ♦ Follow instructions for Steps 2 – 5 described in 'Determining Cantabro Loss for Plant-Produced Mixtures.'

♦ Plant-Produced Mixtures

Determining Cantabro Loss for Plant-Produced Mixtures

Step	Action
1	Compact 4 test specimens according to "Tex-241-F, Superpave Gyratory Compacting of Test Specimens of Bituminous Mixtures."
2	♦ Cool compacted specimens to room temperature and weight ♦ Record and designate the weight as 'A' under 'Calculations.'
3	♦ Dry two specimens for 24 ± 0.5 hours using forced ventilation at room temperature. **Note**: Drying is required to eliminate the water trapped during saturation to measure water accessible air voids ♦ Record the weight of the specimen after drying and designate this weight as B.
4	♦ Immerse two specimens for 24 ± 0.5 hours in a water bath with a constant temperature of 140°F **Note**: this wet conditioning process can start immediately after completing the measurement of water accessible air voids ♦ Dry the specimens for 24 ± 0.5 hours using forced ventilation at room temperature ♦ Determine the final weight of the dry specimens ♦ Record the weight of the specimen after drying and designate this weight as B.
3	Place the test specimen in the Los Angeles testing machine. *NOTE:* Do not include the steel balls.
4	Rotate the Los Angeles machine at a speed of 30 to 33 revolutions per minute for 300 revolutions.
5	♦ After the 300 revolutions, discard the loose material broken off the test specimen. Do not include any of this material in the weight ♦ Weigh the test specimen ♦ Record and designate this weight as 'C' under 'Calculations.'

Section 5

Calculations

Calculate the Cantabro Loss using the following formula:

$$CL = \frac{A-(C-(B-A))}{A} * 100\ (\%)$$

Where:

♦CL = Cantabro Loss, %

♦ A = Initial weight of test specimen

♦ B = Weight of the specimen after drying

♦ C = Final weight of test specimen.

Section 6

Report Forms

Use the reporting form ‘Cantabro’ to report both results from dry and wet conditioned specimens.

Section 7

Archived Versions

The following archived versions of "Tex-245-F, Cantabro Loss" are available:

- 245-1104 for the test procedure effective November 2004 through September 2005.

REFERENCES

1. Alvarez, A. E., A. Epps Martin, C. Estakhri, J. Button, C. Glover, and S. H. Jung. *Synthesis of Current Practice on the Design, Construction, and Maintenance of Porous Friction Courses*. Report FHWA/TX-06/0-5262-1, Texas Transportation Institute, Texas A&M University, College Station, Texas, 2006. http://tti.tamu.edu/documents/0-5262-1.pdf
2. Brown, J. R. *Pervious Bitumen–Macadam Surfacings Laid to Reduce Splash and Spray at Stonebridge, Warwickshire*. Report No. LR 563, Transportation Road Research Laboratory, 1973. England.
3. Ruiz, A., R. Alberola, F. Pérez, and B. Sánchez. Porous Asphalt Mixtures in Spain. In *Transportation Research Record: Journal of the Transportation Research Board*, No. 1265, TRB, National Research Council, Washington, D.C., 1990, pp. 87-94.
4. Khalid, H., and F. Pérez. Performance and Durability of Bituminous Materials. *Performance Assessment of Spanish and British Porous Asphalts*, 1996, pp. 137-157. Published by E & FN Spon, London.
5. Button, J. W., E. G. Fernando, and D. R. Middleton. *Synthesis of Pavement Issues Related to High-Speed Corridors*. Report No. 0-4756-1. Texas Transportation Institute, Texas A&M University, College Station, Texas, 2004.
6. Kearfott, P., M. Barrett, and J. F. Malina, Jr. *Stormwater Quality Documentation of Roadside Shoulders Borrow Ditches*. CRWR Online Report 05-02, Center for Research in Water Resources, The University of Texas at Austin, Austin, Texas, 2005. http://www.crwr.utexas.edu/online.shtml.
7. Kandhal, P. *Design, Construction, and Maintenance of Open-Graded Asphalt Friction Courses*. Information series 115. National Asphalt Pavement Association, Lanham, MD, 2002.
8. Watson, D. E., K. A. Moore, K. Williams, and L. A. Cooley. Refinement of New-Generation Open-Graded Friction Course Mix Design. In *Transportation Research Record: Journal of the Transportation Research Board*, No. 1832, TRB, National Research Council, Washington, D.C., 2003, pp. 78-85.

9. Watson, D. E., L. A. Cooley Jr., K. A. Moore, and K. Williams. Laboratory Performance Testing of Open-Graded Friction Course Mixtures. In *Transportation Research Record: Journal of the Transportation Research Board*, No. 1891, TRB, National Research Council, Washington, D.C., 2004, pp. 40-47.
10. Texas Department of Transportation. *200-F Bituminous Test Procedures Manual*. Austin, TX, 2005.
11. Texas Department of Transportation. *Standard Specifications for Construction and Maintenance of Highways, Streets, and Bridges Adopted by the Texas Department of Transportation.* Austin, TX, 2004.
12. Texas Department of Transportation. *500-C Asphalt Test Procedures Manual*. Austin, TX, 2004.
13. Crouch, L. K., D. Badoe, M. Cates, T. A. Borden, A. Copeland, C. T. Walker, T. Dunn, R. Maxwell, and W. Goodwin. *Bulk Specific Gravity of Compacted Bituminous Mixtures: Finding a More Widely Applicable Method*. Publication TNSPR RES 1153, Tennessee Technological University, 2003. Cookeville, TN
14. InstroTek®. *CoreLok® Operator's Guide. Version 20.* Incorporated. Raleigh, NC, 2003.
15. Masad, E., E. Arambula, R. A. Ketcham, A. R. Abbas, and A. Epps Martin. Nondestructive Measurements of Moisture Transport in Asphalt Mixtures. *Journal of the Association of Asphalt Paving Technologist* (in press), 2007.
16. Masad, E. X-Ray Computed Tomography of Aggregates and Asphalt Mixes. *Materials Evaluation*, July 2004, pp. 775-783.
17. American Association of State Highway and Transportation Officials (AASHTO). Theoretical Maximum Specific Gravity and Density of Hot–Mix Asphalt Paving Mixtures. AASHTO T 209-05, Standard Specifications for Transportation Materials and Methods of Sampling and Testing. 2005.
18. Burr, B. L., C. J. Glover, R. R. Davison, and J. A. Bullin. New Apparatus and Procedure for the Extraction and Recovery of Asphalt Binder from Pavement Mixtures. In *Transportation Research Record: Journal of the Transportation Research Board*, No. 1391, TRB, National Research Council, Washington, D.C., 1993, pp. 20-29.

19. American Standard of Testing Materials (ASTM). Standard Provisional Test Method for Measurement of Permeability of Bituminous Paving Mixtures Using a Flexible Wall Permeameter. ASTM Designation: PS 129-01. 2001.
20. Centro de Estudios y Experimentación de Obras Públicas (CEDEX). Spanish Standard NLT-327/88.
21. Centro de Estudios y Experimentación de Obras Públicas (CEDEX). Spanish Standard NLT-352/86.
22. Zhou, F., S. Hu, and T. Scullion. *Integrated Asphalt (Overlay) Mixture Design, Balancing Rutting and Cracking Requirements*. Report No. FHWA/TX-06/0-5123-1. Texas Transportation Institute, Texas A&M University, College Station, TX, 2006.
23. Birgisson, B., R. Roque, M. Tia, and E. Masad. *Development and Evaluation of Test Methods to Evaluate Water Damage and Effectiveness of Antistripping Agents*. Project Number 4910-4504-722-12, Florida Department of Transportation, University of Florida (Gainesville), 2005.
24. Centro de Estudios y Experimentación de Obras Públicas (CEDEX). Spanish Standard NLT-362/92.
25. Van Oss, C. J. *Interfacial Forces in Aqueous Media.* Marcel Dekker Inc., New York, 1994.
26. Van Oss, C. J., M. K. Chaudhury, and R. J. Good. Interfacial Lifshitz-van der Waals and Polar Interactions in Macroscopic Systems. *Chemical Reviews,* Vol. 88, No. 6, 1988, pp. 927-941.
27. Hefer, A. W., A. Bhasin, and N. L. Dallas. Bitumen Surface Energy Characterization Using a Contact Angle Approach. *Journal of Materials in Civil Engineering © ASCE*, Vol. 18, No. 6, 2006, pp. 759-767.
28. Lytton, R. L., E. Masad, C. Zollinger, R. Bulut, and D. Little. *Measurements of Surface Energy and its Relationship to Moisture Damage*. Report FHWA/TX-05/0-4524-2. Texas Transportation Institute, Texas A&M University, College Station, Texas, 2005.
29. Lytton, R. L. *Adhesive Fracture in Asphalt Concrete Mixtures*. In J. Youtcheff (Ed.), submitted for publication, 2004.
30. Molenaar, A. A. A., A. J. J. Meerkerk, M. Miradi, and T. van der Steen. Performance of Porous Asphalt Concrete. In *Annual Meeting and Technical Sessions, Association of Asphalt*

Paving Technologist. CD-ROM. Association of Asphalt Paving Technologist, Savannah, Georgia, 2006, pp. 1-42.

31. Glover, C., R. Davison, C. Domke, Y. Ruan, P. Juristyarini, D. Knorr, and S. H. Jung. *Development of a New Method for Assessing Asphalt Binder Durability with Field Validation*. Report No FHWA/TX-05/1872-2. Texas Department of Transportation, Texas A&M University, College Station, TX, 2005.
32. Huber, G. Performance Survey on Open-Graded Friction Course Mixes. Synthesis of Highway Practice 284. Transportation Research Board, National Research Council, Washington, D.C., 2000.
33. Texas Department of Transportation. *Technical Advisory. Hamburg Wheel Test*. Austin, TX, 2006.
34. Estakhri, C., S. Rebala, and D. Little. *Laboratory Evaluation of Crumb-Rubber Modified (CRM) Binders and Mixtures*. Report No FHWA/TX-94/1332-1. Texas Transportation Institute, Texas A&M University, College Station, TX, 1993.
35. Vassiliev, N. Y., R. R. Davison, and C. J. Glover. Development of a Stirred Airflow Test Procedure for Short-Term Aging of Asphaltic Materials. *Bituminous Binders*, No. 1810, 2002, pp. 25-32.
36. Burr, B. L., R. R. Davison, C. J. Glover, and J. A. Bullin. Solvent Removal from Asphalt. In *Transportation Research Record: Journal of the Transportation Research Board*, No. 1269, TRB, National Research Council, Washington, D.C., 1990, pp. 1-8.
37. Glover, C. J., R. Davison, C. H. Domke, Y. Ruan, P. Juristyarini, D. B. Knorr, and S. H. Jung. *Development of a New Method for Assessing Asphalt Binder Durability with Field Validation*. Report FHWA/TX-05/1872-2, Texas Transportation Institute, Texas A&M University, College Station, Texas, 2005.
38. Ruan, Y., R. R. Davison, and C. J. Glover. An Investigation of Asphalt Durability: Relationships between Ductility and Rheological Properties for Unmodified Asphalts. *Petroleum Science and Technology*, Vol. 21, Nos. 1-2, 2003, pp. 231-254.
39. Woo, W. J., E. Ofori-Abebresse, A. Chowdhury, J. Hilbrich, Z. Kraus, A. Epps Martin, and C. J. Glover. *Polymer Modified Asphalt Durability in Pavements*. Report FHWA/TX-

07/4688-1, Texas Transportation Institute, Texas A&M University, College Station, Texas. 2007.

40. Way, G. B. ADOT's Use of Crumb Rubber in Asphalt Pavements, http://www.rubberpavements.org/RPA_News/sep97/page3.html.